I. A PHOTOMETRIC EVALUATION OF QUENCHING OILS

II. X-RAY STUDIES OF 2, 4 DINITROPHENYLHYDRAZINE DERIVATIVES

BY

WILBUR IRVING KAYE

B. S., J. B. Stetson University, 1942

THESIS

SUBMITTED IN PARTIAL FULFILLMENT OF THE REQUIREMENTS
FOR THE DEGREE OF DOCTOR OF PHILOSOPHY IN CHEMISTRY
IN THE GRADUATE SCHOOL OF THE UNIVERSITY
OF ILLINOIS, 1945

URBANA, ILLINOIS

UNIVERSITY OF ILLINOIS

THE GRADUATE SCHOOL

January 8, 1945

I HEREBY RECOMMEND THAT THE THESIS PREPARED UNDER MY SUPERVISION BY Wilbur Irving Kaye

ENTITLED I. A Photometric Evaluation of Quenching Oils

II. X-Ray Studies of 2, 4 Dinitrophenylhydrazine Derivatives.

BE ACCEPTED* AS FULFILLING THIS PART OF THE REQUIREMENTS FOR THE DEGREE OF Doctor of Philosophy in Chemistry

George R. Clark
In Charge of Thesis

Wm. C. Rose
Head of Department

Recommendation concurred in†

H A Nye
J. H. Reedy
S Frederick Smith

Committee on Final Examination†

*Subject to successful final examination in the case of the doctorate.
†Required for doctor's degree but not for master's.

500—1-44—27421

ACKNOWLEDGMENT

The author wishes to express his appreciation to Dr. G. L. Clark for his guidance and inspiration in the development of the problem and to his wife, Virginia, for her valuable help in carrying this work out.

TABLE OF CONTENTS

Part I

A Photometric Evaluation of Quenching Oils

A. Introduction 1

B. History
1. Products of Oxidation 2
2. Rates of Oxidation 2
3. Mechanism of Additive Action 3
4. Filtering 4
5. Optical Evaluation 4

C. Experimental
1. Types of Oils 6
2. Appartus 6
3. Experimental Curves and Numerical Rating of Oils 7
4. Dilution Effects 11
5. Laboratory Method of Oxidizing Quenching Oils 19
6. Study of Additive Action 27
7. Changes in Oil in the Quenching Tank 29
8. Theory of Optical Evaluation of Oil Deterioration 37

D. Summary 44

E. Bibliography 45

Part II

X-Ray Studies of 2, 4 Dinitrophenylhydrazine Derivatives

A. Introduction 47

B. History 48

C. Description of the Weissenberg Method 51

D. Structure of Formaldehyde 2, 4 Dinitrophenylhydrazone
1. Preparation 61
2. Properties of the Crystals 61
3. Experimental X-Ray Data 62
4. Orientation of the Molecule in the Unit Cell 73

E. Acetaldehyde 2, 4 Dinitrophenylhydrzaone (platelets)
1. Preparation 76
2. Properties 76
3. Experimental X-Ray Data 77

F. Acetaldehyde 2, 4 Dinitrophenylhydrazone (orange Needles)
1. Preparation 86
2. Properties 86
3. Experimental X-Ray Data 88

G. Crotonaldehyde 2, 4 Dintrophenylhydrazone
1. Preparation 92
2. Properties 92
3. Experimental X-Ray Data 92

H. Butyraldehyde 2, 4 Dinitrophenylhydrazone
1. Preparation 99
2. Properties of Yellow Needles 99
3. Experimental X-Ray Data (Yellow Needles) 100
4. Properties-Orange Needles 105
5. Experimental X-Ray Data 105
6. Amber Platelets 110

I. Furfuraldehyde 2, 4 Dinitrophenylhydrazone
1. Preparation 112
2. Experimental X-Ray Data 113

J. Qualitative X-Ray Analysis of Aldehydes in Micro Quantities
1. Introduction 119
2. Apparatus 119
3. Technique of Qualitative Analysis 125
4. Evaluation of Powder Patterns 126

K. Quantitative X-Ray Analysis
1. Introduction 132
2. Quantitative X-Ray Analysis of Mixtures of NaCl and KCl 133
3. Quantitative X-Ray Analysis of Aldehydes 145

L. Discussion of the Strong Outer Spacing 151

M. Summary 154

N. Bibliography 158

I

A Photometric Evaluation of Quenching Oils

Introduction

At the request of the Delco Remy Division of the General Motors Corporation the oxidation stability of quenching oils was studied. It has been found that the strain induced in aluminum airplane castings on quenching in oil greatly increased with ageing of the quenching oil. These castings of aluminum alloy were quenched rapidly from a temperature of 480° C. (900°F.) in a quenching oil maintained at approximately 45° C. This hot quenching of the metal oxidized the oil producing a byproduct which in some manner impaired the heat conduction properties of the oil. A study of the heat conducting properties seemed to be beyond the scope of the equipment immediately available for use; however, it was highly desireable to devise some method of studying and evaluating the oxidation stability of various quenching oils so that the one of highest quality might be selected with assurance of optimum performance and life in 5000 gallon lots. The method chosen was one based on spectrophotometric absorption values of the oils at different stages of use.

History

Products of Oxidation

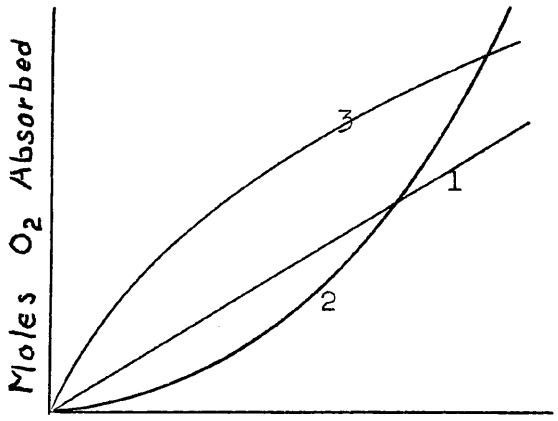
Fenske[1] in heating lubricating oils at 140-170° C. accounted for most of the oxygen absorbed. His results indicate that about half of the oxygen goes into the formation of water while the remainder may be accounted as CO_2, CO, volatile acids (formic, propionic), fixed acids (phenols, esters) and isopentane insolubles (polymers and lacquers). The isopentane insolubles or "precipitables" have been classified according to solubility, color and melting point but there appears to be no clear line of demarcation. They probably are low molecular weight polymers (less than 2000). Their solubility is low in isopentane and moderate in chloroform, ether, and benzene.[2]

Rates of Oxidation

Fenske[1] reports the rate of oxidation to double with each 10 degree rise in temperature between 140° and 180° C. He has likewise found the rate of production of volatile and fixed acids, lacquers, and precipitables to follow a simple logarithmic function. Small discrepancies with precipitables has been assigned to the "solubility" of these products in isopentane.

Three types of curves become evident when the length of heating time is graphed against the amount of oxygen absorbed. The accompanying graph illustrates this. Curve one is

characteristic of relatively pure hydrocarbon oils and indicates a uniform rate of oxidation. Curve two shows a "period of induction" where the rate of oxidation is slight. After a short time the oil usually oxidizes at a rate



equal to or greater than that of a saturated hydrocarbon. This period of induction may be ascribed to the effect of some natural or added inhibitor. Curve three is characteristic of oils heated in the presence of a metallic catalyst. In lubricating oils the metals usually catalyzing oxidation are lead, iron and copper; however, in the quenching of aluminum alloys, a trace of copper is thought to be the predominant catalyst.

Mechanism of Additive Action

Most additives used in lubricating oils contain the following essential ingredients: detergents, anti-oxidants, film strengtheners, and polar compounds designed to improve the lubrication at the surface of the metal. Additives used in quenching oils act primarily to improve oxidation stability and heat conduction.

The detergents minimize sludge formation, maintain a clean metal surface by inhibiting lacquer formation and buffer acids produced on oxidation.[3]

Most anti-oxidants contain hydroxyl or amine groups or compounds of P, S, Se, Sb, As, and Ge which unfortunately are not very stable toward oxidation. Their mechanism of oxidation has been represented by several theories. Among them is the peroxide theory which postulates the formation of a hydrocarbon peroxide with oxidation of the hydrocarbon oil. Without an inhibitor present this hydrocarbon peroxide would cause polymerization. In the presence of an inhibitor the oxygen is removed and the hydrocarbon restored.[4] One other function of the anti-oxidant lies in poisoning the metallic catalysts by complexing or precipitating to form a protective coating. Phosphites have recently been found to increase the proportion of water formed by absorbed oxygen[1], while forming phosphides with suspended metals.

Filtering

A method widely used to purify petroleum oils utilizes adsorption properties of clays. The oil is heated at 120-300° C. with the clay (0.1 to 1 lb. per gal.) in closed vessels for short periods of time (½ to 1 hour) filtered while hot.[4] The filtration-adsorption process acts to remove insoluble lacquers as well as acids and polar groups by adsorption of the hydroxyl groups on silicon atoms in the clay.[6]

Optical Evaluations

Throughout the history of petroleum analysis, color has been used in a qualitative sense in testing for purity. The older methods of visual comparison with colored disks or standards is gradually giving way to more reliable photometric

methods utilizing standard color filters[5]. Further refinements of these color tests lie in the use of prism or grating instruments capable of measuring light transmission through oils at any wave length in or near the visible region.

Experimental

Types of Oils

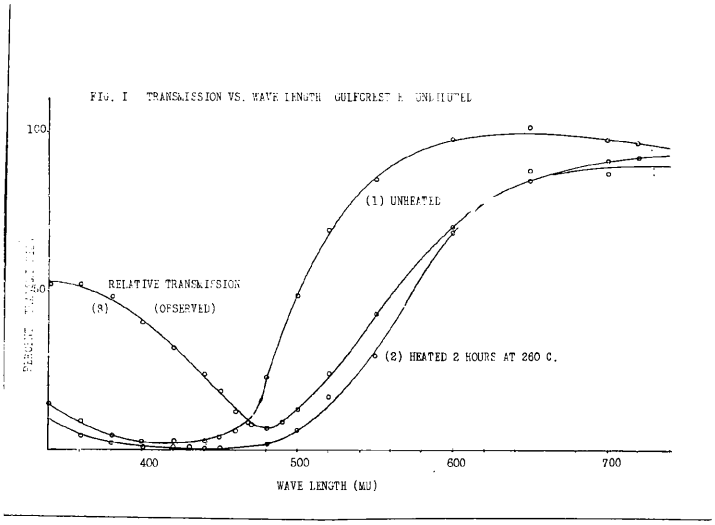
Approximately 35 different commercial quenching oils were tested spectrophotometrically for oxidation stability, but only those showing promise of good stability were investigated further. These paraffin base oils were of light color, API gravity near 30, and boiling largely between 300-400° C. Some of the quenching oil samples contained commercial polar and non-polar additives designed to increase the stability of the oil and impart desireable heat conduction properties. All of the oils contained varying amounts of aromatic compounds of a lower stability than the bulk of the saturated hydrocarbons.

Apparatus

In this work a Cenco-Sheard Spectrophotelometer was used. The sensitivity below 400mu was low with darker colored oils. In this range with dark colored oils an error of 5% in the transmission readings was possible. In the rest of the range an error of 2% limits the accuracy. The large slit width required in testing dark colored oils in the ultraviolet range lead to a spectral width of the transmission reading as much as 10 mu. The error due to overlapping orders was small but appreciable as determined by the use of filters. In order to obtain a satisfactory accuracy with dark colored oils it was necessary to dilute the samples. Petroleum ether was chosen as a cheap, easily handled solvent.

Experimental Curves and Numerical Rating of Oils

If the transmission versus wave length values for a typical quenching oil are plotted the curve (1) in fig. I



is obtained. Curve two represents the spectral curve for the same oil heated 2 hours at 260° C. If the ratio quotient of these two curves be plotted with the transmission value of the unheated oil at 100 we obtain a curve similar to function (3) on the graph. Acturally transmission values for this curve were obtained by setting the transmission of the unheated oil at full scale deflection on the spectrophotometer; then by placing the heated oil in the path of light the per cent "relative transmission" of the heated to unheated oil may be read immediately. Table I lists the calculated and observed values for these relative transmissions. The value of the relative transmission curves lies in their evaluation of the oxidation products formed in the oil. The exact nature of the oxidation

DATA

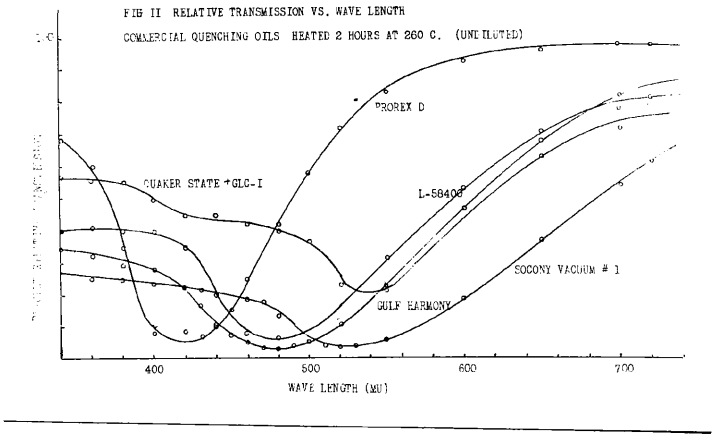
Transmission Vs. Wave Length

Table I. Gulf Crest 2 Heated at 260° C for 2 hours (undiluted)

Wave Length	T_1 Unheated	T_2 Heated	T_1/T_2 (calc.)	T_1/T_2 (obs.)
340	15	10	66	52
360	9.0	4.5	64	52
380	4.5	2.5	55	48
400	3.0	1.3	43	40
420	3.0	1.0	33	32
430	3.0	1.0	33	28
440	3.0	0.8	27	24
450	3.7	0.8	22	19
460	6.0	0.8	13	12
470				8
480	28	1.6	5.7	7
490				9
500	49	6.5	13	13
520	69	17.	25	24
600	98	69	70	70
650	102	88	86	85
700	98	87	89	91
720	97	90	93	92

products producing these curves is unknown, though thought to betied up with the formation of the polymer "precipitables".

These relative transmission curves are observed to vary widely from oil to oil in the position and character of the absorption peak (minimum transmission) as can be seen in fig. II in which several commercial quenching oils are graphically



compared. In general the more highly refined oils show absorption peaks further toward the violet than do oils containing largely aromatic compounds. This shift in absorption peaks is misleading in oils which are evaluated on the basis of visible color only. An oxidized oil of light color may actually contain more oxidation and polymer products than a dark colored oil similarly treated. The data for fig. II are listed in Table II.

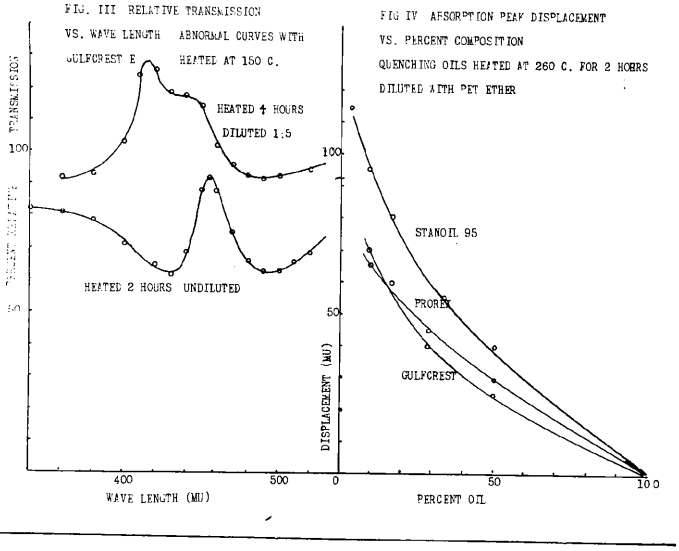
Relative Transmission vs. Wave Length

Table II. Quenching Oils Heated at 260°C. for 2 Hours (undiluted)

Wave Length	Gulf Harmony	Prorex	L-5840	Quaker State	Soc. Vac. #1
340	35	68	40	50	30
360	32	60	41	55	25
380	29	35	40	53	25
400	28	8.0	40	50	23
420	22	8.1	35	45	22
430	16	6.0	29		21
440	11	10.0	20	45	20
450	6.5	15.5	13.5		20
460	4.5	25	8.0	42	19
470	3.0				18
480	3.0	42	6.5	40	13
490	4.0				10
500	5.2	58	9.9	37	6.5
520	11	72	16.5	23	4.0
530					4.0
550	23	83	32	21	6.0
600	45	93	53	47	19
650	64	96	71	68	37
700	72	98	78	82	54
720	76	98	81	80	61

Dilution Effects

Abnormal color curves are sometimes observed when oils containing inhibitors are heated at a low temperature (150° C.) An example of this may be seen in fig. III. The oil, Gulfcrest E, used in the plotting of this graph (data tabulated in table III) was a highly refined amber colored oil containing only non-polar additives. A further study might show some interesting factors involved in these abnormal transmission curves. The shift of the peak observed between the two curves in fig. III



is not due to heating but is a dilution effect.

When working with dark colored oils or light colored oils having a large absorption in the near ultra-violet region it is necessary to dilute the samples with a neutral solvent to obtain a maximum sensitivity. A high boiling petroleum ether was chosen. Dilution with corresponding amounts of ethyl ether or chloroform resulted in curves similar to those

DATA

Table III. Abnormal Curves in the Transmission vs. Wave length

GulfCrest E Heated 150°C:

Wave Length	2 hrs. (undil)	4 hrs. (dil. 1:5)
340	82	
360	81	92
380	79	93
400	71	103
410		124
420	65	125
425		120
430	62	118
440	69	118
450	88	115
455	92	
460	88	102
470	75	96
480	66	93
490	63	92
500	63	93
510	66	
520	69	95
540	78	98

diluted with petroleum ether with only a slight difference noted in the higher relative transmission values of the oils diluted in chloroform. This change of the transmission values is believed to be associated with the solubility of the "insolubles" in chloroform over than in the isopentane of the petroleum ether. The use of a low boiling petroleum ether (isopentane) is not practical since it rapidly precipitates the polymers from the more highly oxidized oils. Dilutions were accomplished with the aid of pipettes.

The most obvious result of dilution is the large shift in the absorption peak. This amounts to as much as 110 mu in oils dilutedto 5% with petroleum ether. All oils investigated exhibited approximately the same displacement of the absorption peak with dilution. Fig. IV and Table IV illustrate this effect. The prorex oil is a highly purified almost colorless oil containing no additives whereas the Stanoil 95 is an average good quality oil containing no additives. From this it will be noted that the shift in absorption is not dependent on purity.

It is obvious that Beer's law will not be rigorously followed by a solution showing such a large shift of the absorption peak as is exhibited with heated quenching oils. The curves shown in the three graphs labeled fig. V and Tables V show that there is a uniform change upon dilution in the general nature of the curves. The region of the curve on the ultra-

DATA

Table IV. Percent Composition vs. Absorption Peak Displacement. Heated at 260°C. for 2 hours. Diluted with Pet. Ether.

% Oil	GulfCrest E		Stanoil 95		Prorex	
100	480	0	510	0	43	0
50	455	25	470	40	400	30
33.3			455	55		
28.6	440	40			385	45
16.7	420	60	430	80	370	60
9.1	410	70	415	95	365	65
4.1			400	110		

DATA

Table V. Transmission vs. Wave Length for Diluted Quenching Oils-GulfCrest 4 heated at 260°C. for 2 Hours.

	Undil.	1:1	2:5	1:5	1:10
360mu	52	68	73	81	83
380	48	63	68	74	80
400	40	55	58	53	51
410			44		
420	32	40	29	28	44
430		29	21	29	45
440	24	22	20.5	34	57
460	12	17	29	47	69
470	7	19			
480	7	22	40	68	77
490	9				
500	13	36	55	73	83
520	24				
550	43	68	81	89	92

DATA

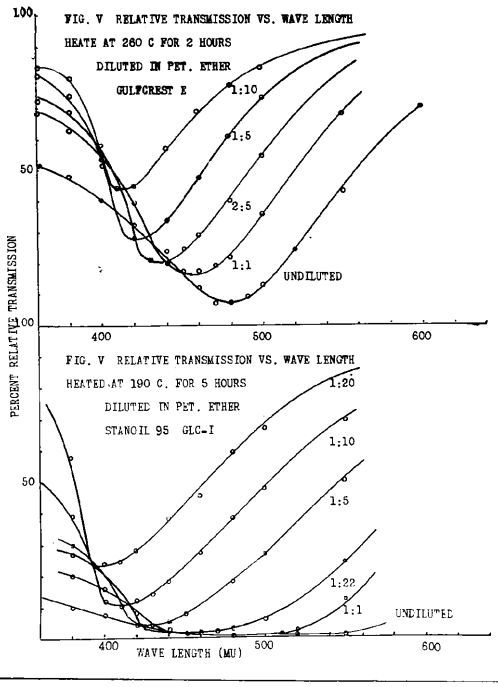
Table V. Stanoil 95 plus Lard Oil plus Additive 1, Heated at 190°C. for 5 hours.

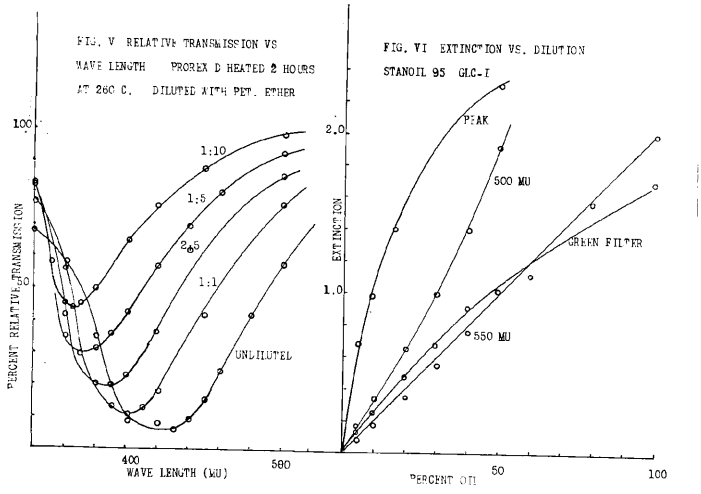
	Undil.	1:1	2:5	1:5	1:10	1:20
380	10	20	20	30	49	60
390						21
400	8	16	16	20	1	18
410		12		10	10.8	20
420	5	8	4.9	4.2	12	23
430			4.0	14		
440	3	2	1.2	5.8	17	3
450			0.9	7.0		
460	1	0.9				
470		0.5	1.0		27	44
480	.4	0.7	2.0	17.0	40	54
500	0.1	1.2	5.0	27	48	64
520	0.0	3.8	10			
530	0.1					
550	1	11	21	51	69	78

DATA

Table V. Transmission vs. Wave Length for Diluted Quenching Oils. Prorex D. Heated at 260°C. for 2 Hours.

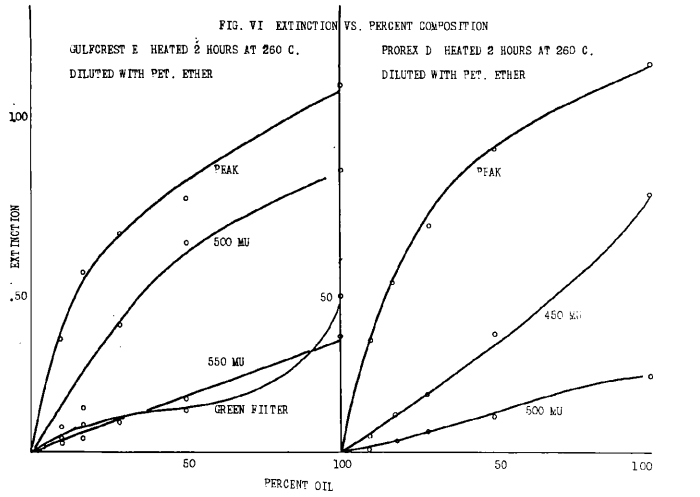
	Undil.	1:1	2:5	1:5	1:10
340	68	77	82		83
360	60	47	42	35	45
370		32		29	48
380	35	20	20	31	50
390		13	19	36	
400	8.0	11	23	42	65
410		13			
420	8.1	18	36	57	76
430	6.0				
440	10	42	62	69	
460	25			81	88
480	42		88		
500	58	77	86	92	99
550	83	92	96		100
600	93				
650	96				
700	98				





violet side of the peak exhibits a steeper slope than the curve on the red side. These properties must be considered before investigating Beer's law.

To study the extent to which Beer's law is followed, the percent composition (by volume) is plotted against the extinction (log 1/T) at the peak absorption and at a constant wave length (500 and 550 mu). The graphs in fig. VI from table VI



shows a curved line for extinctions at peak absorption in the case of the three oils plotted. At 550 mu the curve, though of lower slope, approaches a straight line. When a photelometer with a green filter (Cenco) is used (see fig. XI) curve is a modification of those at 500 and 550 mu for any given oil. From these data it is apparent that Beer's law may be used to correct for dilution only to a rough approximation when the wave length is given.

Laboratory Method of Oxidizing Quenching Oils

It is possible to study the relative rates of oxidation of oils by heating a series of oil samples under known conditions of time and temperature and comparing the relative transmission values. In this study the samples were heated in

Table VI. Quenching Oils Heated at 190°C. for 5 Hours. Diluted with Petroleum Ether (High Boiling)

Stanoil 95 Plus Lard Oil Plus GLC-1

Dilution	% Conc.	Transmission	Extinction	at abs. peak
	100	0		510
1:1	50	0.5	2.30	470
1:2	33.3	0.9	2.045	455
1:5	14.7	4.0	1.398	430
1:10	9.1	10.5	0.980	415
1:20	4.7	23.0	0.638	400

Table VI. Stanoil 95 Plus Lard Oil Plus GLC-I. Transmission and Extinction at 550 mu.

Dilution	% Conc.	Transmission	Extinction
	100	1.0	2.00
1:1	50	11.0	0.958
1:2	33.3	22	0.658
1:5	16.7	50	0.303
1:10	9.1	69	0.161
1:20	4.7	80	0.096

"VI"

Table VI. [illegible] with Petroleum Ether (Fifth Solution)

GulfCrest

Dilution	% Conc.	Transmission	Extinction	at [illegible]
	100	7.0	1.155	480
1:1	50	16.0	0.796	455
2:5	28.6	29.5	0.[illegible]68	440
1:5	16.7	28.0	0.554	420
1:10	9.1	44.5	0.352	410

Table VI. GulfCrest E Transmission and Extinction at 450 mu.

Dilution	% Conc.	Transmission	Extinction
	100	43	0.367
1:1	50	68	0.168
2:5	28.6	81 (ext.)	0.092
1:5	16.7	91 (ext.)	0.041
1:10	9.1	93 (ext.)	0.029

Table VI. GulfCrest E Transmission and Extinction at 500 mu

Dilution	% Conc.	Transmission	Extinction
	100	13	0.886
1:1	50	22	0.658
2:5	28.6	40	0.398
1:5	16.7	73	0.136
1:10	9.1	83	0.079

DATA

Table VI. Quenching Oils Heated at 260°C. for 2 Hours. Diluted with Petroleum Ether (High Boiling)

Prorex D

Dilution	% Conc.	Transmission	Extinction	Abs. Peak
	100	6.0	1.22	430 mu
1:1	50	11.0	0.958	400
2:5	28.6	19.5	0.710	390
1:5	16.7	29	0.538	370
1:10	9.1	44	0.358	365

Table VI. Prorex D Transmission and Extinction at 450 mu.

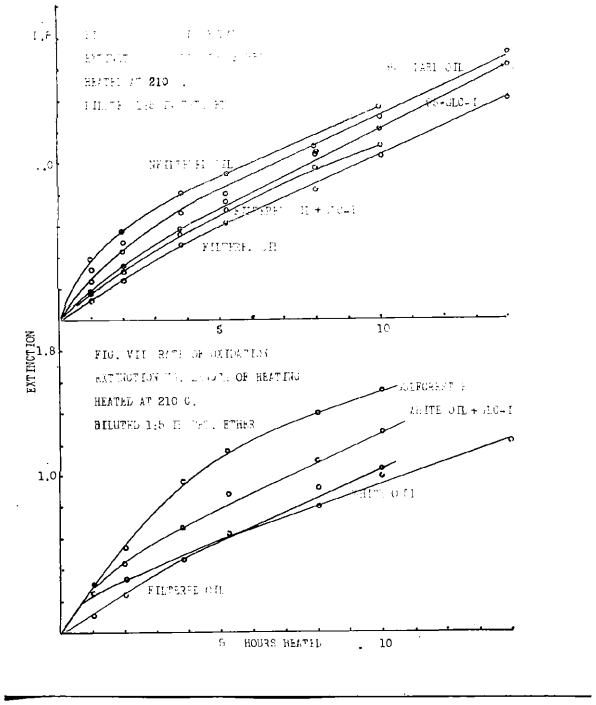
Dilution	% Conc.	Transmission	Extinction
	100	15.5	0.810
1:1	50	42	0.37
2:5	28.6	65	0.187
1:5	16.7	76	0.120
1:10	9.1	88	0.056

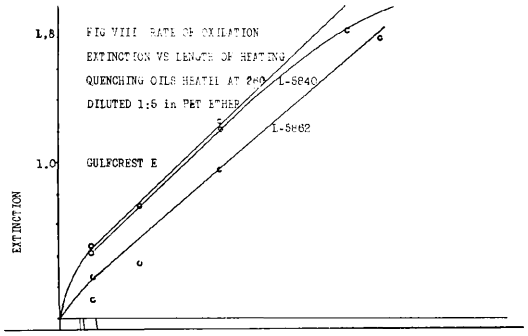
Table VI. Prorex D Transmission and Extinction at 500 mu.

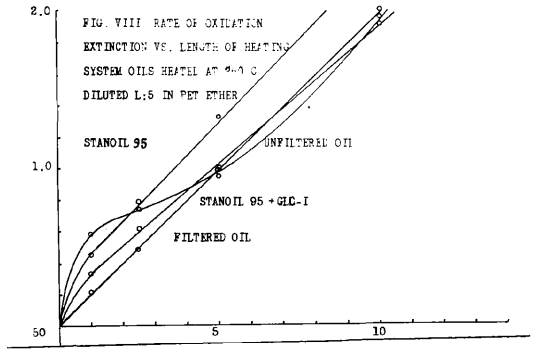
Dilution	% Conc.	Transmission	Extinction
	100	58	0.238
1:1	50	77	0.113
2:5	28.6	86	0.065
1:5	16.7	92	0.036
1:10	9.1	98	0.008

test tubes immersed in an oil bath whose temperature was maintained within 5 degrees of the desired temperature. Only samples from the same series have been compared with each other as this temperature control is not sufficiently accurate to correlate samples from different series without the aid of a common sample. The rates of oxidation as shown by this method are not maximum rates of oxidation because of the mechanical hindrance of the test tubes in permitting the maximum rate of oxygen absorption.

The graphs in figs. VII and VIII show the effect of heating various commercial quenching oils at 210° and 260°C.







The data for figs. VII and VIII are listed in tables VII and VIII. For the figures extinctions are plotted against time of heating; all oils being diluted 1:5 with high boiling petroleum ether. The slope of such a curve is a measure of the rate of oxidation. In general, the better quenching oils show a period of rapid oxidation followed by a uniform decomposition. Stanoil 95 is an example of such an oil.

The addition of an anti-oxidant retards the initial rate of oxidation, but it soon approaches the same rate as the untreated oil. Heating in the presence of a metal catalyst (aluminum turnings) further accelerates initial oxidation in most circumstances. If the oil is drastically purified and its rate of oxidation plotted, from the beginning a uniform rate of oxidation is observed. The conclusions to be drawn from these curves are that oils containing aromatic components experience a rapid initial oxidation, while anti-oxidants inhibit oxidation and catalysts accelerate oxidation. As soom as the less stable components are removed the remainder of the oil (presumably of stable napthenic or paraffinic nature) oxidizes at a uniform rate. Hence, insofar as oxidation stability of quenching oils at a high temperature is concerned, the initial composition of the oil is the determining factor.

Fenske[1] reports the rate of oxidation of lubricating oils to double with each 10 degree rise in temperature between 140° and 180° C. While keeping in mind that maximum rate of absorption of oxygen was not attained in the samples subjected

Data

Quenching Oils Heated at 210 5°C. Diluted 1:5 (16.7%) with Petroleum Ether (High Boiling)

Table VII. Percent Relative Transmission and Extinctions at the Absorption Peak

Sample	1 hr.	2 hr.	3 5/6	5 1/4	8	10	14
Stanoil 95	55 0.260 (420)	38 0.420 (420)	23 0.638 (420)	14 0.854 (420)	9.0 1.04 (430)	6.0 1.22 (430)	
Stanoil 95 Lard Oil	55 0.260 (420)	36 0.440 (420)	23 0.638 (420)	16 0.796 (420)	9.0 1.04 (430)	5.3 1.28 (430)	2.0 1.70 (435)
Stanoil 95 Lard Oil GLC-1	67 0.172 (420)	45 0.346 (420)	22 0.658 (420)	17 0.770 (420)	9.0 1.04 (430)	5.1 1.29 (430)	2.8 1.55 (440)
Stanoil 95 Lard Oil Al turnings	48 0.318 (420)	33 0.481 (420)	16 0.796 (425)	12 0.920 (420)	9.0 1.04 (430)	5.3 1.28 (430)	
System Oil 2/11 unfiltered	40 0.398 (480)	28 0.554 (490)	15 0.824 (490)	12 0.920 (485)	8.3 1.08 (480)	4.5 1.35 (500)	
System Oil 2/11 filtered	79 0.103 (415)	56 0.253 (410)	34 0.468 (415)	25 0.610 (415)	15.7 0.804 (420)	9.1 1.04 (420)	40 1.40 (430)
System Oil 2/11 filtered 0.3% GLC-1	76 0.120 (420)	49 0.310 (410)	28 0.553 (415)	20 0.698 (420)	10.8 0.966 (420)	8.0 1.10 (420)	
White Oil (OHI)	55 0.260 (345)	46 0.336 (355)	33 0.471 (360)	24 0.619 (350)	12 0.922 (370)	10.2 0.991 (370)	7.0 1.22 (380)
White Oil GLC-1	51 0.292 (360)	36 0.444 (360)	17 0.769 (370)	13 0.881 (375)	8.2 1.09 (380)	5.4 1.27 (390)	
GulfCrest E.	50 0.301 (420)	30 0.522 (430)	11 0.960 (430)	7.0 1.15 (430)	4.0 1.40 (440)	2.9 1.54 (450)	3.5 1.46 (440)

DATA

Quenching Oils Heated at 200 5°C. Diluted 1:5 (16.7%) with Petroleum Ether (High Boiling)

Table VIII. Percent Relative Transmission at Absorption Peak.

Sample	1 hr.	2 1/2 hr.	5 hr.	10 hr.
Stanoil 95 Lard Oil	33 (420)	18 (420)	4.7 (430)	0.7 (450)
Stanoil 95 Lard Oil GLC-1	46 (420)	24 (420)	10.5 (435)	1.2 (445)
System Oil 2/11 Unfiltered	20 (480)	10 (490)	10.5 (485)	1.1 (505)
System Oil 2/11 Filtered	01 (420)	33 (410)	11.3 (420)	1.0 (440)
L-5840	37 (420)	19 (420)	6.2 (430)	1.5 (445)
L-5862	53 (420)	46 (430)	11.5 (420)	1.6 (440)

Table VIII. Extinctions at Absorption Peak

Sample	1 hr.	2 1/2 hr.	5 hr.	10 hr.
Stanoil 95 Lard Oil GLC-1	0.338	0.619	0.980	1.92
Stanoil 95 Lard Oil	0.482	0.744	1.30	2.15
System Oil 2/11 unfiltered	0.585	0.766	0.980	1.96
System Oil 2/11 filtered	0.214	0.482	0.547	2.10
L-5840	0.431	0.721	1.21	1.82
L-5862	0.276	0.338	0.940	1.80
GulfCrest E	0.468	0.721	1.26	2.22

to colorimetric tests, it appears that this rate of oxidation with rise in temperature is not as large in the range 200-260°C. except during the short initial oxidation. In these tests the rate of oxidation has doubled in the 50 degree rise between 210° and 260° C.

Study of Additive Action

By the use of the spectrophotelometer it is possible to study the anti-oxidant properties of additives. In general additives containing anti-oxidants inhibit the oxidation of the less stable components of the oil. When the anti-oxidant is added to a highly purified oil containing no catalysts it is observed that the oxidation of the oil is accelerated. This effect may be ascribed to the oxidation of the anti-oxidant itself. In table IX are compiled the relative transmission values at peak absorption for Stanoil 95 with the additive and its components and for the Stanoil 95 drastically purified (filtered system oil) by long oxidation and filtration with clays. In both oils the methyl dichloro stearate (MDS) has little effect on the oxidation of the oil. The detergent Mon. 303 and Thialkene show the largest inhibitor action on thenew Stanoil 95 while producing but slight effect on the filtered oil. It will be noted that the over-all additive action most closely approximates that of the detergent Mon. 303 alone.

Table X demonstrates the effect of heating the quenching oil with a metal. The aluminum used in this series was in the form of turnings obtained from an aluminum alloy casting. Two

DATA

Study of Additive Action

Table IX. Relative Transmission Values at Peak Absorption

	Undiluted	Heated at 200°C.
	1 1/2 Hr.	3 1/2 Hr.
System Oil filtered	32 (445)	7 (445)
S. O. Filtered GLC-I 0.3%	27	8.5
S. O. Filtered MDS 0.06%	31	10
S. O. Filtered Lon 303 0.12%	27	8.0
S. O. Filtered Thialkene 0.12%	34	11
Stanoil 95	15 (165)	3.9 (435)
Stanoil 95 GLC-1 0.3%	24	7.7
Stanoil 95 MDS 0.06%	15	4.2
Stanoil 95 Lon 303 0.12%	22	7.3
Stanoil 95 Thialkene 0.12%	21	8.0

Table X. Transmission Values at Peak Absorption

Heated 3 Hours at 210°C.

Sample	Pet. Ether
Stanoil 95 Lard Oil	28 (420mu)
Stanoil 95 Lard Oil Al	31.5
Stanoil 95 Lard Oil GLC-1	43
Stanoil 95 Lard Oil GLC-1 Al	39
Stanoil 95 Lard Oil GLC-II	34
Stanoil 95 Lard Oil GLC-II Al	42

types of additives have been introduced into samples of the oil: GLC-1, the same as discussed above and GLC-II containing a phosphite. In all cases the additive has a beneficial effect in inhibiting oxidation. The effect of the aluminum turnings is relatively slight. The increased stability produced by heating the plain Stanoil 95 and Lard oil with aluminum may be attributed to the formation of an aluminum soap with the acids produced by oxidation. The additive GLC-1 seems to react with the metal in such a way asto limit its value in inhibiting oxidation, while the second additive, GLC-II is favored by the presence of the aluminum.

Changes in Oil in the Quenching Tank

A series of quenching oil samples from the quenching tanks at the Delco Remy Bedford Aluminum Foundry were obtained. The base of this quenching oil is Stanoil 95 to which had been added 0.85% Lard oil for wetting purposes. Subsequent heating tests indicate little decomposition of the Lard oil over that of the quenching oil when heated at 260° C. To the Stanoil 95 and lard oil was added 0.3% of the additive GLC-1. If relative transmission curves are determined for the unheated Stanoil 95 with Lard oil and GLC-1 with respect to the oil without the additive a slight absorption of light will be observed (table XI, fig. IX). With the freshly added (new) additive absorption of light increases, but after remaining in the oil for several months, the oil actually becomes lighter

Table XI. Relative Transmission Values vs. Wave Length

Wave Length	Stanoil 95 GLC-1 new undiluted	Stanoil 95 GLC-1 old dil. 1:5	Stanoil 95 GLC-II dil. 1:5	Stanoil 95 2/11 filtered dil. 1:5
350	92	100	100	100
380	92	100	100	105
390			110	117
400	91	100	125	126
410			131	122
420	90	103.5	120	115
430		104	118	106
440	88	103	113	106
460	87	102	106	
480	90	102	104	101
500	19	102	102	
550	94		99	100
600	96		98	
	with ref. to Stanoil 95 unheated		heated 4 hrs. 115°C. relative to filtered oil unheated.	

in color. The effect of decreased light absorption is even more marked in the case of the additive GLC-II freshly added. In this instance the absorption peak occurs near the absorption peak of the heated oils.

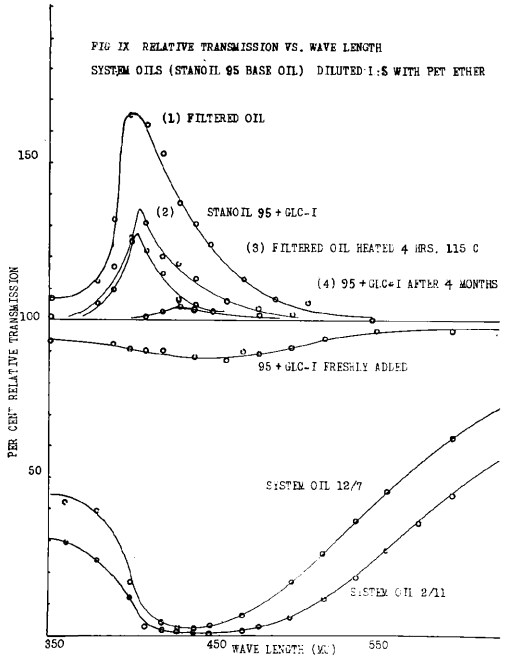


Table XII lists the transmission values for samples of quenching oils taken from the same quenching tank at different dates. These samples have not been heated subsequent to removal from the quenching tanks and are relative to the Stanoil 95 with lard oil and GLC-I (all diluted 1:5 with petroleum ether). The transmission values show increasing oxidation over a period of four months when the oil was filtered with a clay adsorbent. The filtered oil has a peak transmission 170% greater than the original oil at approximately the same wave length of the absorption peaks.

DATA

Relative Transmission Values of Untreated Quenching Oils

Table XII. Transmission Values of System Oils Relative to Stanoil 95 0.85% Lard Oil 0.3% GLC-1 Diluted 1:5 with Petroleum Ether

Wave Length	12/7	12/13	1/12	2/11 unfil.	2/11 fil.
340	43	40	32	30	112
360	42	37	30	29	115
380	39	32	25	24	117
390					137
400	17	16	12	12	170
410			5	2.2	167
420	3.7	3.1	2.6	1.7	158
430	2.6	2.0	1.8	1.2	142
440	2.3	1.8	1.2	1.0	135
450	2.9	2.0	1.1	1.0	129
460	4.0	2.3	1.3	1.2	
470	6.0	3.4	2.0	1.8	117
480	8.7	5.0	3.0	2.5	
500	17	11	7.0	5.2	111
520	26	19	13	11	
540	36	29	21	18	104
560	46	39	31	27	
600	63	56	47	44	100
650	75	72	62	61	102
700	86	82	79	76	

If these system oils (from the quenching tanks) are heated and the relative transmission curves of the laboratory heated to unheated oils are determined, some information may be had as to the stability of the oil at any time during use in the tank. These values(for peak relative transmission) are given in table XIII. It might be expected that the stability of the oils remains constant after the initial heating period (in the quenching tank) but consideration must also be given to the part that new additions of oil, additive and dissolved aluminum play as the oil is used over a period of time. The filtered oil is observed to be far superior in stability than even the new oil. There is a good correlation between these relative transmission values and the strain induced in the aluminum alloy castings quenched in the respective oils. The strain values in table XIII are the amount of bow in inches in the casting during stress relief when the casting is sawed nearly through with a series of parallel sawcuts by a standard procedure for the foundry.

Experience in motor performance has shown that a bow less than 0.050 in. has never resulted in failure, but that it is essential to maintain a value less than this maximum. The relation between relative transmission and bow is not linear in this instance, but this could hardly be expected with an oil which is continually being renewed with fresh oil, two additions of two additive blends, and other variables operating. However, in quenching in this 5000 gallon tank and in 150 gallon tanks in which single casting were

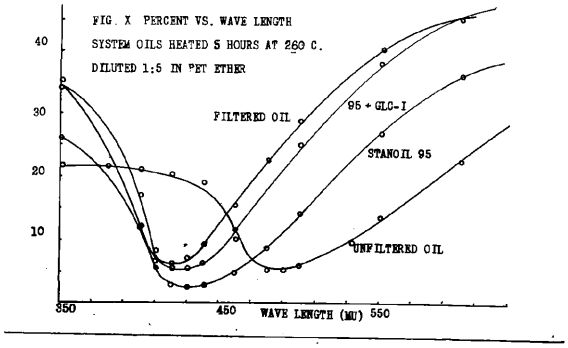
D.T.D.

Stability of System Oils

Table XIII. Relative Transmission at Maximum Absorption Heated at 200°C. Diluted 1:5 with Petroleum Ether

Sample	Average Strain in castings in inches of flow on stress relief	Heated 1 hr.	2 hr.
Stanoil 95	0.055	48 (420)	35 (420)
Lard Oil G.O-1	.095		
12/7	.095	34 (465)	12 (480)
12/18	.065	42 (470)	19 (475)
1/12	.045	66 (480)	37 (480)
2/11	.052	54 (475)	29 (485)
Unfiltered			
2/11	.030	85 (410)	62 (410)
Filtered			
9/11 (6 months use of oil without further filtering	.045	70 (410)	58 (410)

submerged, the lower the relative transmission index number, the higher the residual strain in the castings. It is to be noted that the variations in strain follow the index numbers in table VI (relative changes of the oil at any given stage on further oxidation) and not those of table V (rationof the transmission of the oil at any stage in the tank to that of the original unused oil. A more thorough investigation of temperature and length of the heating might bring the correlation still closer. A further effect may be seen in table XI tabulating transmission values for filtered Stanoil 95 heated for 4 hours at 115° C. Some inhibitor appears to be in this oil, perhaps a stable product from the original additive or from the clay adsorbent. The nature of the transmission versus wave length curves for a few of the system oils is given in table XIV, and fig. X. It is interesting to note the correlation between the absorption curves for samples heated in the laboratory alone and the oils from the quenching tanks (unfiltered system oils).



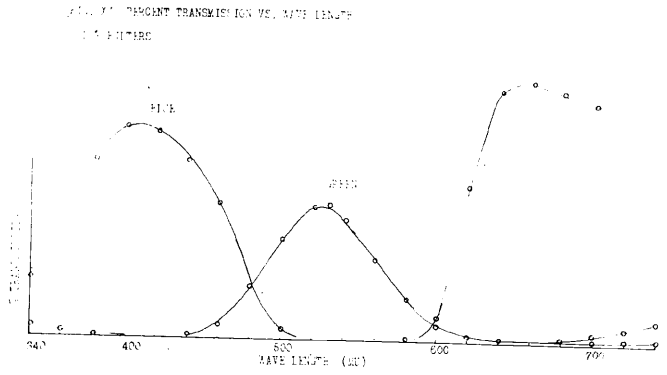
For routine laboratory tests designed to evaluate the stability of oils, a filter photelometer may be used to

Data

Table XIV. Relative Transmission vs. Wave Length. Oyster Oil (Stanoil 95 base) Heated 5 Hours at 260° C. Diluted 1:5 with Petroleum Ether

Wave Length	Stanoil 95	Stanoil 95 Lard oil GLC-I	Oyster oil unfiltered	Oyster oil filtered
350	58	68	43	70
380			42	58
400	24	34	42	24
410	11	16		13
420	5.6	10.5	40	11.3
430	4.7	10.5		14
440	5.2	13	38	18
460	6.8	23	20	31
470			14	45
480	17		10.5	
490			10.5	
500	28	50	12	58
550	54	76	27	80
600	82		45	90

advantage because of the availability of the smaller instrument and the rapidity with which the tests may be made. Care, however, must be taken in evaluating oils of an unknown nature because of the wide variation in wave length at the absorpiton peaks. A filter should be chosen having a maximum transmission in the range of minimum transmission of the oil. Consideration should be taken of the infra-red transmission of the filter since the oils themselves are quite transparent in the near infra-red range. Several commercial filters have been found unsatisfactory in this respect. Typical filter transmission curves are shown in fig. XI, table XV.



Theory of Optical Evaluation of Oil Deterioration

The above data suggest a theory upon which the observed phenomenon may be explained. Two basic readings may be observed; the natural and relative transmissions which mean natural color and color induced in the oils upon heating.

DATA

Table XV Transmission vs. Wave Length of Gene Filters

Wave Length	Blue	Green	Red
300	13	20	18
340	18	4	4
360	41	2	2
380	55	1	2
400	65	1	< 1
420	63	1	< 1
440	55	1	
460	32	4	< 1
480	10	15	< 1
500	3	31	< 1
520	< 1	41	
530		42	
540	< 1	37	< 1
560		25	
580	< 1	13	< 1
600		5	1
610			8
620	< 1	2	48
640		1	78
660	< 1	1	81
680		1	78
700	3	1	75
740	6	1	71
800	28	2	42

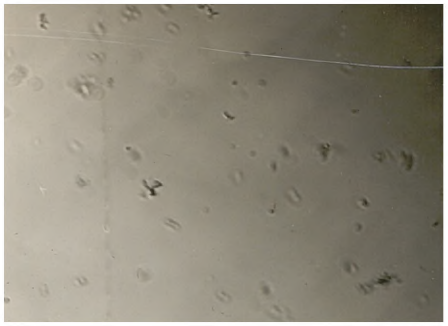
The natural transmission curves are broad and affected to a lesser extent by heating and diluting than the relative transmission curves. The natural transmission curves are the result of colored materials originally present in the oil in addition to any products of oxidation, while the relative transmission curves are characteristic of the heated products of the oil alone. There appear to be three fundamental processes at work in the oil to produce the relative transmission values. These are: absorption, fluorescence and scattering. To what extent each of these processes enter has not been determined though scattering is believed to play a large part.

The large shift in the absorption peak on dilution does not seem adequately explained on the basis of a purely absorption phenomenon postulating the formation of some complex between the oil and the solvent. If this were the case, various solvents would be expected to react differently in displacing the peak and absorbing light. The slight differences in peak displacement noted between petroleum ether and chloroform seem very small in comparison with the over-all displacement.

Fluorescence of petroleum oils is a well known fact. Nearly all the oils investigated have exhibited some fluorescence. With some, the fluorescent material seems to be produced upon heating. The oils usually fluoresece to produce a greenish blue color. This is quite noticeable if the oil sample in the spectrophotelometer is observed at right angles to the incident light. The shift of the absorption peak on dilution

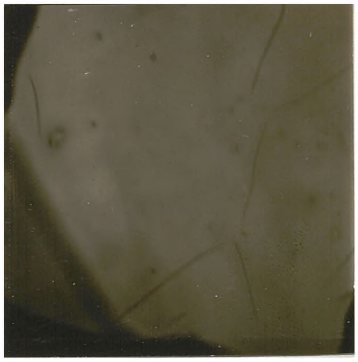
might be partially explained in the basis of fluorescence but such an explanation suffers the same disadvantages as the absorption theory. An undiluted sample produces an absorption peak in the blue range because of absorption of blue and violet light to produce a fluorescent green light. If fluorescence were the cause of the light absorption, then the transmission curves would be expected to show a steeper slope on the long wave length side of the absorption peak instead of on the short wave length side. There are two main reasons for this, one that the light absorbed in producing fluorescence must be of a shorter wave length than the fluorescent light (apparently blue green) and the other the effect of natural absorption of the oil on the fluorescent light. Furthermore, all the oils seem to show nearly the same displacement of the peak on dilution in spite of the wide variance of natural fluorescence.

The remaining explanation lies in scattering of the light. The presence of finely divided particles suspended in oxidized oils has been known for some time. The "precipitables" are probably a class of these particles. The word "class" is used since the precipitables can be only the larger of the particles. The accompanying photographs illustrate the type of particles to be found in the oil. Photograph I was taken of a undiluted heated oil sample at 600 magnification with a Zeiss 0.65 N.A. objective lense in a Zeiss Ultraphot. The particles appear spherical with a tendency to coalesce. Measurement of the size



Photograph I

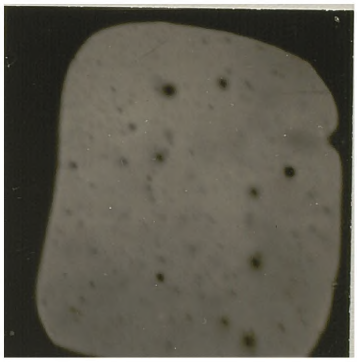
Zeiss Ultraphot 0.65 N. A. objective 600x Heated Quenching Oil



Photograph II

Electron Micrograph 1000x

Unheated filtered system oil

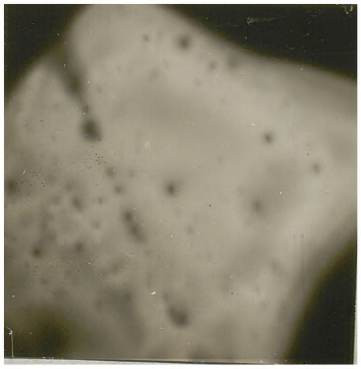


Photograph III

Electron Micrograph 1000x

Filtered system oil heated

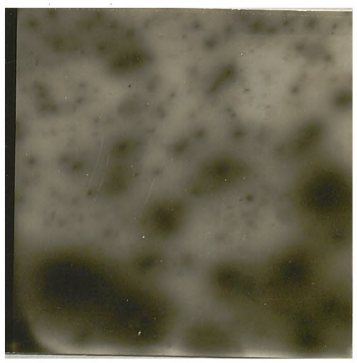
14 hours at 210° C.



Photograph IV

Electron micrograph 1000x

White oil heated 14 hrs. 210°C.



Photograph V

Electron micrograph 2000x

Stanoil 95, Lard oil, GLC-1

Heated 14 hours at 210°C.

of these particles leads to approximately 0.5u. Photographs II-V are electron micrographs at 1000 to 2000 diameters. The specimens were diluted approximately 1 to 20 with benzene; a drop of this solution applied to a collodion film backed with a 200 mesh copper screen. The excess oil was removed and the sample placed in the upper portion of the sample holder in order to secure a low magnification. Photograph II at 1000 x showing relatively few particles was taken of unheated filtered system oil. The dark lines visible are creases in the collodion film. Part of the picture is framed by the copper screen. After heating this filtered system oil for 14 hours at 210°C. a large number of round particles are framed as can be seen in photograph III. Photograph IV of white oil heated 15 hours at 210 indicates the formation of a similar product from a pure paraffin or stable naphthene. Photograph V is of Stanoil 95 with Lard oil and additive GLC-I heated 14 hours at 210°C. A larger distribution of particle sizes may be noted. This photograph is characteristic of the average quenching oil. It is interesting that any particles appear since they might be expected to dissolve in the benzene if they are the "precipitables".

If these particles have a diameter near or smaller than the wave length of light they will scatter the light. Consequently, an oil producing an absorption peak in the violet should be expected to contain particles of smaller size than an oil with an absorption peak in the blue. This is observed in the case of white oil versus Stanoil 95. The electron

microscope pictures do not show this so readily as an optical microscope because of the small field of view. The particles in the heated white oil are barely visible with an oil immersion lens while the particles in the heated Stanoil 95 are quite visible.

The shift of the absorption peak with dilution may be explained on the basis of scattering if the assumption is made that with increasing dilution the size of the particles become smaller.

If these relative transmission curves are actually a measurement of the amount of particles in the oil, the results may indicate the mechanism by which the conduction properties of a quenching oil change on use. The presence or growth of large quantities of particles may have a large influence on the heat conduction from a hot casting. This is indicated by the fact that when particles are completely removed by filtration as proved by electron micrographs, the residual strain in castings quenched in this oil as measured by the bow when the castings are sawed nearly through vertically is decidedly lower than that found in castings quenched in the same oil before filtration. Furthermore after this filtration following months of deterioration of the oil, remarkable stability is maintained, since in six months of continuous use the average strain in castings has increased only from 0.030 to 0.045 inches.

Summary

1. Spectrophotometric curves are found to be a characteristic and integrating measure of quenching oil stability and performance as determined by residual strains in quenched aluminum alloy castings; single numerical values of ratios of transmission of deteriorated to original oils enable pre-rating of oils before introduction into tanks.

2. Effects of dilution, additives, catalytic effects of metal surfaces, sludge formation and filtration and adsorption are indicated.

3. The most stable and effective quenching oil judged spectrophotometrically and practically in terms of casting strain is one which has been subjected to oxidizing conditions and quenching use in the presence of additives, and then filtered through activated clay. Subsequent oxidation of the oil is then uniformly linear with time. In these oils additives have comparatively little effect.

4. Electron micrographs prove the formation of insoluble sludge particles from oxidation of unstable aromatic and naphthenic fractions of oil. These are almost completely absent only in the filtered used oil. These particles may have the largest single effect on thermal conductivity in the quenching of castings.

BIBLIOGRAPHY

(1) Fenske, M. R., Stevenson, C.E., Rusk, R. A., Lawson, N. D., Cannon, M. R., and Kock, E. F., Ind. and Eng. Chem., Anal. Ed., 13, 51 (1941)

(2) Ludeman, C. G., Ind. and Eng. Chem., Anal. Ed., 12, 520, (1940)

(3) Waters, G. W., and Burnham, H. D., Ind. and Eng. Chem. Ind. Ed., 36, 263 (1944)

(4) Gruse, W. A., and Stevens, D. R., The Chemical Technology of Petroleum, McGraw-Hill, 1942, p. 133

(5) Diller, I. N., Gray, R. J., and Wilson, J. W., Ind. and Eng. Chem., Anal. Ed., 14, 607 (1942)

(6) Kalichevsky, Stagner, Chemical Refining of Petroleum Oils, ACS Monograph 63 2nd. Ed. Reinhold Pub. Co. 1942

II

X-Ray Studies

of

2, 4 Dinitrophenylhydrazine

Derivatives

Introduction

This section is concerned with the structure of a series of aldehyde 2, 4 dinitrophenylhydrazones and the analysis of aldehydes as follows from the techniques used in these structural identifications. In particular the following items are treated.

1. A method of approach to the study of the structure of complex organic compounds.

2. Presentation of fundamental data concerning the unit cell and space group for a number of aldehyde 2, 4 dinitrophenylhydrazones, with some indication as to the probable orientation of the molecule in the unit cell.

3. Further information concerning the nature of the different crystalline modifications of certain of the aldehyde 2, 4 dinitrophenylhydrazones.

4. The application of the x-ray powder method to the qualitative analysis of classes of organic compounds; in particular aldehydes from the powder patterns of the 2, 4 dinitrophenylhydrazine derivatives.

5. Data necessary for the qualitative identification of some aldehydes.

6. Development of techniques for the quantitative analysis of pure and mixed aldehydes.

7. Data necessary for the quantitative analysis of the aldehyde 2, 4 dinitrophenylhydrazones.

History

In the past few years a considerable amount of research has been undertaken to work out systematic and practical methods of organic analysis for carbonyl compounds using a solution of 2, 4 dinitrophenylhydrazine. The use of this reagent in the classification and identification of aldehydes and ketones was first pesented as long ago as 1894 (1,2). More recently (1930) Allen (3) brought this method into prominance for the classification of aliphatic as well as aromatic compounds.

The reagent is usually prepared by dissolving 2, 4 dinitrophenylhydrazine in ethyl alcohol acidified with either hydrochloric or sulfuric acids. The addition of an aldehyde or ketone to such a solution usually results in the rapid formation of crystals of the 2, 4 dintirophenylhydrazone. If the aldehyde or ketone initially does not contain any great amount of impurities and if the derivative is carefully purified by recrystallization, the aldehyde or ketone can be classified from the color, optical properties and melting point of the derivative.

When the unknown substance contains a mixture of aldehydes or ketones the problem of identification becomes difficult since the melting point, which is the most widely used test, is so easily lowered by the presence of impurities. Recourse is then usually taken to separation of the aldehyde or ketone by fractional distillation or crystallization before identification with the 2, 4 dinitrophenylhydrazine reagent. Such a procedure is time consuming and any improvement may beconsidered valuable.

Two instrumental methods have been used for the identification of the derivatives of aldehydes and ketones which are affected to a lesser extent by the presence of impurities than is the melting point. These are dependent upon optical crystallographic properties of the derivative (4, 5, 6, 7) and the x-ray powder patterns (8).

Bryant (4, 5) has given a probable crystal system for the 2, 4 dinitrophenylhydrazine derivatives of formaldehyde and acetaldehyde as monoclinic while the n-butyraldehyde derivative was reported as orthorhombic.

In a series of articles concerned with the study of protein hydrolysates (8) the x-ray powder method was used to distinguish between 2, 4 dinitrophenylhydrazine derivatives of acetaldehyde, propionaldehyde, and acetone. The x-ray powder photographs were recorded on flat cassets placed 3 cm. from the sample, two patterns of samples to be compared being recorded on two sides of the same film.

The major field of contention in the use of 2, 4 dinitrophenylhydrazine as a reagent for the identification of aldehydes and ketones lies in the rather large number of modifications which have been reported from time to time. The exact nature of these modifications has caused much speculation. Two modifications of acetaldehyde have been clearly shown to exist (4-8) as well as two modifications of derivatives of the furan series (9). Still other modifications of these and other compounds seem likely in view of the varied reports of crystalline properties and melting points.

Bredereck (9) considered the possibility of cis-trans isomers and desmatropy as explanations for the two markedly different forms of furfuraldehyde 2, 4 dinitrophenylhydrazone. These two forms were red and yellow respectively in color; the first being prepared by recrystallization from hot pyridine while the yellow form was prepared by crystallization from alcohol and acetone.

In the case of the acetaldehyde 2, 4 dinitrophenylhdrazone the two modifications are yellow and orange-red in color, the atable form, prepared by fusion or sublimation of the stable form, melted at 147°C. Bryant (7) assumed that the two were polymorphs whereas Campbell (10) believed them to be theresult of insufficient purification. Allen and Richmond (11) pointed to the fact that they might have been the result of the acid catalyst used in the preparation of the derivatives since they have always observed a lower melting point of the derivative prepared with sulfuric acid than with hydrochloric acid.

The use of 2, 4 dinitrophenylhydrazine reagent in the quantitative estimation of aldehydes and ketones has been reported by Iddles and Jackson (12) who presented a good bibliography of the earlier work. They studied the effects of time, temperature and concentration upon the yields obtained. Yields greater then 95% were reported for simple aliphatic aldehydes; the yield increased with the molecular weight of the carbonyl compound.

Description of the Weissenberg Method

K. Weissenberg (13) described in 1924 a new x-ray goniometer and camera which has found wide use in the determination of the structure of materials which can be obtained in the form of reasonably sized single crystals. Many authors (14, 15, 16), particularly Buerger (17) have discussed the theory and operation of the camera lies in spreading the diffracted x-ray beam from a single layer line into a pattern of spots enabling the unequivocal indexing of each diffracted beam.

The crystal is mounted in a special holder (fig. 1, 2)

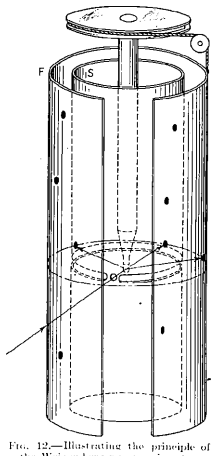


FIG. 12.—Illustrating the principle of the Weissenberg x-ray goniometer.

Fig. 1. Schematic Diagram of Weissenberg Camera

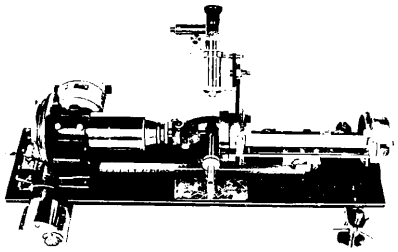


FIG. 135.—Weissenberg-Seemann goniometer.

Fig. 2. Photograph of Weissenberg Camera

permitting the rapid alignment of the crystal. A cylindrical shield fits over the crystal and allows only the diffracted beam from a particular zone, or layer line to pass through

and register on the film, while a mechanical device rotates the crystal and simultaneously translates the film parallel to the axis of crystal rotation.

There are two readings necessary for indexing each spot (fig. 3); the distance from the center of the film

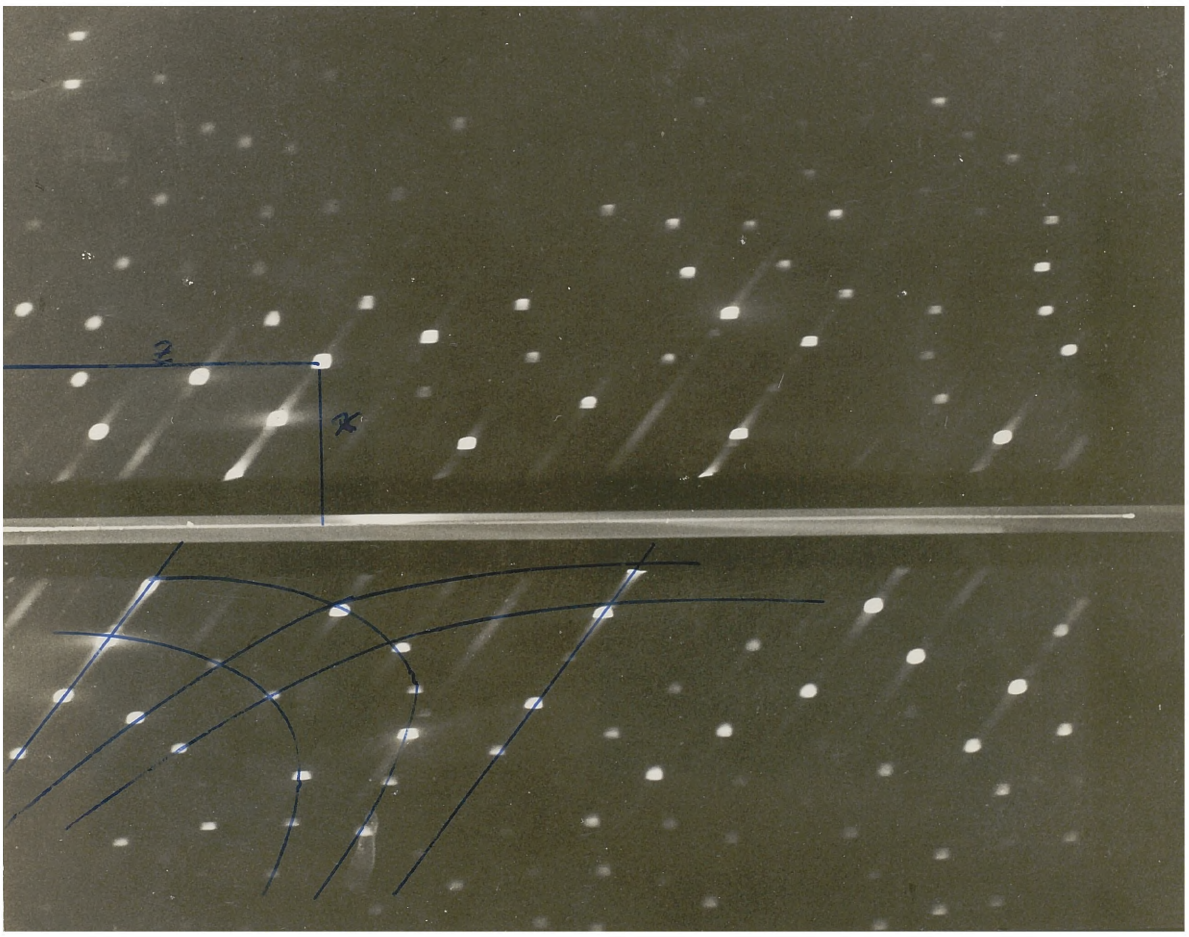


Fig. 3. Zero Layer Line Weissenberg Photograph of Acetone 2, 4 Dinitrophenylhydrazone Cu K radiation.

outward (x) and the distance from the end of the film to the spot in question (z). The first reading (x) determines

the usual interplanar distance "d" while the second value (z) determines the angle between the planes and permits the construction of the reciprocal lattice of the crystal.

In order to be able to interpret the Weissenberg patterns the instrumental constants relating the above x and z readings withtheir respective angular values ϕ and ω must be known. 2ϕ isthe relection angle where ϕ is the familiar angle in Bragg's law. is the angle through which thecrystal rotates from some arbitrary starting position.

Using the idea of radian measurement it is obvious that

$$2\phi = (360/2\pi r_c)x$$

where $360/2\pi r_c$ is a constant. For the Weissenberg camera used in this work the effective radius of the film, r_c, is 3.55 cm., hence the constant is 1.615 degrees per millimeter.

The constant relating the z measurement with the angular rotation of the crystal depends upon the effective drum diameter upon which the cord moving the film is drawn (fig. 1).

$$\omega = (360/2\pi r_d)z$$

In the present case r_d = 5.73 cm. hence the constant is equal to unity in units of degrees per millimeter.

While the usual Weissenberg pattern may be indexed directly with a little experience it is adviseable at first to draw the reciprocal lattice from the Weissenberg photograph.

Recalling that the reciprocal lattice value (ρ) is a vector in the direction of the normal to the set of parallel

planes in question and of length proportional to the reciprocal of the interplanar distance "d" related by the expression (18)

$\rho d = K$

where K is the radius of the sphere of diffraction, usually the radius of the camera and is the wave length of the x-rays used.

ρ is directly proportional to some function of the hkl values and in fact is proportional to the diagonal of the tetrahedron having the sides of length hkl and the angles between the sides of α, β, γ and where α, β, and γ are the angles between the axes of the unit cell. If a permanent point be fixed at the end of each of the vectors from the various planes in the crystal. With the spots from the Weissenberg pattern transformed into such a reciprocal lattice it becomes a simple matter to index the spots according to their hlk and α, β, γ and values. The Weissenberg camera simplifies the picture somewhat since all of the interferences occurring on a single photograph will have the same l values provided the crystal has been rotated about the c axis. The reciprocal lattice will then be a <u>plane</u> lattice of points whose x and y coordinates are the h and k values of the plane in question.

To construct the reciprocal lattice of the zero layer line consider the circle in fig. 4 to be the projection of the sphere of diffraction and also the radius of the cylindrical

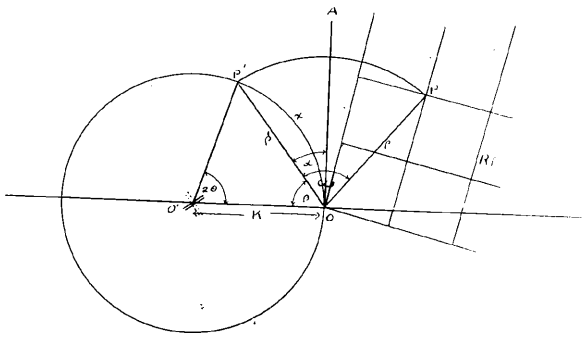


Fig. 4. Reciprocal Lattice Construction

camera. The length of the vector ρ may be given directly in terms of the distance x by the equation relating the arc of a circle to its chord

$$\rho = 2K\sin(360x/4\pi K) = 7.10\sin(8.20x).$$

It is then necessary to find the angle from the reference position OA through which the vector must be rotated to bring it to position in the reciprocal lattice. Assuming that the reciprocal lattice point P occupied the position shown at the beginning of the exposure, it is observed that the crystal will have to rotate through the angle ω before it will be in a position to diffract the x-ray beam. This may be visualized by considering the orientation of the planes in question through the crystal. At the moment of diffraction these planes are at an angle θ to the horizontal x-ray beam OO' but initially they were oriented normal to the vector ρ at position OP. Since we wish to know the angle which ρ (at OP) makes with the

reference line OA we must know the angle $\nu - \alpha$.

$$\alpha = 90 - \beta$$

$$2\beta = 180 - 2\theta$$

$$\alpha = \theta$$

Hence the required angle is $\omega - \theta$.

Now to plot such a reciprocal lattice tabulate the x and z values. ω is given directly when z is measured in millimeters. Tabulate θ and ρ from the x-values and finally tabulate $\omega - \theta$. The two columns of ρ and $\omega - \theta$ values suffice to draw the reciprocal latteice. An example is shown here of an acetone 2, 4 dinitrophenylhydrazone crystal rotated about the c axis. Table I lists the above values from the Weissenberg pattern fig. 3. Fig. 5 shows the constructed reciprocal lattice.

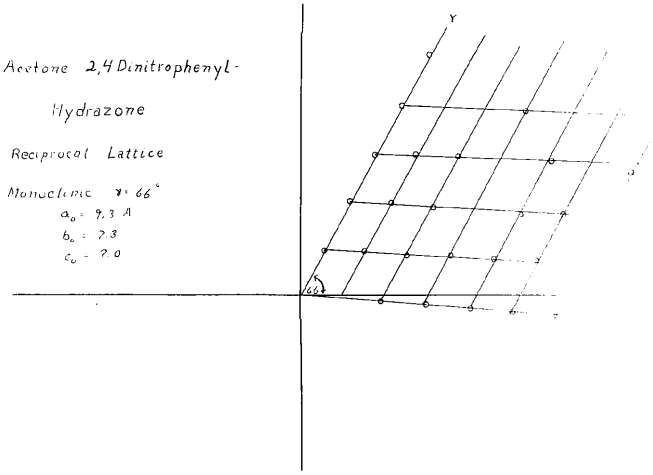


Fig. 5. Reciprocal Lattice of Acetone 2, 4 Dinitrophenylhydrazone

Table I. Reciprocal Lattice Projection

#	x(cm.)	θ	ω	$\omega - \theta$	θ
1.	0.68	5.57	34.0	28.4	0.68
2.	1.44	11.8	40.0	28.2	1.43
3.	2.20	18.0	46.3	28.3	2.16
4.	3.00	24.6	52.5	27.9	2.91
5.	3.90	32.0	59.2	27.2	3.70
6.	1.04	8.5	66.7	58.2	1.04
7.	1.78	14.6	60.8	46.2	1.76
8.	2.41	20.5	61.4	40.9	2.45
9.	1.60	13.1	83.8	70.7	1.58
10.	2.22	18.2	75.8	57.6	2.18
11.	2.97	24.3	74.3	50.0	2.88
12.	2.20	18.0	95.0	77.0	2.16
13.	4.23	34.6	86.7	52.1	3.98
14.	2.80	23.0	103.7	80.7	2.72
15.	3.35	27.5	97.8	70.2	3.22
16.	4.03	33.0	95.8	62.8	3.91
17.	3.43	28.1	111.0	82.9	3.30
18.	4.00	32.8	106.2	73.4	3.80
19.	4.15	34.0	118.3	84.3	3.11
20.	4.70	38.5	115.2	76.7	4.35
21.	5.38	44.0	113.8	69.8	4.87
22.	0.52	42.6	100.0	57.4	0.52
23.	1.13	9.2	104.5	95.3	1.13
24.	1.78	14.6	109.5	94.9	1.77
25.	2.40	19.7	114.5	94.8	2.36

This lattice together with the rotation pattern Fig. 6

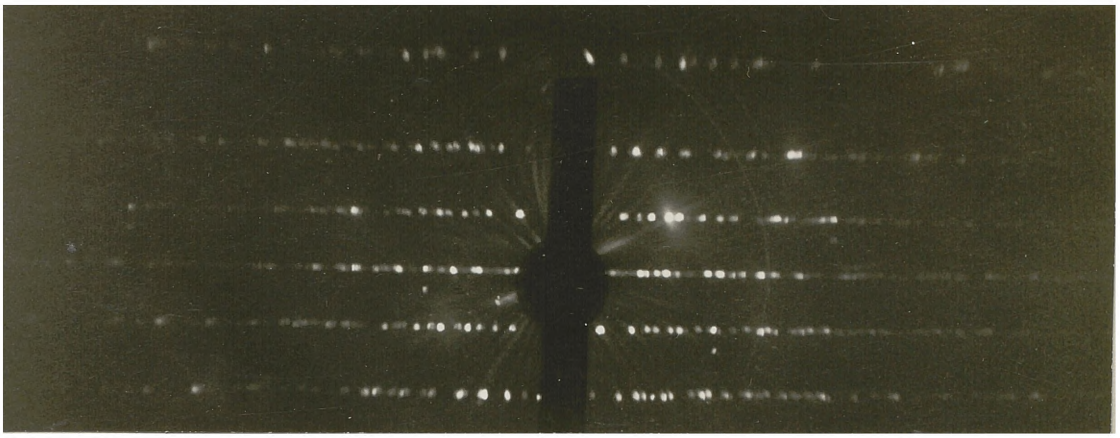


Fig. 6. Rotation Pattern, Acetone 2, 4 Dinitrophenylhydrazone

permits the identification of the unit cell as Monoclinic

a_o = 9.10 A^o γ = 66^o

b_o = 7.3

c_o = 7.05 .

A much more rapid way of indexing a Weissenberg pattern lies in the visual identification of the zones on the film. The zones h00 and 010 of the zero layer line photograph are identified easily as being the straight lines crossing the film at an angle of 52^o from the horizontal. The ω value between these two straight lines gives the angle between these respective axes in the unit cell. Calculation of the "d" values from the x values of the 100 and 010 lines immediately leads to the unit cell length along these axes. Two such zero layer line Weissemberg patterns of a crystal rotated about two axes usually suffices to identify the unit cell dimensions and the

space group. Further knowledge of the intensities of other interferences may be obtained from layer line photographs. These intensities in turn offer a solution to the final structural arrangement of atoms and molecules in the unit cell.

Throughout the work presented here the equi-inclination method of Buerger (19) is used since by this method layer line photographs may be visually identified in the same manner as the zero layer line normal beam photographs. In order to record the layer line by the equi-inclination method it is necessary to introduce thex-ray beam at an angle of $\pm\theta$ as shown in fig. 7. The shield is then moved laterally by the

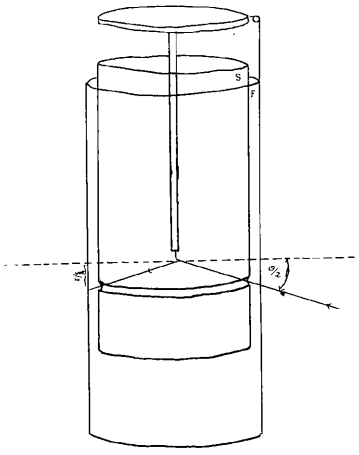


Fig.7. Schematic Diagram of Weissenberg Camera for Equi-inclination photograph.

distance $\frac{1}{2}$ the distance observed between the layer lines in question and the zero layer line of the rotation pattern (fig. 6). Corrections should be made for the difference in diameter of the shield and the film.

Structure of Formaldehyde 2, 4 Dintirophenylhydrazone

Preparation. The formaldehyde 2, 4 dinitrophenylhydrazone was prepared by adding 40% formaldehyde solution to a hot concentrated solution of 2, 4 dinitrophenylhydrazine dissolved in methyl alcohol approximately two normal in hydrogen chloride. When cooled the crystals were filtered and air dried. The crystals were then recrystallized once from hot 90% ethyl alcohol and three times from hot isobutanol. The last recrystallization was slow and resulted in the growth of yellow needles and platelets about 2-5 millimeters in length.

Properties of the crystals. The formaldehyde 2, 4 dinitrophenylhydrazone crystals melted at 166°C. (uncorrected) agreeing with the literature (4, 10). The density of the crystals as measured by floating in a mixture of methyl iodide and ethyl bromide was 1.592 ± 0.010 g/ml.; the density of the liquid being determined with a 25 ml. boot specific gravity bottle. A photomicrograph of a flat yellow platelet is shown in fig. 8. The axial designa-

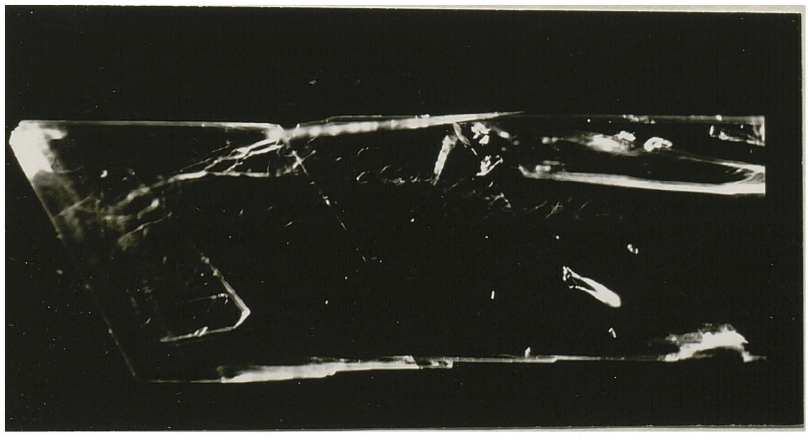
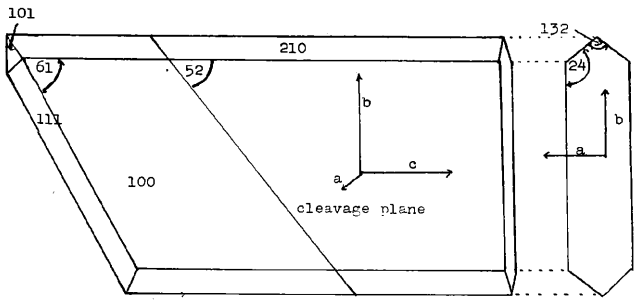


Fig. 8. Photomicrograph of Platelet of Formaldehyde 2, 4 Dinitrophenylhydrazone 60x



Crystal of Formaldehyde 2,4 Dinitrophenyl hydrazone

Fig. 9. Schematic Diagram of Platelet Showing Axial designation and cleavage plane.

tion of this type of crystal is indicated in fig. 9. The needle shaped crystals are similar to the platelets inbbeing elongated along the c axis; the difference being in the growth of the (100) face of the platelets. The angles between the faces along the c axis were measured as the angle through which the needle shaped crystal had to be rotated to bring successive faces into position to reflect, normal to the face of the crystal, a beam of light from a microscope placed on the Weissenberg camera. Experimaental X-ray Data. Figures 10 and 11 are rotation patterns taken with the shield of the Weissenberg camera removed and the film held stationary. These patterns were taken to confirm the axial unit cell lengths along the axis of rotation and to determine the instrument settings for equi-inclination layer line patterns. The crystal was rotated about the "c" axis in fig. 10. The

Illustrations for Formaldehyde 2, 4 Dinitrophenylhydrazone

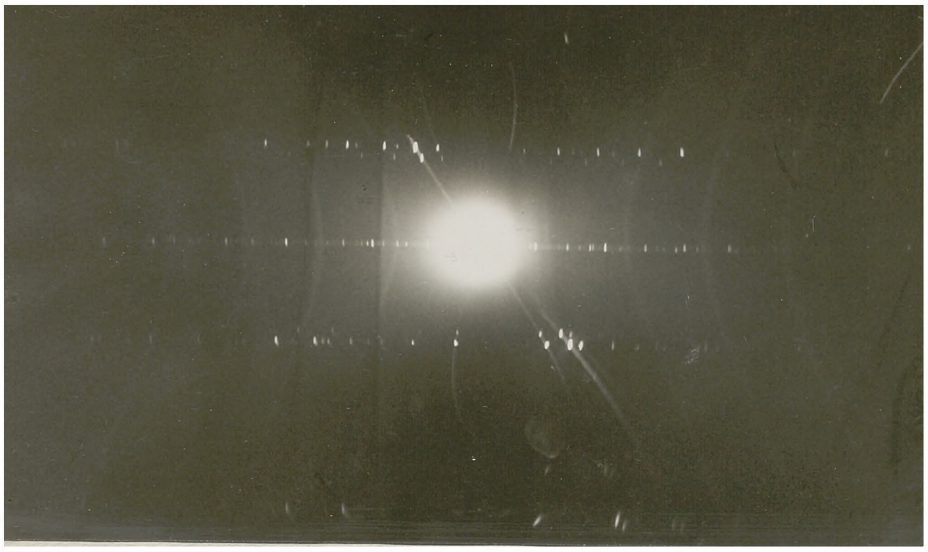


Fig. 10 Rotation Pattern about the "c" axis. Weissenberg Camera, 3.5 cm Radius. Needle shaped crystal.

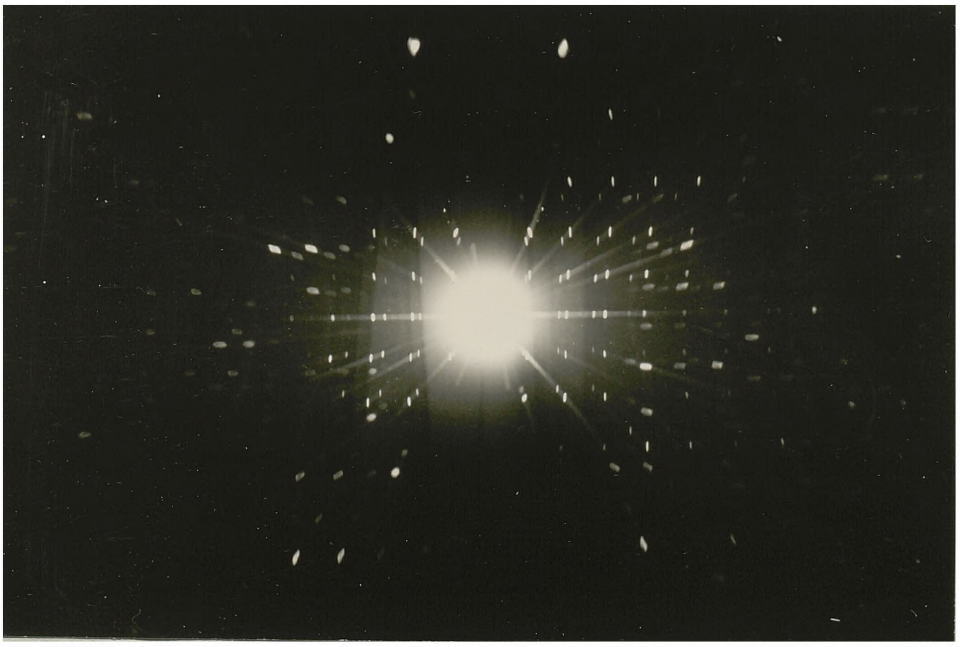


Fig. 11 Rotation Pattern about the "b" axis. Plate shaped crystal.

distance between the first layer line is 2.70 cm. Using the equation (20)

$$d_c = n\lambda/\sin(\tan^{-1}x/2r)$$

where n is the number of the layer line, λ, and x is the distance between the layer lines in question. The c_o value found is 4.34 A. Fig. 11 is a rotation pattern of one of the platelets rotated about the b_o axis. At first this pattern seems to be of a tetragonal unit cell but further examination shows that the a_o value is greaterthan the b_o value. Calculation of b_o by the method outlined above leads to a value of 10.08 A. a_o may be calculated from the spots on the zero layer line by the use of the equation

$$d = \lambda/a\sin(360x/2\pi r)$$

where x is the distance from the center spot to the first spot of the zero layer line. The a_o value so determined is 10.4 A. This pattern appears to be of a tetragonal crystal because of the fact that the hnO interferences (n equal to a constant for the particular layer line) are much more intense than the hnk interferences. Fig. 12 is a Weissenberg zero layer line photograph of a crystal rotated about the c axis. It was taken from a plate shaped crystal with a wide (.060 in.) pinhole collimating system which accounts for the elongated shape of the spots on the film. Unfiltered copper radiation was used hence the K_β interferences may be readily detected just inside of the corresponding K_α interferences. The a_o value as measured from the 400 interference is 10.5 A. while the b_o value is 10.0 A. The angle between the a and b axes is approximately 93^o. The intensities of the OkO interferences are less than the hOO interferences

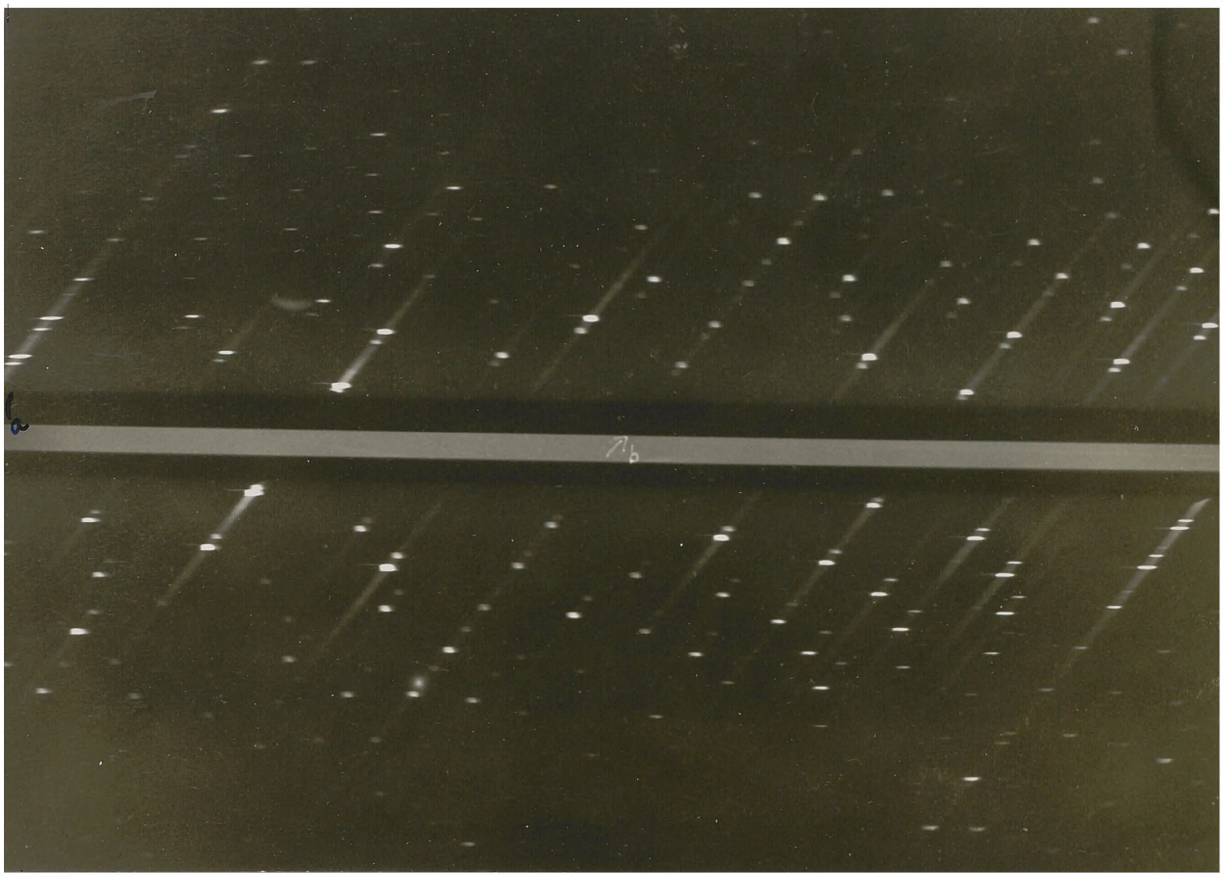


Fig. 12. Weissenberg zerp layer line photograph. Crystal rotated about "c" axis. Camera Radius 3.55 cm. Cu K radiation.

because of the shape of the plate-like sample. No systematic extinctions are observed on this photograph. The expected 010 interference can not be very intense since its white radiation "streak" is not observed.

The pattern of the first layer line about the c axis is shown in fig. 13. No systematic extinctions are observed; however, the $0\bar{2}1$, $\bar{1}11$, $1\bar{1}1$, and $\bar{1}2\bar{1}$ interferences appear unusually intense. Since the crystal was triclinic it was difficult to rotate the crystal about a line normal to the XZ plane of the

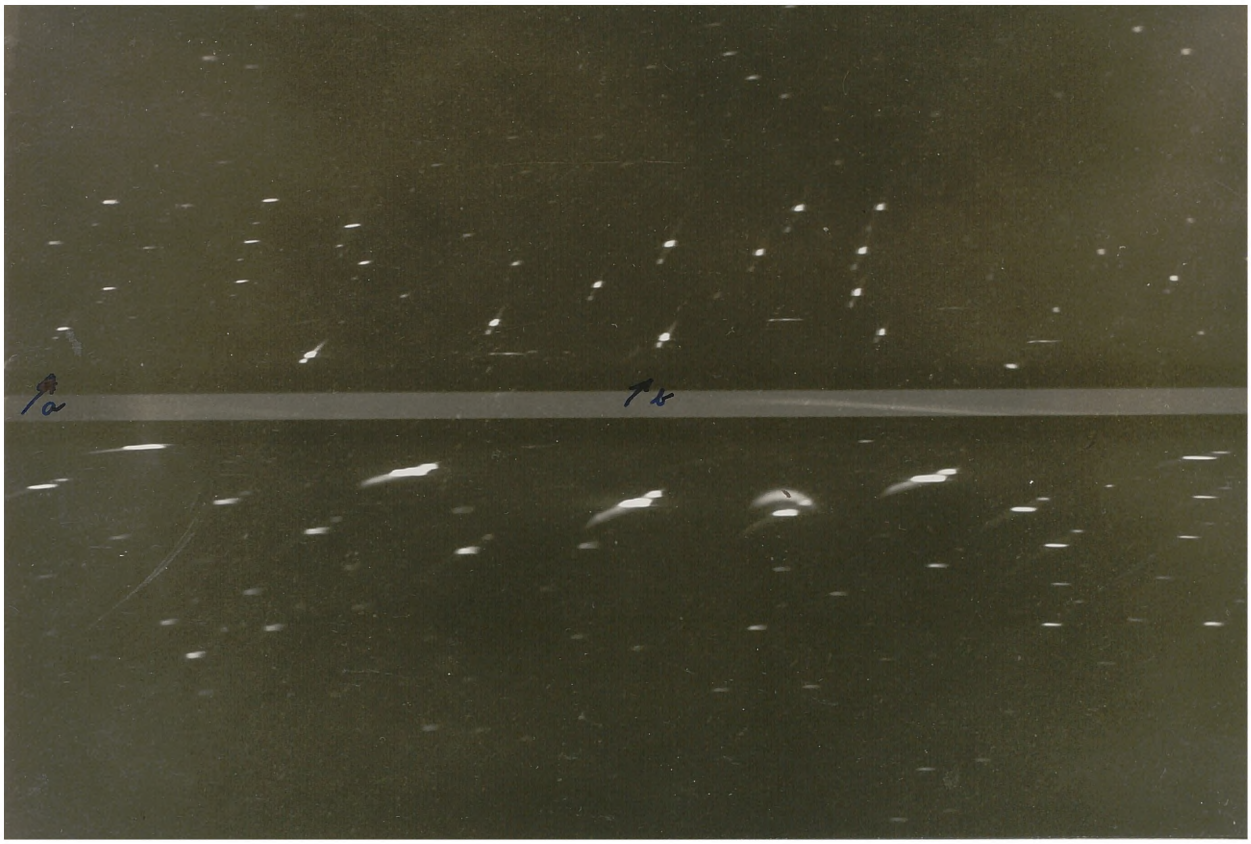


Fig. 13. Weissenberg First layer line Equi-inclination Pattern Crystal rotated about the "c" axis.

crystal. This pattern is observed to have been rotated about an axis lieing a few degrees from the "c" axis because the h0l and 0kl zones do not lie on straight lines. The second layer line about the "c" axis was too far out to enable photographing with the Weissenberg camera.

Another plate-shaped crystal was chosen for a rotation about the "b" axis. Fig. 14 is a Weissenberg pattern of the zero layer line about this axis. The h00 intensities appear greater than the 00l or h0l intensities; however, if considera-

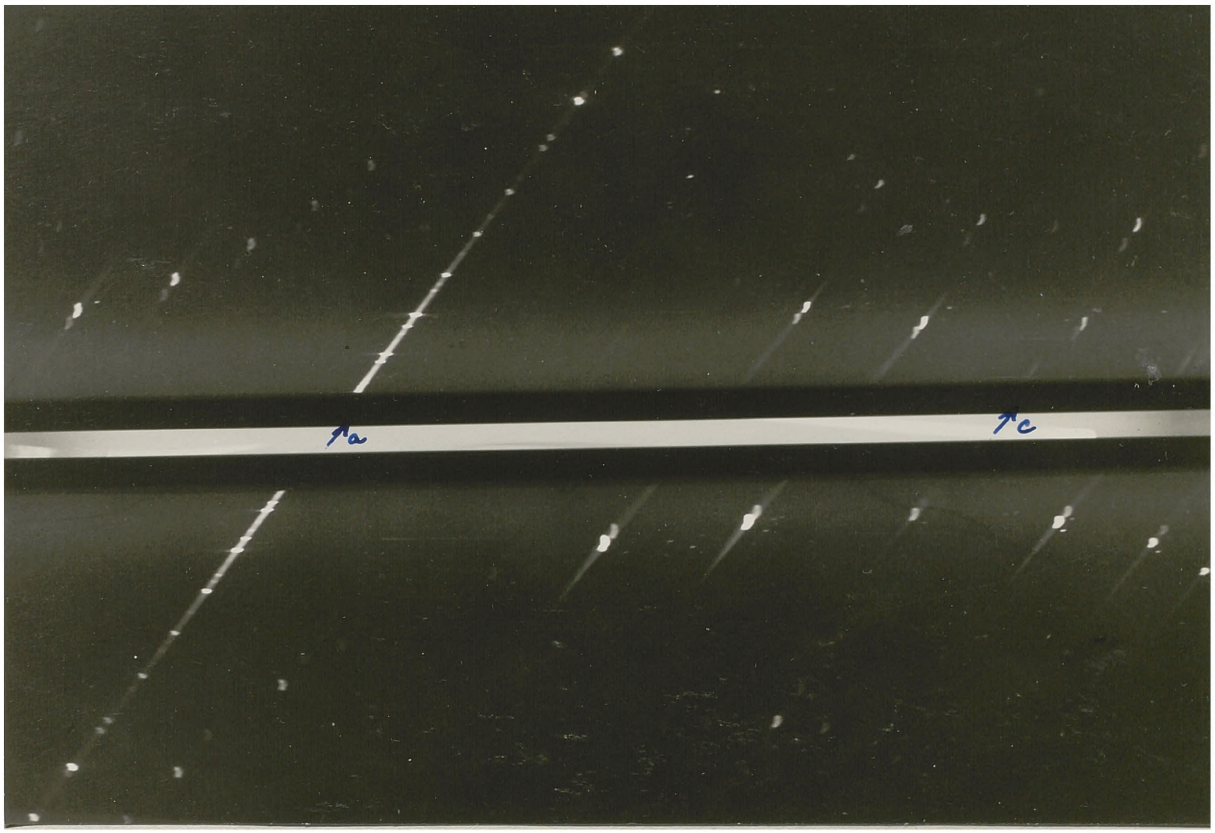


Fig..14. Weissenberg Zero Layer Line Photograph. Crystal Rotated about the "b" Axis.

tion be given to the shape of the crystal the 00l and h0l intensities would be relatively more intense than observed. The angle between the a and c axes appears to be about 94° (average value between the two sides of the film). There appear no systematic extincitions, though the entire zone $h\bar{2}0$ appears to be absent.

The first layer line Weissenberg photograph with the crystal rotated about the "b" axis is shown in fig. 15. No systematic extinctions appear. The h2l zone is very weak while the 111 interference is very strong.

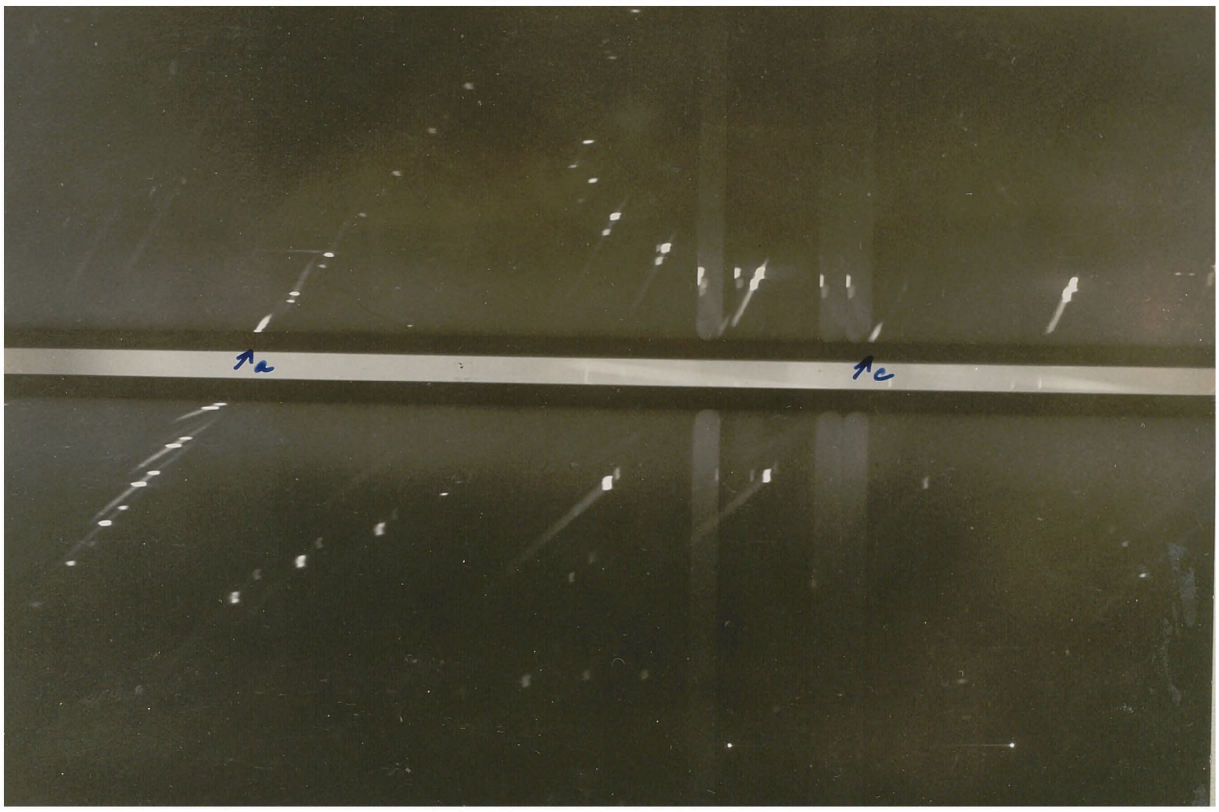


Fig. 15 Weissenberg Equi-inclination First Layer Line Pattern, Crystal Rotated About the "b" axis.

Fig. 16 is of the second layer line with the crystal rotated about the "b" axis. Again no systematic extinctions are observed, while the $0\bar{2}1$ interference is very strong.

The Weissenberg camera used for this work was not built for accurate determination of the unit cell dimensions because the effective radius of the film is small and variable within 5%. For a more accurate determination of the unit cell values the powder pattern was chosen. Fig. 17 is a powder pattern of the formaldehyde 2, 4 dintrophenylhydrazone sample mounted in a 0.35 mm. diameter cellulose acetate tube. A camera of 7.00 cm.

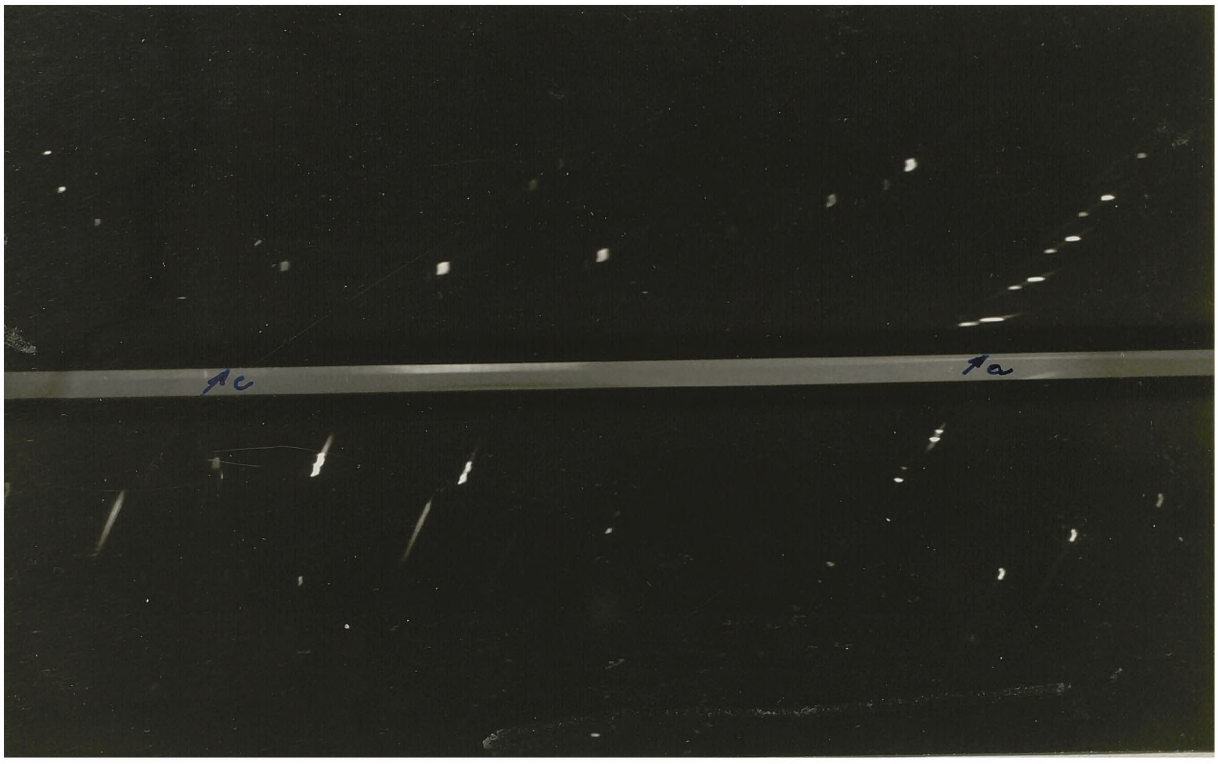


Fig. 16. Weissenberg Equi-inclination Second Layer Line Pattern Crystal Rotated about the "b" axis.



Fig. 17. Powder Pattern, Fine Pinholes, 7.00 cm radius. Agfa Non-Screen film.

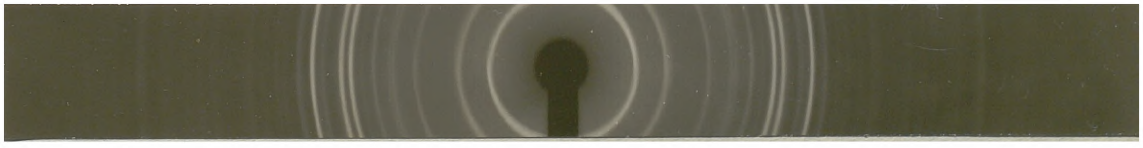


Fig. 18. Powder Pattern, For Intensity Measurements, Eastmen Type A Fine Grain Film.

radius was used with Cu K_α radiation. The sample was oscillated through 30 degrees to smooth out any spots on the Debye-Scherrer rings. A collimating system of 0.010 in. diameter back and front pinholes was used. The use of such small pinholes required an exposure of 24 hours with Agfa-Ansco Non-Screen film.

For accurate measurement of the intensities of the lines another pattern, fig. 18, was taken using Eastman Type A fine grain film with a collimating system of a 0.010 in back pinhole and a 0.025 in. front pinhole. This photograph was then microphotometered with a Leeds and Northrup recording microphotometer.

Table II lists the necessary data for and the conclusions from the reciprocal lattice projections of the powder patterns.

Table II. Data from Powder Patterns, Figures 17 and 18.

#	D	I/I_o	"d"	p	hkl
1.	2.08	0.88	10.3	2.08	100
2.	2.94	0.41	7.35	2.93	110
3.	3.07		7.05	3.06	$\bar{1}10$
4.	4.16	0.24	5.20	4.14	200
5.	4.62		4.62	4.59	210
6.	4.78	0.17	4.42	4.75	120, $\bar{2}10$
7.	4.90	0.14	4.34	4.86	$\bar{1}20$
8.	5.35	0.26	4.05	5.31	101
9.	5.67	0.04	3.84	5.62	$\bar{1}01$
10.	5.00	0.97	3.62	5.94	$1\bar{1}1$
11.	6.24	0.86	3.47	6.19	$\bar{1}\bar{1}1$
12.	6.75		3.21	6.69	$\bar{3}10$
13.	7.07	100	3.08	7.00	$0\bar{2}1$
14.	7.43	0.22	2.93	7.35	$\bar{1}\bar{2}1$

The construction of the reciprocal lattive projection of a triclinic unit cell can not be made with a simple drawing as can be done with orthogonal unit cells. Figures 19 and 20 and 21 are

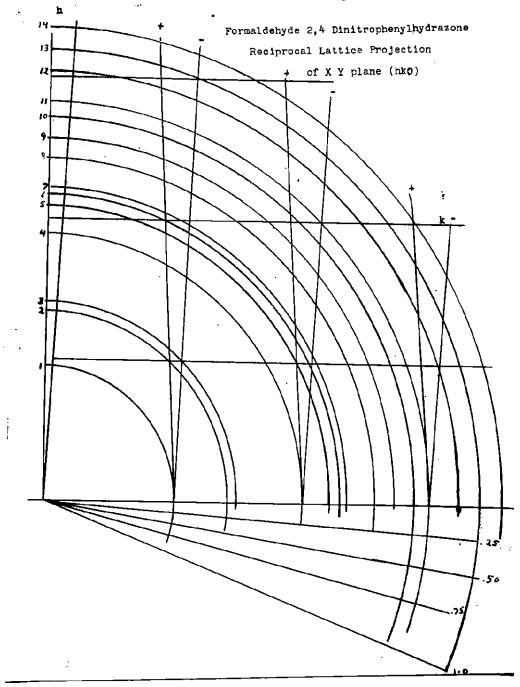


Fig. 19. Reciprocal Lattice Projection in "ab" plane.

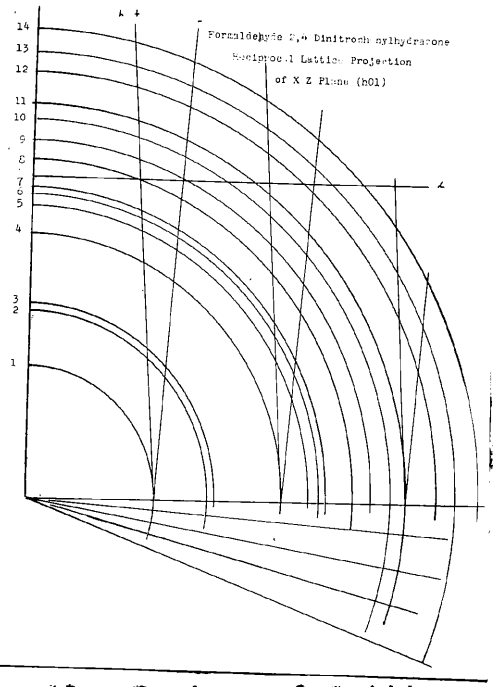


Fig. 20. Reciprocal Lattice Projection in "ac" plane.

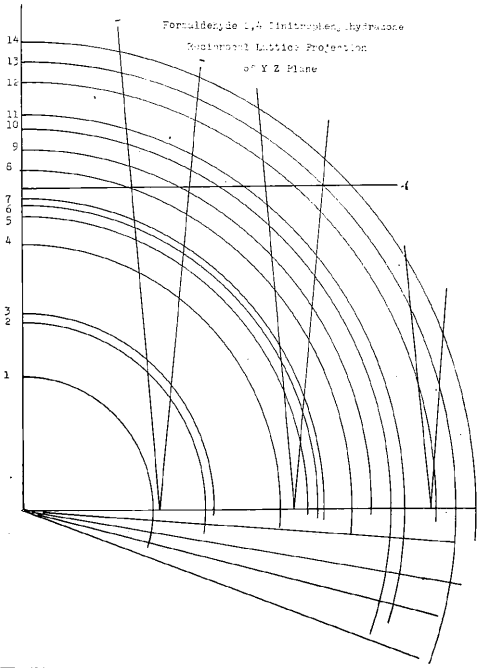


Fig. 21. Reciprocal Lattice Projection in "bc" plane

reciprocal lattice drawings from the powder patterns figs. 17 and 18. From fig. 19 the lines may be indexed as arising from hkO planes; fig. 20 indexes the lines hOl and fig. 21 indexes the linesas from Okl planes. These reciprocal lattice projections have been constructed from data obtained from the Weissenberg patterns in the manner as follows; Consider first the lines from the planes hkO. The interferences from the zero layer line photograph about the c axis (fig. 12) were tabulated in order of decreasing "d" values. The lines on the powder pattern will occur in this same order and may be rapidly indexed until the planes begin to over-lap with the planes having indices Okl, hOl, or hkl. The intensity measurements serve as a check. The Weissenberg pattern of the zero layer line about the b axis (fig. 14) was used in a similar manner to construct the lattice fig. 20. This procedure can not be followed in indexing fig. 21 since no Weissenberg pattern was obtained with the crystal rotated about the "a" axis. However, in fig. 13 it was observed that the $0\bar{2}1$ spot was very intense. Calculation of the "d" value of this spot on the Weissenberg film leads to a value of 3.08 A. This calculation was made using the equation (25)

$$\cos 2\theta = \cos\phi \cos\mu$$

where θ is the Bragg angle, ϕ is equal to $(x/r)360/2\pi$ and $\mu = \tan^{-1} q/r$ where q is the distance from the zero to the first layer line. Knowing that line #13 is the $0\bar{2}1$ line it is possible to draw the reciprocal lattice projection of the Okl plane, (fig. 21).

From the reciprocal lattice projection of the powder pattern it is possible to describe the unit cell with fair accuracy.

We may then say that the unit cell of formaldehyde 2, 4 dinitrophenylhydrazone is triclinic

$a_o = 10.41 \pm .93$ A. $\quad \alpha = 85^o$

$b_o = 10.00 \pm .05 \quad \beta = 86^o$

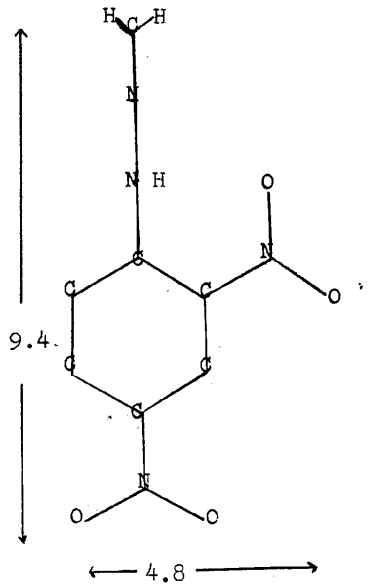
$c_o = 4.23 \pm .03 \quad \gamma = 87^o$

Since there were no systematic extinctions observed, the space group must be P_1 or P_I^- (23). From the measured density of the crystal, the number of molecules per unit cell is 2.08 according to the formula

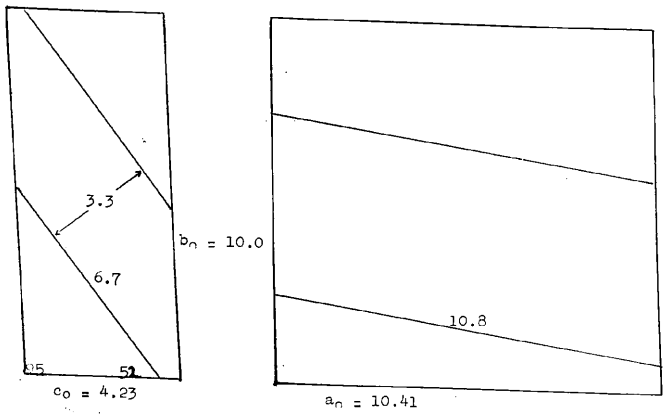
$$n = pV/1.65M$$

where p is the density, V the volume of the unit cell in cubic angstoms and M is the molecular weight. This indicates two molecules per unit cell. The space group P_1 has one equivalent position per unit cell while space group P_I^- has two (24). Hence we may ascribe the space group $P_1^- - C_i^1$ to this crystal.

Orientation of the Molecule in the Unit Cell: The cleavage plane, the intensities of interferences, and the theoretical size of the molecule lead to some estimation of the orientation of the molecule in the unit cell. The size of the molecule may be determined from the atomic, covalent, and Van der Waals bond lengths and bond angles as reported for other compounds (26). Fig. 22 illustrates a schematic diagram of the formaldehyde 2, 4 dinitrophenylhydrazone molecule with the corresponding bond lengths drawn to scale. Assuming that the molecule lies in a plane, the length of the molecule with the Van der Waals radii considered for the end atoms is 12.9 A; without the Van der Waals radii considered for the length of the molecule is 9.4 A. With the Van der Waals radii considered the width of the molecule will be approximately



Formaldehyde 2,4Dinitrophenyl-Hydrazone



Unit Cell for Formaldehyde 2,4Dinitrophenylhydrazone

Fig. 22. Molecular Model Fig. 23. Plan of the Unit Cell

6.3 A. at the narrowest portion of the molecule and 8.3 at the widest portion. The thickness of the molecule may be taken as that of the benzene ring or 3.7 A. Fig. 23 shows the proposed angle at which the molecule is oriented in the unit cell. This angle lies in the bc plane and was determined by the cleavage plane through the crystal. At this angle the molecules must lie side to side hence the width of the molecule must include the Van der Waals radii. The observed width agrees with the above calculated minimum width of the molecule hence the broad "nitrobenzene" portion of the molecule must fit into the narrower end chain portion. The fact that the molecules fit side to side is further evidence by the definit angle of cleavage in this plane. Furthermore the $0\bar{2}1$ plane of the unit cell agrees

with this orientation of the molecule and we should expect a strong diffraction beam from this plane.

In the ab plane there was observed no definite cleavage angle. The Unit cell is not long enough to permit the molecule to lie parallel to the a axis since then the molecules would have to lie end to end and the Van der Waals radii would have to be considered. If the molecule were considered to lie on the diagonal of this plane the molecules might lie end to end but under these conditions we should expect a definite cleavage angle in this plane. This angle has not been observed. It is possible to place the molecule in the unit cell tilted at some angle between that parallel to the a axis and the diagonal. Fig. 23 illustrates how this could be accomplished. The effective length of the molecule would then be in the neighborhood of 10.8 A. This is but little more than the length of the molecule without adding the Van der Waals radii. The high intensity of the $1\bar{1}1$ and $1\bar{2}1$ interferences further substantiates this molecular orientation in the unit cell.

Consideration should be given to the possibility that the molecule is not strictly coplanar before endeavoring to obtain a more accurate representation of the unit cell. The small distance (3.3A.) between the molecules lieing side by side requires that the molecules fit together very closely, perhaps by hydrogen bonding between N-H and N-O groups.

Acetaldehyde 2, 4 Dinitrophenylhydrazone (platelets)

Preparation. The acetaldehyde 2, 4 dinitrophenylhydrazone was prepared by adding cold acetaldehyde, prepared by distilling paraldehyde acidified with sulfuric acid, to a solution of 2, 4 dinitrophenylhydrazine in methyl alcohol approximately 2 N in hydrogen chloride. After standing one hour the crystals were filtered and air dried. The compound was then recrystallized six times from hot 90% ethyl alcohol. The final rectystallization, from n-propyl alcohol, resulted in yellow rectangular plates 1-3 mm. on the long side.

Properties. The crystals melted at 166°C. (uncorrected). The literature (7, 10) records melting points of 168.5°C. for crystals prepared under these conditions. The density of the crystals as measured by floating in a mixture of ethyl bromide and methyl iodide was 1.541 ± .005 g/ml. Fig. 24 is a photomicrograph of one of these yellow platelets. When fragmenting these crystals, no definite cleavage plane was observed. The

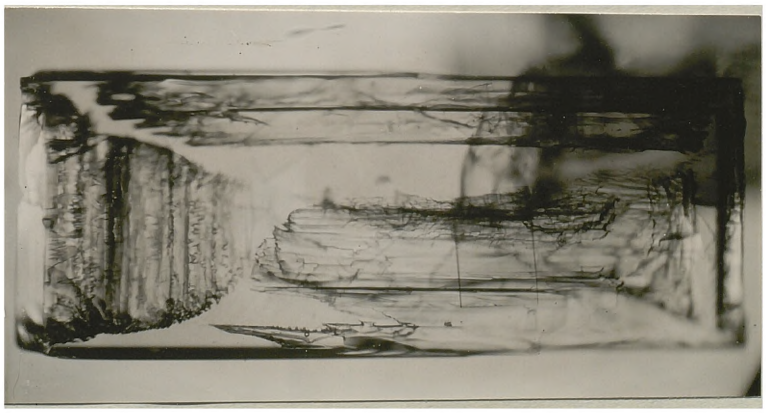
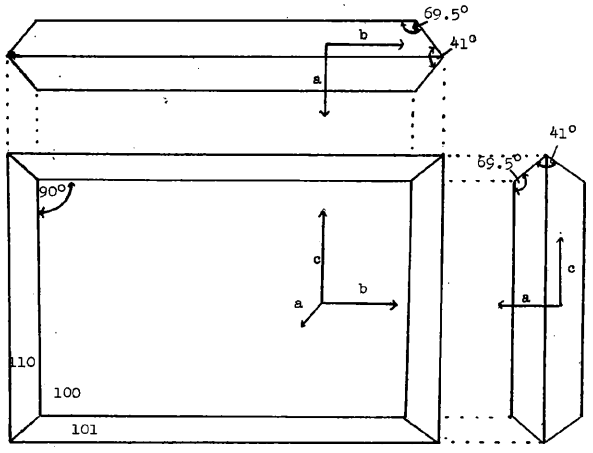


Fig. 24 Photomicrograph of the yellow platelets, 50x.

axial designation of this crystal isgiven in figure 25. The angles between the faces were measured with the Weissenberg goniometer. The angle of 69.5° leads to an axial unit cell ratio of 3.74.



Axial Designation For Acetaldehyde 2,4 Dinitrophenylhydrazine Crystal (common)

Fig. 25. Axial designation of yellow platelet.

Experimental X-Ray Data. Figure 26 is a rotation pattern of the crystal rotated about the "b" axis. The b_o unit cell length calculated from this pattern is 7.22 A.

Fig. 27 is a rotation pattern of the crystal rotated about the "c" axis giving a c_o value of 7.22 A. The layer lines on figures 26 and 27 may be superimposed, hence have the same value.

Figure 28 is a Weissenberg pattern of the zero layer line with the crystal rotated about the "b" axis. The h00 and 00l interferences occur only when h and l are even. Otherwise no systematic extinctions occur. Several anomalous weak spots occur on this pattern probably arising from imperfections in the crystal (see fig. 24). The angle between the a and c axis is observed to be 90 degrees.

Illustrations for Acetaldehyde 2, 4 Dinitrophenylhydrazone

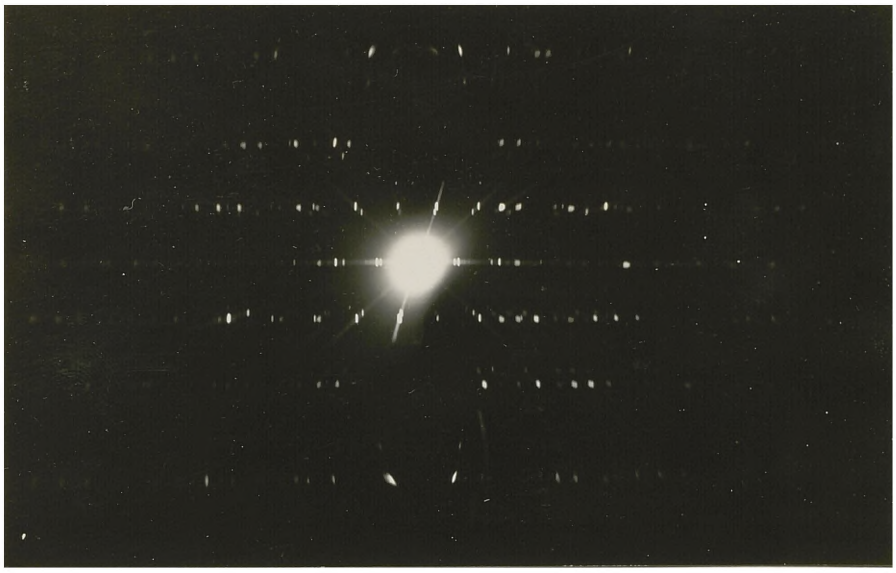


Fig. 26. Rotation Pattern, Crystal rotated about "b" axis.

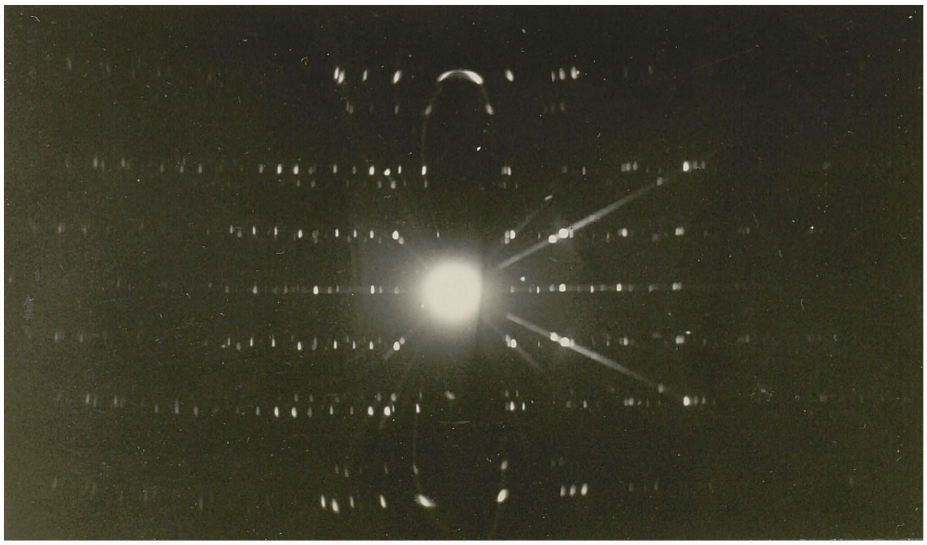


Fig. 27. Rotation Pattern, Crystal rotated about "c" axis.

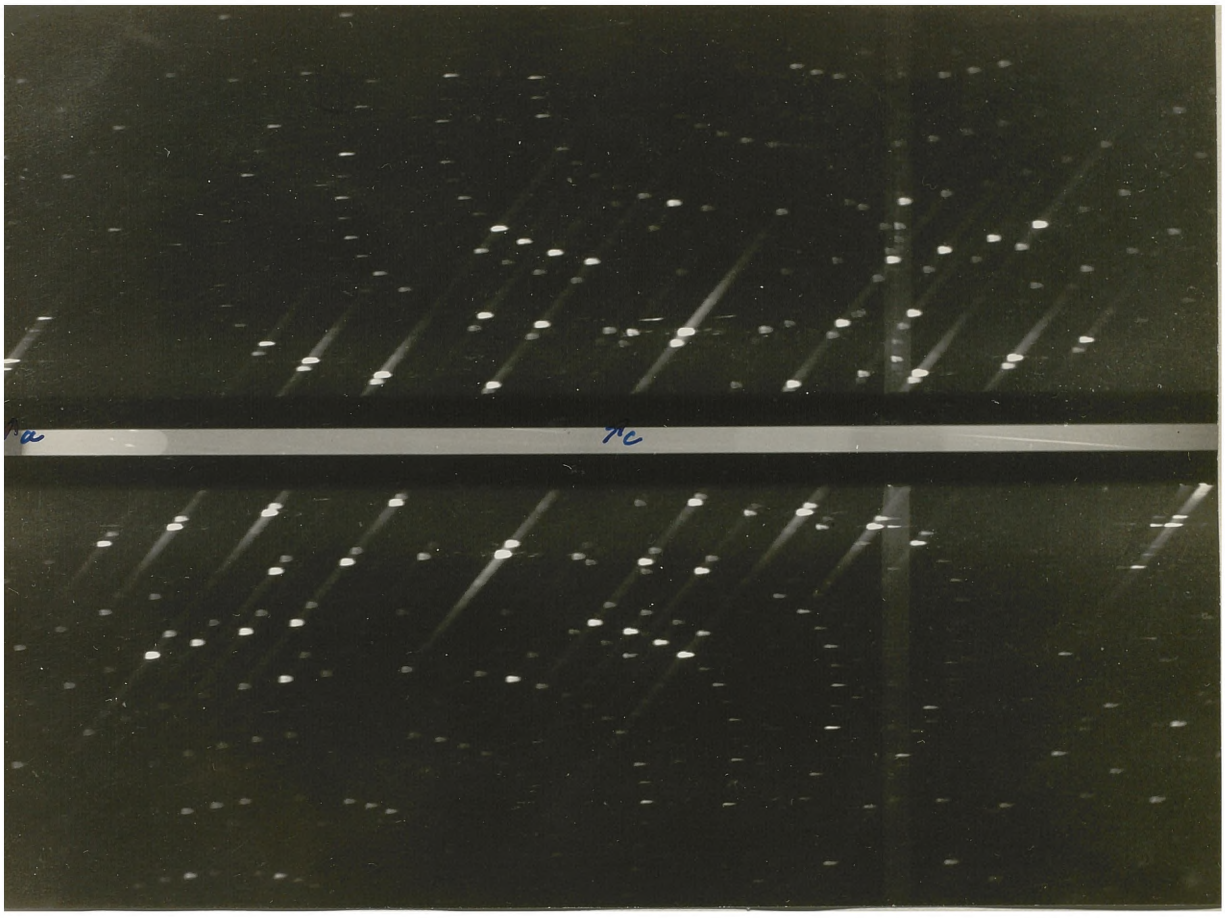


Fig. 28. Weissenberg Zero Layer, Line, Crystal Rotated About the "b" axis.

The first layer line photograph (fig. 29) with the crystal rotated about the "b" axis exhibits systematic extinctions only where h is even, i. e. h0l present only where h is odd.

Fig. 30 is a Weissenberg zero layer line photograph with the crystal rotated about the "c" axis. A large number of extinctions occur which make the interpretation of the pattern difficult at first. However, if the film of fig. 30 be superimposed upon the film for fig. 28 the interpretation becomes obvious. The fact that the two patterns may be superimposed

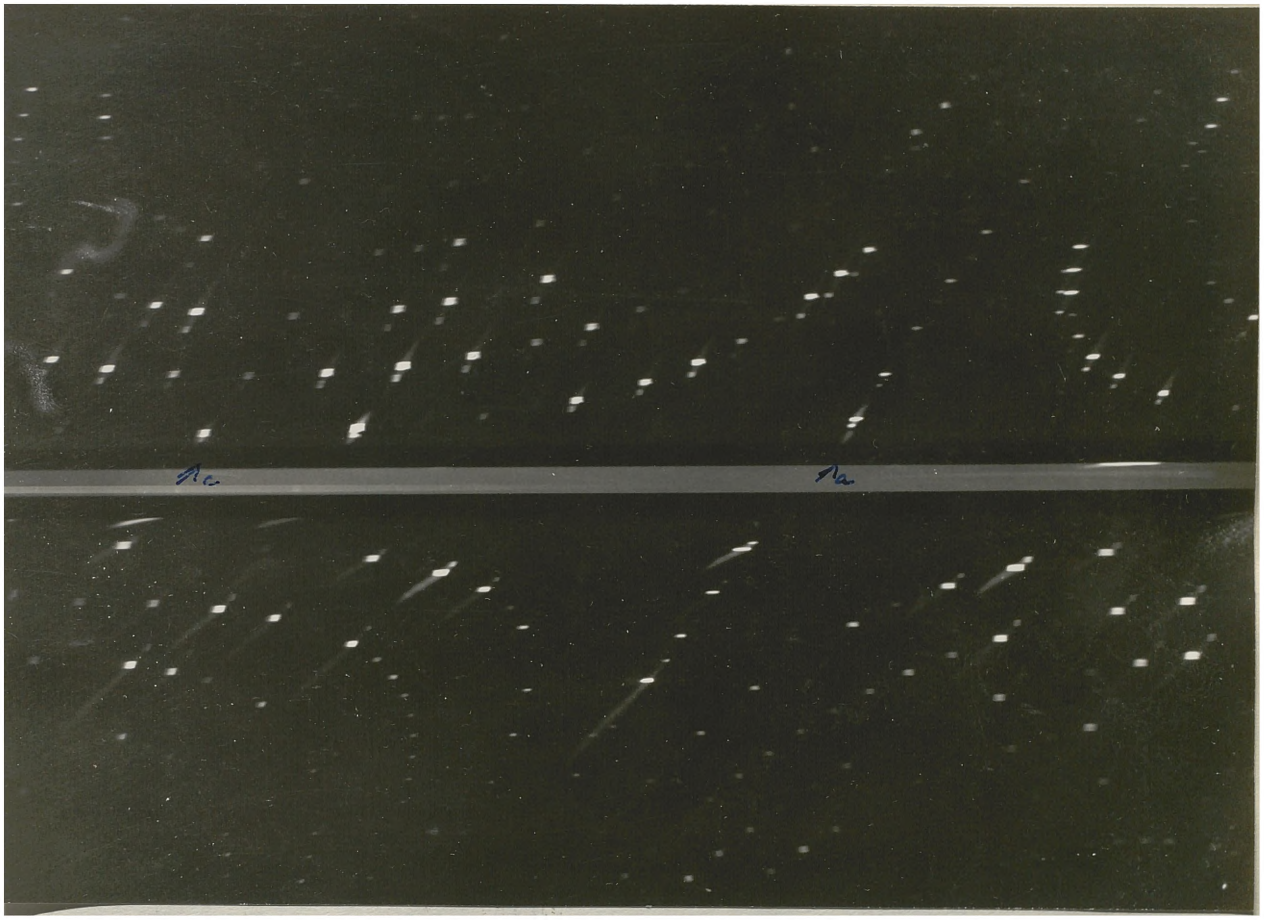


Fig. 29. Weissenberg Equi-inclination First Layer Line Photograph, Crystal Rotated About "b" Axis

conclusively establishes the tetragonal unit cell. Then it is observed that the interferences hkO are extinct where h plus k equals an odd number. hOO and OkO interferences also exist only where h and k are even numbers. The intensities of the hkO interferences are different from the corresponding $\bar{h}$kO interferences.

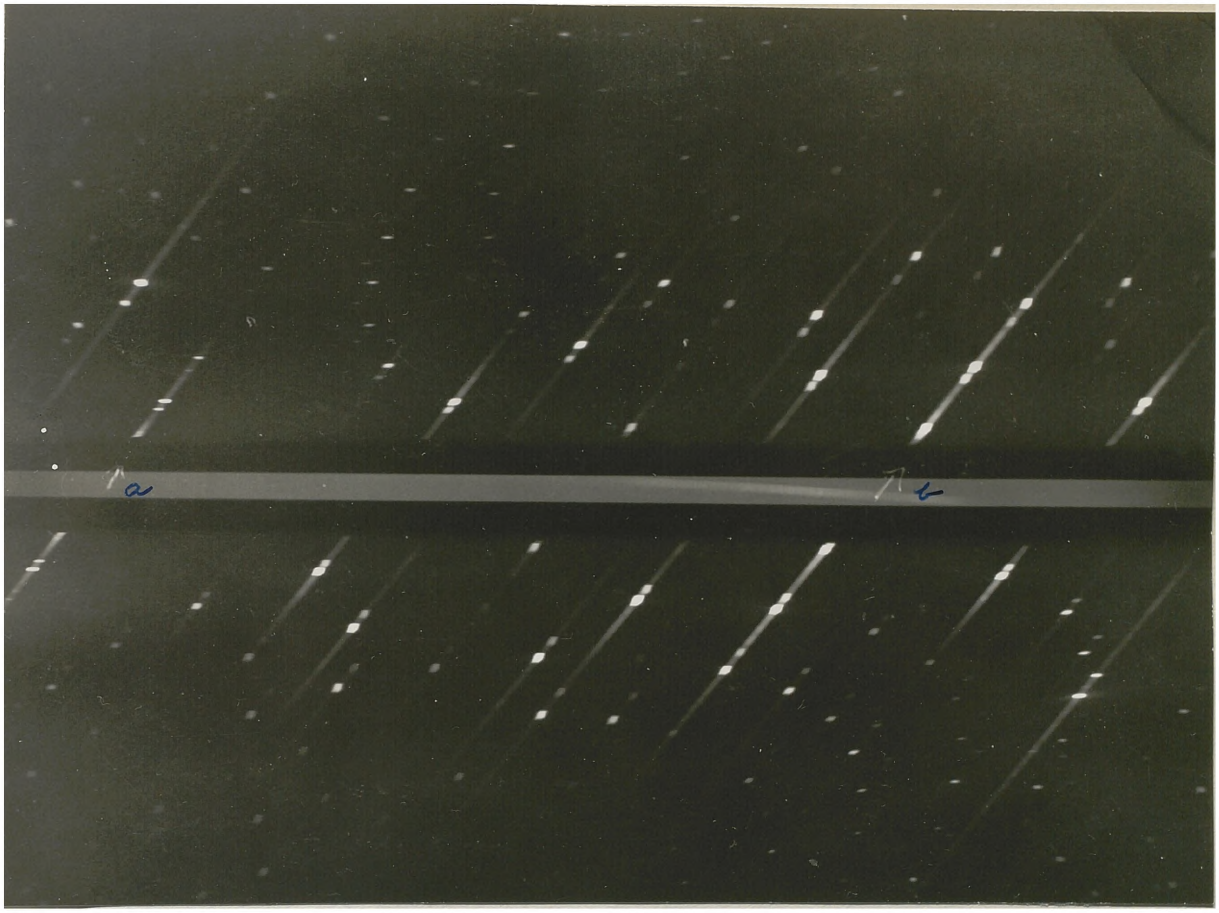


Fig. 30. Weissenberg Zero Layer Line Photograph, Crystal Roatated About "c" Axis.

Figure 31 is the first layer line equi-inclination photograph with the crystal rotated about the "c" axis. No systematic extinctions are observed. The 021, 111, and 121 spots are very intense.

Fig. 32 is a powder pattern taken with a 7.00 cm. powder camera with 0.025 in. diameter front and back pinholes. The sample was mounted in a 0.35 mm. diameter cellulose acetate tube and rotated 360° during the exposure. Eastman type a fine grain film was used requiring an 11 hour exposure. The film was then microphotometered with the Leeds and Northrup Microphotometer.



Fig. 31. Weissenberg Equi-inclination First Layer Line Photograph, Crystal Rotated About "c" Axis.

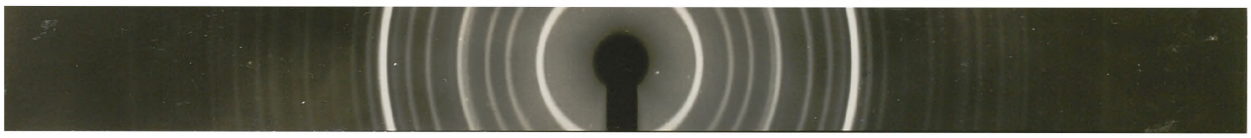


Fig. 32. Powder Pattern. 7.00cm. radius. CuK_{α} Radiation Eastman Type A film. 0.025 in. pinholes.

Table III. Powder Pattern Calculations for Fig. 32.

	D	I	"d"	D	hkl
1.	2.25	0.70	9.35	2.29	200
2.	3.21	018	6.70	3.20	110
3.	3.[illegible]0	0.13	5.68	3.75	201
4.	4.39	0.14	4.05	4.37	111
5.	4.6[illegible]	0.37	4.65	4.57	310, 400
6.	4.82	0.06	4.41	4.79	211
7.	5.50	0.21	3.96	5.46	401, 311
8.	6.08	0.18	3.57	6.03	020, 002
9.	6.33		3.43	6.28	411
10.	6.47	0.12	3.36	6.41	202, 220
11.	6.76	1.00	3.21	6.70	021
12.	6.82		3.18	6.75	112, 131
13.	7.19	0.14	3.03	7.12	212, 221, 511
14.	7.63	0.07	2.86	7.54	312, 231

Table III lists the data obtained from the powder pattern and enables the construction of the reciprocal lattice projection, fig. 33.

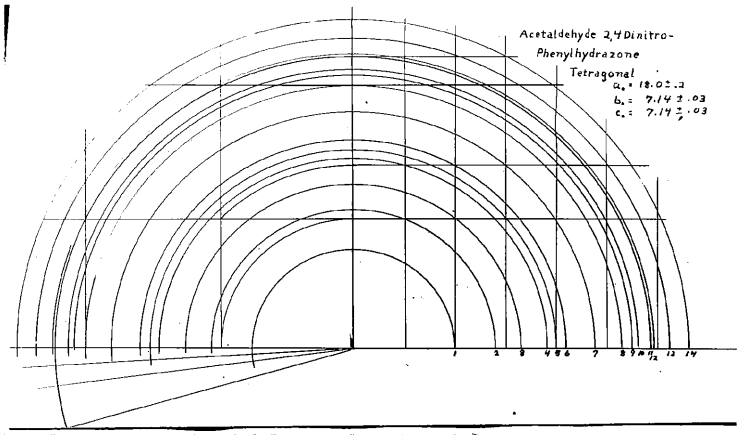


Fig. 33. Reciprocal Lattice Projection.

A further refinement of the measurement of the long unit cell dimension a_o was accomplished by the use of an off-center oscillation pattern fig. 34, taken with the 7.00 cm. camera.

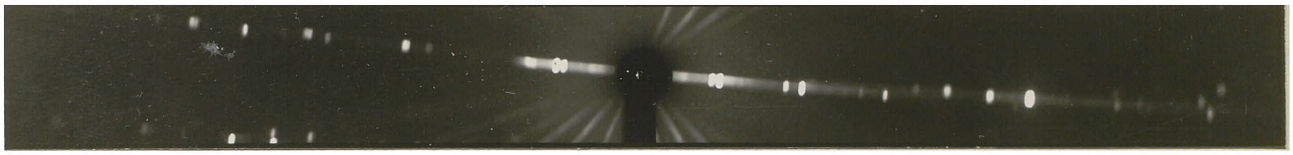


Fig. 34. Off-center Oscillation Pattern, 7.00 cm. radius. CuK Oscillated through 30°.

The crystal for this pattern was obtained by recrystallization from hot benzene. These crystals were larger andmore perfect than those from n-propyl alcohol. The crystal was oscillated through 30° with the "a" axis of the crystal in such a position as to record the h00 zone and at the same time the crystal was so placed to rotate about an axis lieing a few degrees from the c axis. By doing this it was possible to distinguish between the zones h00, h10, h20 etc., since these zones will each lie on essentially straight lines on the film and will lie a few degrees off from each other, all passing through the central spot.

The identification of the spots follows most easily from observations of the corresponding spots on the Weissenberg pattern noting the relative order of "d" values and the intensities of the interferences.

Shrinkage of the film, Eastman No-Screen, was determined by measurement of the total film length before and after development and found to be 0.5%. Corrections were then made on all the measured "radii" of the spots.

The c_o value measured on this film from the distance between the observed layer lines was 7.26 A.; however, the true c_o value may more accurately be determined from the powder pattern.

The a_o value was calculated from the measurement of the observed 600 spot and found to have a value 6 x 3.115 = 18.69±10A.

From the reciprocal lattice projection and the off center oscillation pattern the unit cell for acetaldehyde 2, 4 dinitrophenylhydrazone is tetragonal

a_o = 18.69 ±.10 A.

b_o = 7.14 ±.05

c_o = 7.14 ±.05

The axial ratio of 3.74 obtained from the optical measurement of the angle between thefaces, agrees within the experimental errors with the ratio of the above values (3.82). From the above unit cell data, the density and molecular weight, the number of molecules per unit cell is calculated to be 3.96, hence n = 4. The hkO interferences occur only where h+k = 2n, hOO only where h = 2n, OkO only where k = 2n, and OOl only where l = 2n; hence the space group is probably $P4_{2/n} - C4h^4$ (21).

Acetaldehyde 2, 4 Dinitrophenylhydrazone

Orange Needles

Preparation. In the course of preparing crystals of acetaldehyde 2, 4 dinitrophenylhydrazone a new modification of the crystals was observed. The usual habit of acetaldehyde 2, 4 dinitrophenylhydrazone when crystallized from n-propyl alcohol is plate-like and yellow in color. However, when the hot solution was observed during crystallization, and orange needle-like form of the crystal was seen growing until the temperature fell to approximately 75° C. when the yellow plate-like modification began to crystallize. At this temperature the solution was decanted. The crystals remaining in the bottom of the dish were predominantly of the orange needle-like form and were further separated from the yellow platelets under a binocular microscope to give pure samples. Attempts to prepare the orange needles in pure quantities by hot evaporation were not successful.

Properties. The melting point of the pure orange crystals is 165° C. (uncorrected). The two forms reported in the literature have melting points at 147° and 164° - 169° C. (7, 25). Apparently the orange needles are different from either of these forms. The compound melting at 164°- 169° may be identified as the yellow plate-like form. The modification melting at 147° has not been prepared. The depression in the melting point of mixture of the yellow and orange forms was not very large (m.p. 162°).

The density of the orange crystals as measured by floating in a mixture of ethyl bromide and methyl iodide was 1.51 ± .02 g/ml. The slight solubility and small size of the crystals made this

determination difficult.

Fig. 34_a is a photomicrograph of the orange needles. 50X. The angles, measured on the Weissenberg goniometer, between the faces parallel to the length of the needles were 63° and 117°. A definite cleavage plane was observed almost parallel to the 11 plane through the crystal.

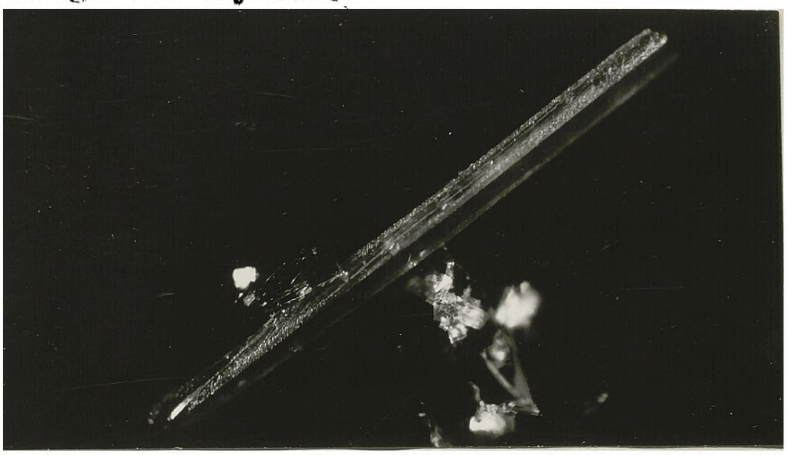


Fig. 34_a Photomicrpgraph of Orange Needle 50X.

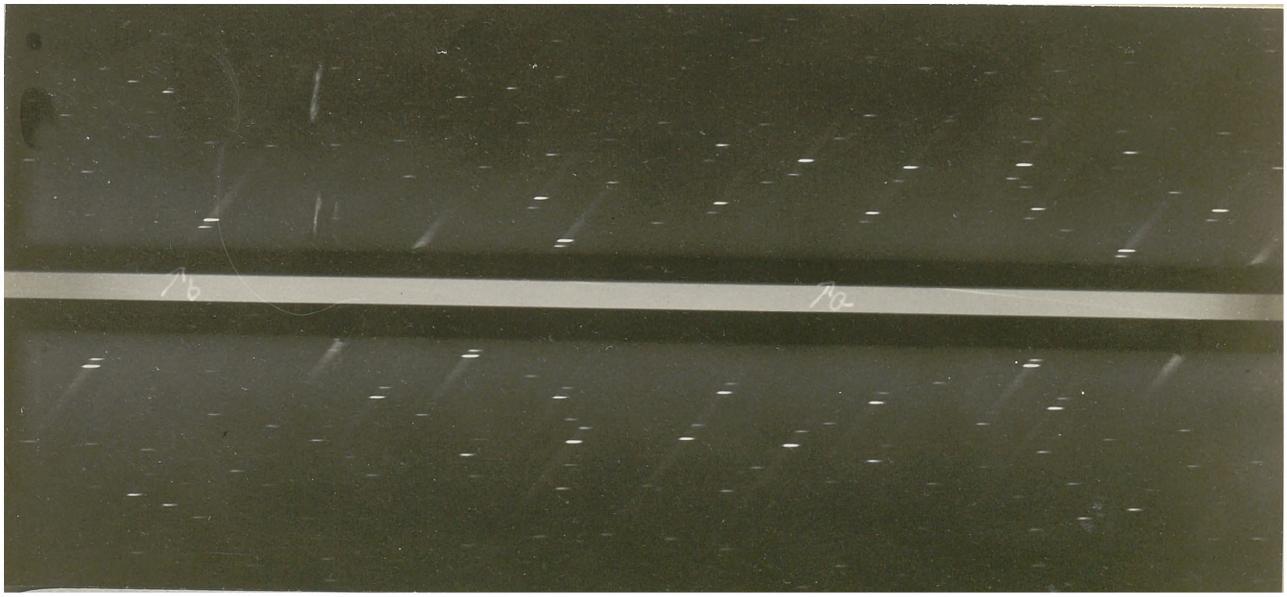


Fig. 35. Weissenberg Zero Layer Line Photograph, Crystal Rotated About the "c" Axis.

Experimental X-Ray Data. Fig. 35 is a Weissenberg zero layer line photograph of the needle-like crystal rotated about the "c" axis (length of crystal). The angle between the a and b axes is observed to be $90^{\circ} \pm 1^{\circ}$. The fact that the other unit cell angles α and β are 90° may be inferred from the fact that the zero layer line lays perpendicular to the c axis of crystal rotation. Extinctions are observed only for h00 and 0k0 interferences where h and k are odd.

For more accurate measurement of the unit cell values an oscillation pattern, fig. 36, and a powder pattern, fig. 37, were taken with the 7.00 cm. camera. In fig. 36 the crystal was mounted to oscillate 45° about an axis lying a few degrees from the "c" axis. The spots are tabulated in table IV, corrections being made for a 0.5% shrinkage of the film. The hkl values were easily indexed by observation of the relative "d" values and intensities on the Weissenberg pattern fig. 35. The relative intensity measurements in fig. 37 were measured by use of the microphotometer. If the powder patterns, figs. 37 and 32 of the two forms of acetaldehyde 2, 4 dinitrophenylhydrazone are compared they will be found to be surprisingly similar both in "c" values and intensities.

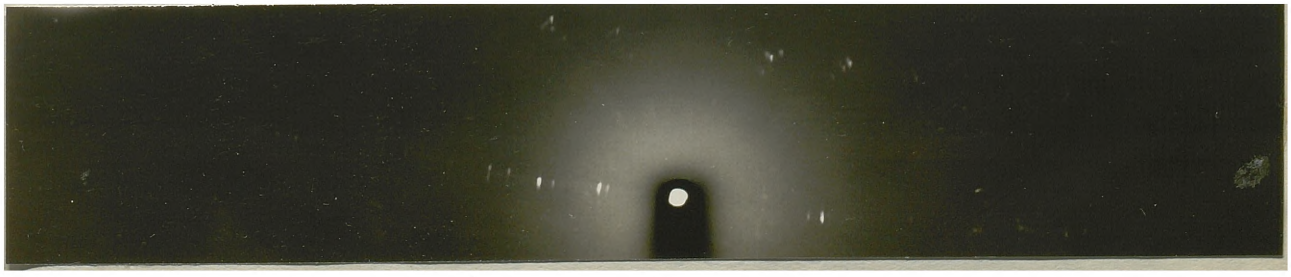


Fig. 36. Oscillation Pattern. 45° 7.00 cm. Radius, CuKα.

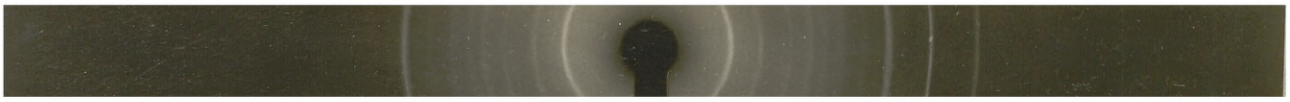


Fig. 37. Powder Pattern.

Table IV. Analysis of Oscillation Pattern, fig. 36.

#	R	D	D(corr.)	I	"θ"	hkl
1-R.	1.19	2.38	2.39	1.0	9.0	110
2.	2.00	4.00	4.02	1.0	5.38	020
3.	2.71	5.42	5.45	0.5	3.98	320
4.	3.27	6.54	6.57	0.1	3.30	230
5.	3.51	7.02	7.06	0.1	3.08	330
6.	3.90	7.80	7.84	0.2	2.78	430
7.	4.21	8.42	8.46	0.1	2.585	140
8.	4.76	952	9.57	0.1	2.300	240
9.	5.13	10.26	10.31	0.1	2.140	440
10.	5.43	10.86	10.91	0.2	2.025	350
11.	5.70	11.40	11.46	0.2	1.932	450
12.	6.02	12.04	12.10	0.1	1.834	550
13-L	2.00	4.00	4.02	1.0	5.38	020
14.	3.22	6.44	6.47	0.2	3.36	230
15.	4.11	822	8.26	0.2	2.645	040
16.	4.20	8.40	8.44	0.1	2.585	140
17.	5.41	10.82	10.87	0.2	2.934	350
18.	5.68	11.36	11.42	0.1	1.935	360
19.	6.00	12.00	12.06	0.1	1.840	370

Table V. Analysis of Powder Pattern fig. 37.

#	D	D(corr.)	I	"d"	hkl
1.	2.33	2.34	1.00	9.2	110
2.	3.18	3.19	0.38	6.8	210
3.	3.98	4.00	0.22	5.44	020
4.	4.55	5.47	0.32	4.73	011
5.	4.94	4.96	0.30	4.29	400
6.	5.42(d)	5.45	0.25	3.98	410, 320
7.	6.02	6.05	0.15	3.59	021
8.	6.75	6.78	0.92	3.20	121

The c_o value of the unit cell as calculated from the distance between the layer lines on fig. 36 is 5.06 ± .05 A. The a_o and b_o values were calculated from the data in tables IV and V. The unit cell may then be classed as Orthorhombic.

a_o = 17.3 ± .4 A. (4 x d400)

b_o = 10.6 ± .2 (4 x d040)

c_o = 5.06 ± .05 (rotation pattern)

The measurements on a_o were checked by calculation fro the "d" value of the 550 interference of fig. 36. a_o calculated this way equals 17.5 A. Furthermore, the external faces parallel to the length of thecrystal are identified as 110 faves since the axial ratio b_o/a_o determines and angle of 31.8° which is very nearly equal to half the angle 63° observed between the vaces as measured on the Weissenberg goniometer.

Using the extinction data the space group is probabley $P2_12_12$ or $P2_12_12_1$. The Weissenberg patterns being difficult to obtain, with the crystal rotated about any axis other than the c axis, the complete extinction data were not available.

The above unit cell dimensions together with a molecular weight of 224 and a density of 1.51 determines the number of molecules per unit cellas 3.88, the true value probably being 4. Both of the above space groups contain 4 equivalent positions per unit cell.

Crotonaldehyde 2, 4 Dinitrophenylhydrazone

Preparation. The crotonaldehyde 2, 4 dinitrophenylhydrazone sample was prepared by adding crotonaldehye to a solution of methyl alcohol and hydrogen chloride (approximately 2N.). The crystals were filtered and washed with ethyl alcohol, then recrystallized slowly from hot benzene forming in brilliant red needles.

Properties. Fig. 38 is a photomicrograph of a group of these crystals. The melting point, 190°C., of these crystals agrees with the literature (26). The density of the crystals as measured by floating in a mixture of ethylene chloride and carbon tetrachloride was 1.43±.01 g/ml.



Fig. 38. Photomicrograph of red crystals 20X

Experimental X-Ray Data. Fig. 39 is a zero layer line Weissenberg photograph of the crystal rotated about the "c" axis. From this photograph the unit cell values are roughly

$\gamma = 90°$, $a_o = 17.8$ A., $b_o = 12.3$ A.

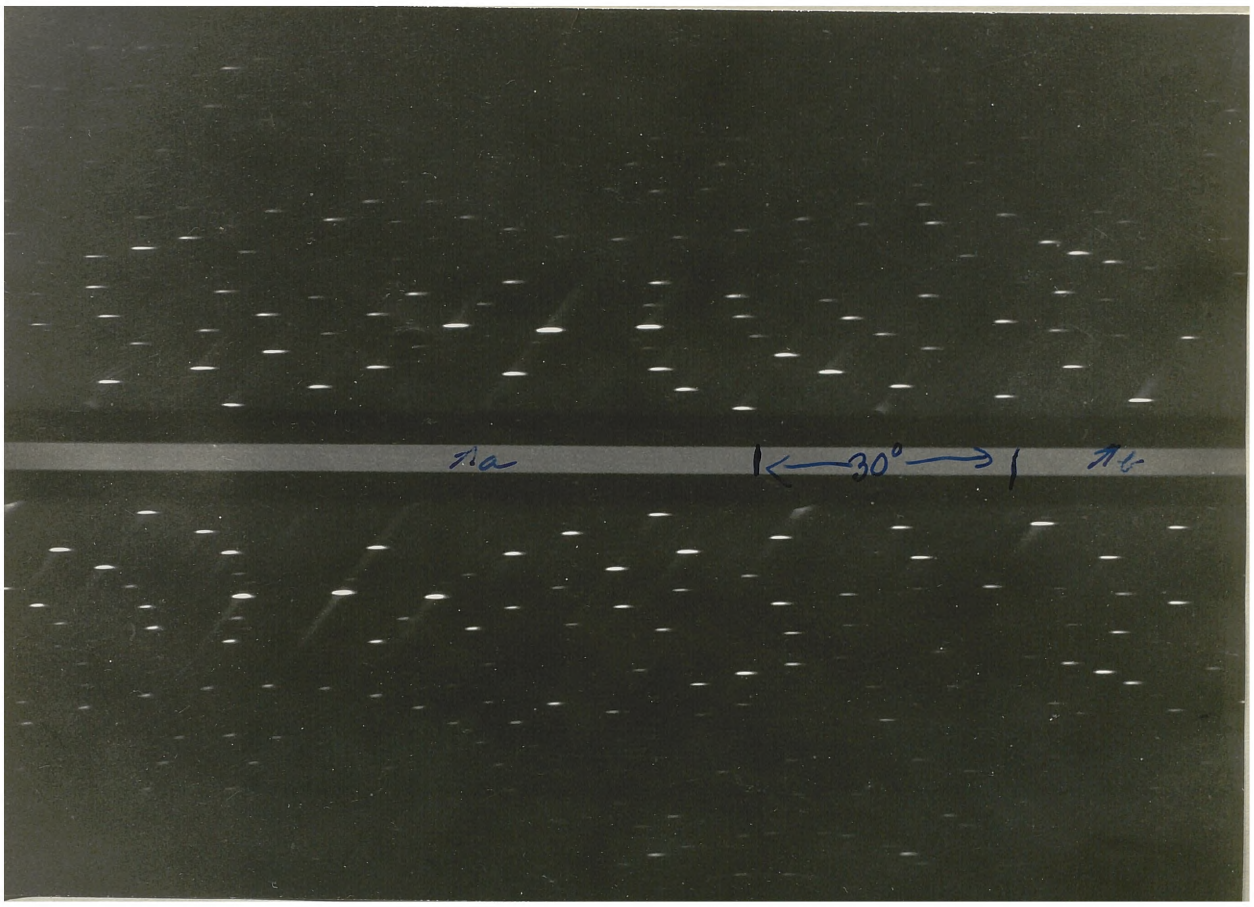


Fig. 39. Weissenberg Zero Layer Line Weissenberg photograph, Crystal Rotated about "c" Axis.

Extinctions occur for h00 and 0k0 only where h and k are odd. Fig. 40 is the first layer line equi-inclination Weissenberg photograph with the crystal rotated about the "c" axis. Systematic extinctions appear to exist for h0l where h is odd. The 401 interference appears to be unusually intense and is probably an indication of the orientation of the molecule in the unit cell.

The fact that the 0kl zone is not a straight line in fig. 40 indicates that the angle α of the unit cell is slightly different from 90°.

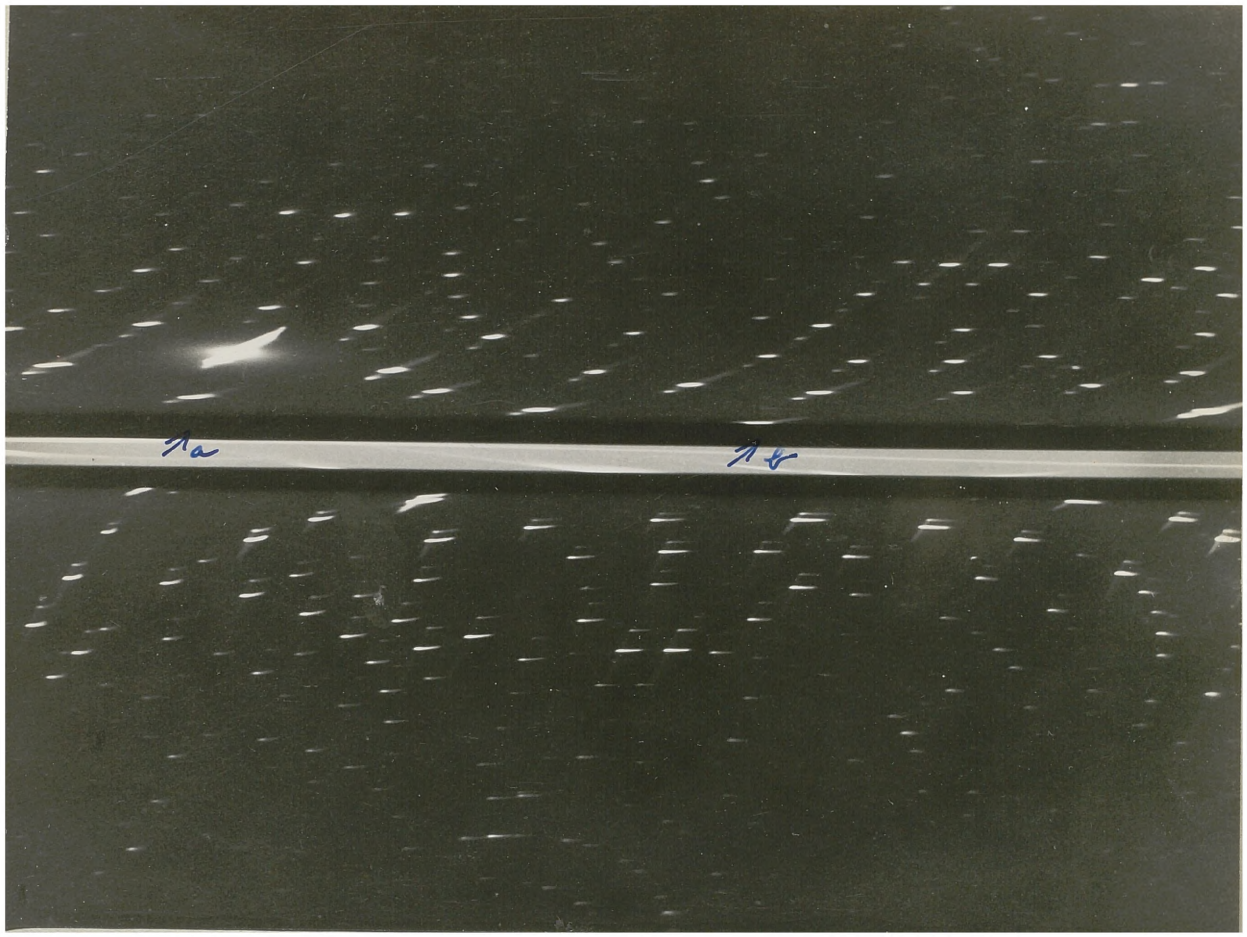


Fig. 40. Weissenberg First Layer Line Equi-Inclination Photograph. Crystal Rotated about "c" Axis.

For more accurate measurements of the unit cell values, a_o and b_o and c_o, an oscillation pattern (30°), fig. 41, was analyzed. The c_o value calculated from the distance between the layer lines was 4.63 A. correction being made for a 0.5% shrinkage of the film.

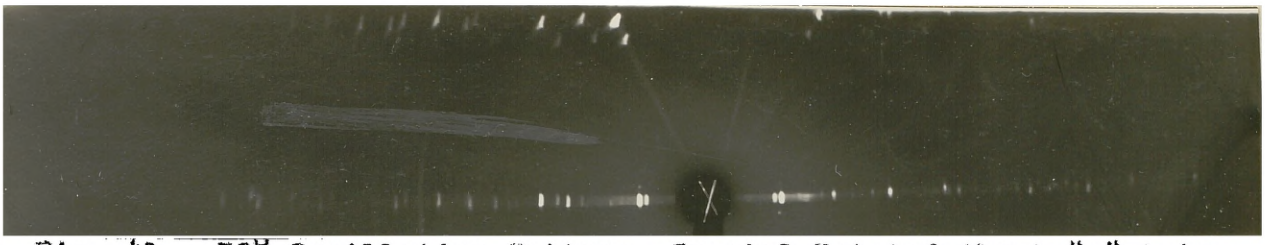


Fig. 41. 30° Oscillation Pattern. Crystal Rotated About "c" Axis.

Table VI lists the data obtained from measurements on the interferences lieing on one side of the zero layer line. The range of oscillation was determined by visual observation of the oscillation and Weissenberg patterns. This range of oscillation is marked in ink on the Weissenberg pattern fig. 39. The spots were identified by comparison of the relative "d" values and intensities.

The b_o value calculated from the 080 interference on this oscillation pattern is 8 x 1.635 or 13.08 ± .05 A. a_o may not be calculated directly from this pattern since no h00 spots were recorded on it; however, from calculation of the 360 spot (#13) a_o equals 18.90 ± .50 A.

Fig. 42 is a powder pattern of the sample taken with the 7.00 cm. camera. Table VII lists the data from this pattern.

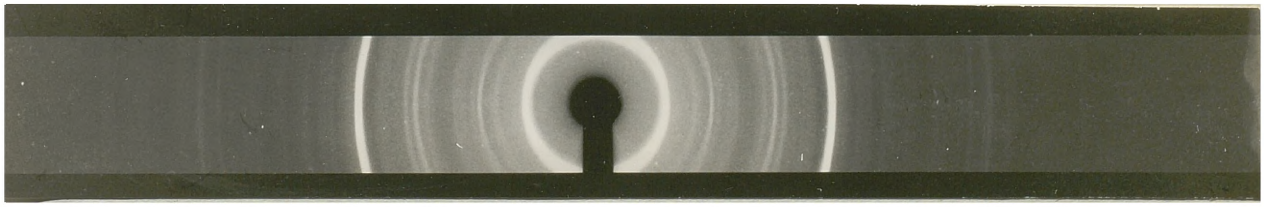


Fig. 42. Powder Pattern. 7.00 cm. Radius. CuK$_\alpha$ Radiation.

Assuming = 90° the unit cell is Orthorhombic

a_o = 18.90 ± .60 A.

b_o = 13.08 ± .05

c_o = 4.63 ± .05

Table VI. Oscillation Pattern Data: Crotonaldehyde 2, 4 Dinitrophenylhydrazone. 7.00 cm. Radius. CuK_α

#	R	D	D(corr.)	I	"d"	p	hkl
1.	1.00	2.00	2.01	10	10.7	2.01	110
2.	1.75	3.50	3.52	0.4	6.12	3.50	120
3.	2.00	4.00	4.02	0.1	5.38	4.00	220
4.	2.54	5.08	5.11	0.5	4.19	5.07	130
5.	3.31	6.62	6.65	0.3	3.26	6.58	040
6.	3.38	6.76	6.80	0.1	3.19	6.72	140
7.	3.51	7.02	7.06	0.2	3.09	6.96	240
8.	3.73	7.46	7.50	0.1	2.91	7.40	340
9.	4.31	8.62	8.67	0.1	2.525	8.52	250
10.	4.49	8.98	9.02	0.2	2.432	8.89	350
11.	5.02	10.04	10.10	0.2	2.183	9.89	060
12.	5.17	10.34	10.40		2.123	10.15	260
13.	5.33	10.66	10.72		2.060	10.45	360
14.	5.96	11.92	11.99		1.850	11.61	170
15.	6.82	13.64	13.71		1.635	13.71	080
16.	7.86	15.72	15.80		1.431	11.98	290
17.	8.16	16.32	16.40		1.392	15.58	490
18.	8.77	17.54	17.63		1.310	16.52	1 10 0
19.	9.36	18.72	18.82		1.237	17.40	1 11 0
20.	9.62	19.24	19.34		1.208	17.84	2 11 0
21.	10.40	20.80	20.92		1.149		

Table VII Powder Pattern Data: Crotonaldehyde 2, 4 Dinitrophenyl-hydrazone. 7.00 cm. Radius. CuK_{α}

#	D	I	"d"	p	hkl
1.	1.99	1.0	10.9	1.99	110
2.	2.80	0.2	7.70	2.79	210
3.	3.27	0.3	6.60	3.26	020
4.	3.48	0.1	6.20	3.47	120
5.	3.80	0.1	5.67	3.78	310
6.	3.99	0.1	5.43	3.97	220
7.	4.78	0.2	4.43	4.75	320
8.	5.18	0.4	4.15	5.14	201 111
9.	5.35	0.3	4.05	5.31	230
10.	6.65	1.0	3.26	6.59	401
11.	6.74	1.0	3.22	6.68	520,321,140
12.	10.63	0.2	2.078	10.39	
13.	11.14	0.2	1.986		

The number of molecules per unit cell as calculated from the density, 1.43, molecular weight, 251, and the above unit cell values equals 3.97 or 4.

The space group is probably $P2_12_12$ or $P2_12_12_1$; however, other possibilities exist since complete extinction data are not available.

Butyraldehyde 2, 4 Dinitrophenylhydrazone

Preparation: Three crystallographically different butyraldehyde 2, 4 dinitrophenylhydrazones have been identified. The more stable form grows in yellow needles while the second grows in orange needles and the third in amber platelets. The samples were prepared in the same manner as the other derivatives using a hydrogen chloride methyl alcohol solution of 2, 4 dinitrophenylhydrazine. The two needle-like forms have been identified crystallizing from methyl alcohol, ethyl alcohol, benzene, and acetone, hence they can not be alcoholates. When the crystallization from methyl alcohol was allowed to proceed rapidly the resulting mass of crystals was orange in color. When these crystals were allowed to stand in the methyl alcohol for three hours they were observed to be almost entirely converted to an equal mass of yellow crystals. X-ray powder photographs proved that this change occurred in the crystallographic system of the compound (see figures 47 and 52).

Properties of the Yellow Needles: The melting point of the yellow needles was observed to be 123°C. (uncorrected). The literature records melting points of 122° C. (4) and 123° C. (3, 27). The density of these crystals was not determined since they dissolved too readily in the organic solvents used for density measurements; however, the density was found to lie within the limits of 1.36 and 1.43 g/ml. Fig. 43 is a photomicrograph of the yellow needles obtained by evaporation of an acetone solution. No definite cleavage plane was observed.

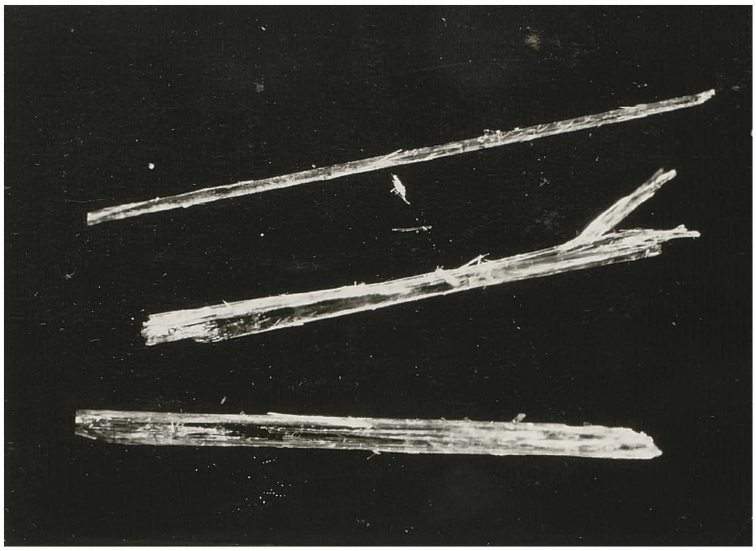


Fig. 43. Photomicrograph of the yellow needles. 100X

Experimental X-Ray Data - Yellow Needles: Fig. 44 is a 30° oscillation pattern of a crystal rotated about the "c" axis. The co value calculated from this pattern was 4.90 A. Fig. 45 is a Weissenberg zero layer line photograph of a yellow needle rotatedd about the "c" axis, while fig. 46 is a Weiss equi-inclination photograph of the first layer line. The crystal used in these patterns was obviously twinned; however, one "orientation" predominates. Upon superimposing these patterns (fig. 45 and 46) the extinctions become:

h10	present	only	when	$k = 2n$
hk0	"	"	"	$h + k = 2n$
h00	"	"	"	$h = 4n$
0k0	"	"	"	$k = 4n$
h01	"	"	"	$h = 4n$
hkl	"	"	"	$h = 2n$
hkl	absent	when		$h = 2n$, $k = 2n$

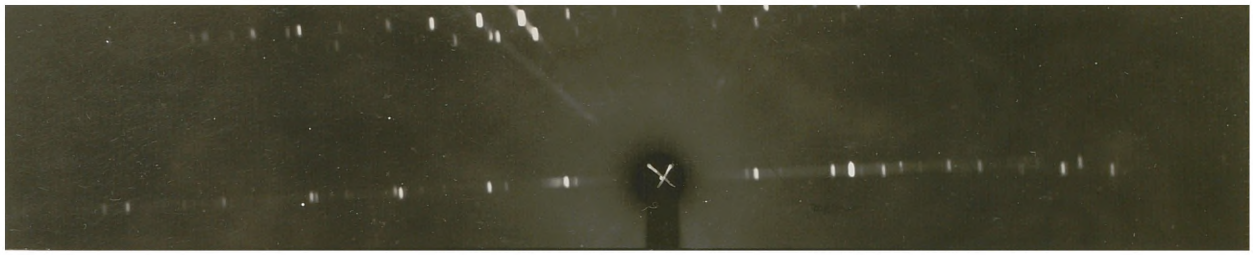


Fig. 44. 30° Oscillation Pattern Crystal Rotated About "c" Axis. Yellow Needles.

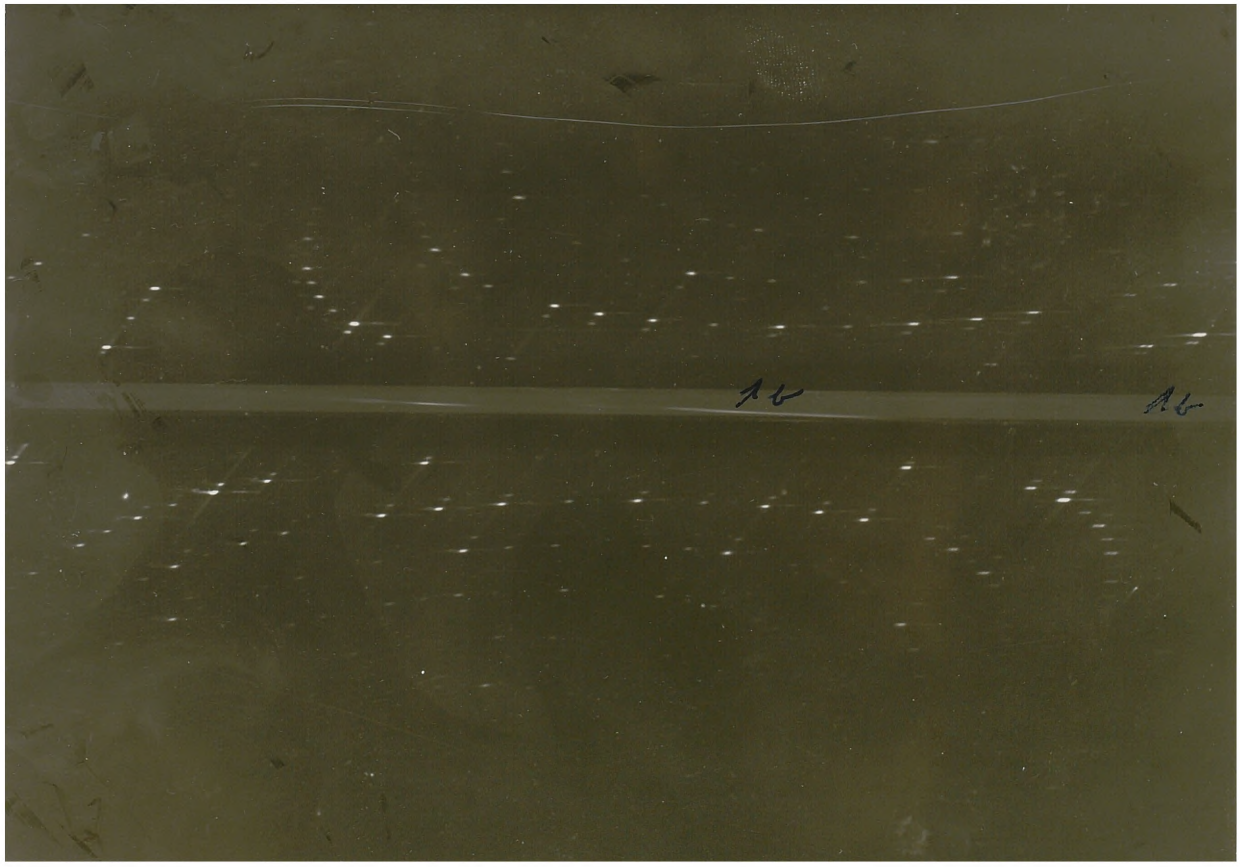


Fig. 45. Weissenberg Zero Layer Line Photograph. Crystal Rotated About "c" Axis. Yellow Needles.

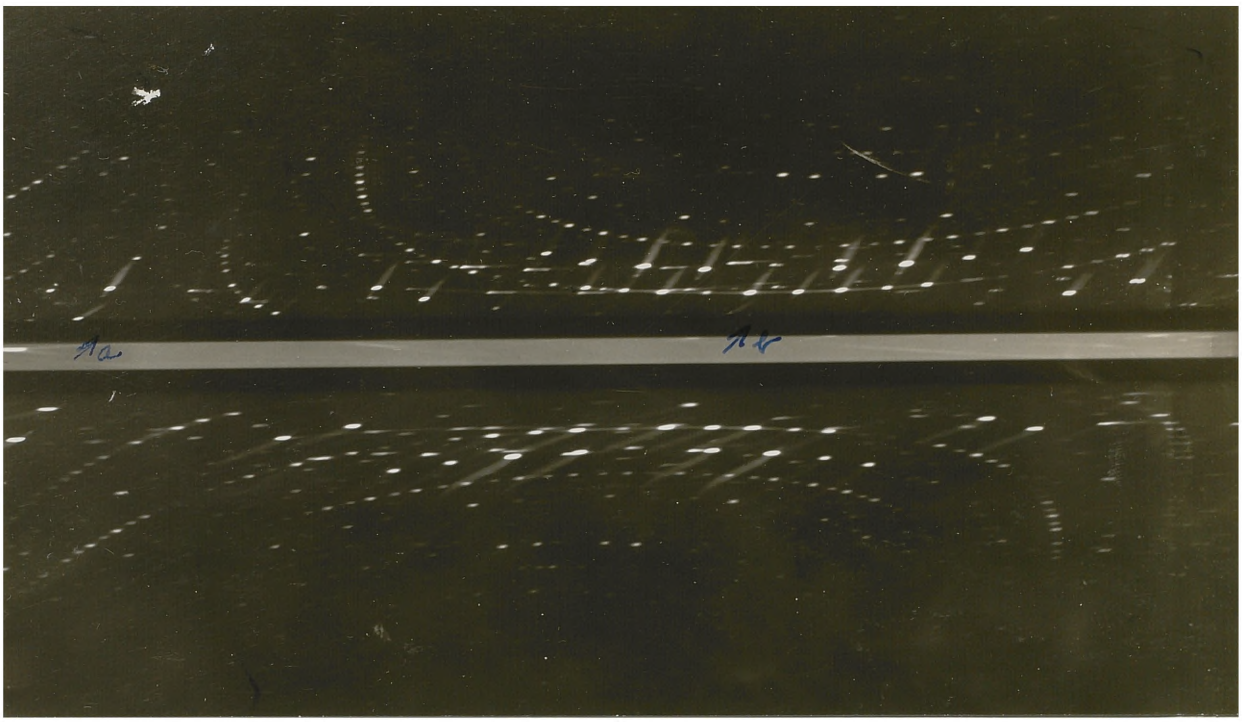


Fig. 46. Weissenberg First Layer Line Equi-inclination Photograph. Crystal Rotated About "c" Axis. Yellow Needles.

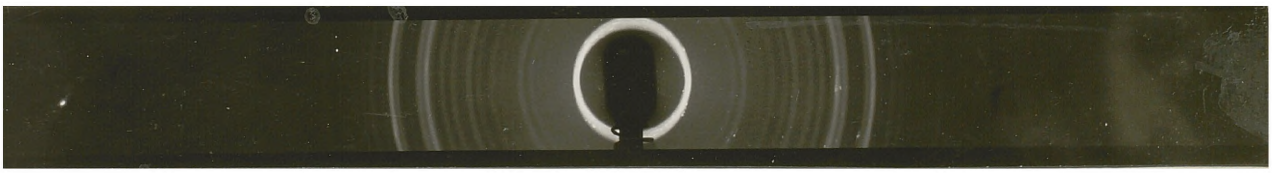


Fig. 47. Powder Pattern. Yellow Needles. 7.00 cm. radius. CuK_{α}.

Knowing these extinction data the unit cell dimensions were calculated roughly from the Weissenberg pattern (fig. 45) and are:

$\gamma = 90^{\circ}$ $(\alpha = \beta = 90^{\circ})$

$a_o = 54 \pm 3.0$ Å $(42 \times d_{4800})$

$b_o = 17.9 \pm 1.00$ $(12 \times d_{0124})$

$c_o = 4.90 \pm .05$

Fig. 47 is the powder pattern of the yellow needles. The data from this pattern are tabulated in Table VIII. The hkl values were determined by visual comparison with the Weissenberg pattern (fig. 45.). The relative line intensities were calculated from the microphotometer tracing of fig. 47.

Table VIII.Powder Pattern. N-butyl 2, 4 dinitrophenylhydrazine

Yellow Needles

#	D	I	"d"	hkl
1.	1.54	1.0	14.0	400
2.	2.86	.05	7.60	420
3.	3.14	.08	6.85	800
4.	3.68	.03	5.86	620
5.	3.92	.04	5.52	820
6.	4.33	.05	5.00	1020
7.	4.48	.09	4.70	1200
8.	4.70		4.42	.040
9.	5.20	.07	4.24	
10.	5.33	.07	4.05	
11.	5.77	.32	3.77	
12.	5.99	.18	3.63	
13.	6.30	.03	3.44	
14.	6.60	.13	3.29	
15.	6.77	.31	3.21	
16.	6.95	.03	3.12	
17.	7.30	.05	2.98	
18.	7.53	.03	2.98	

Properties.- Orange Needles: The melting point of the orange needles was 122° C. This melting point is observed to be very close to that of the yellow form. Likewise, the melting point of a mixture of the two froms is very nearly the same (121-122°C.). The density of the orange form lies in the same range as that of the yellow form, i.e. 1.26-143 g/ml. Fig. 48 is a photomicrograph (20X) of these orange needles. A cleavage plane is observed almost

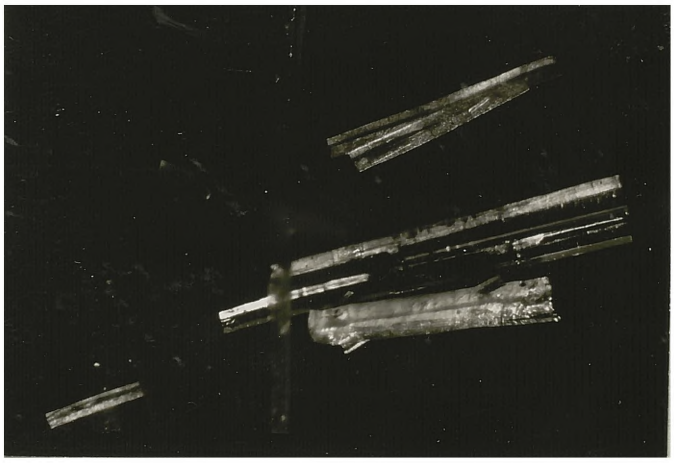


Fig. 48. Photomicrograph of Orange Needles 20X

parallel to the 001 plane (c axis through the length of the needle).

Experimental X-Ray Data - Orange Needles: Fig. 49 is a rotation pattern, 3.5 cm. radius, of the orange needles. The c_o value calculated from the distance between the layer lines is 7.0 A. Fig. 50 is a Weissenberg zero layer line photograph with the crystal rotated about the "c" axis. Fig. 51 is the first layer line equi-inclination pattern. From these two patterns the extinction data are:

h00 present only where h = 2n

0k0 " " " k = 2n

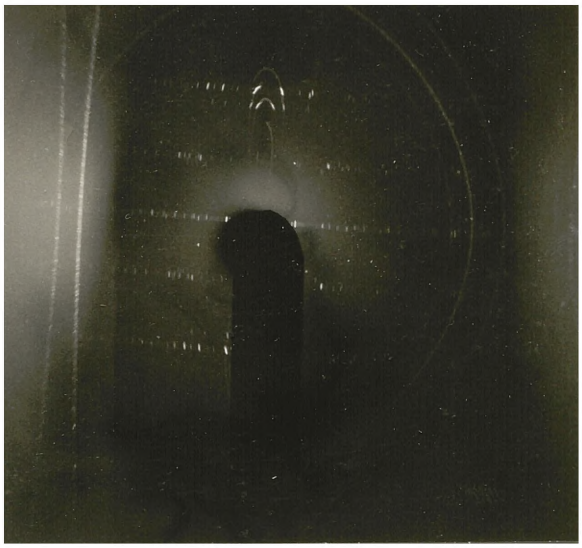


Fig. 49. Rotation Pattern of Orange Needles 3.5 cm. radius.

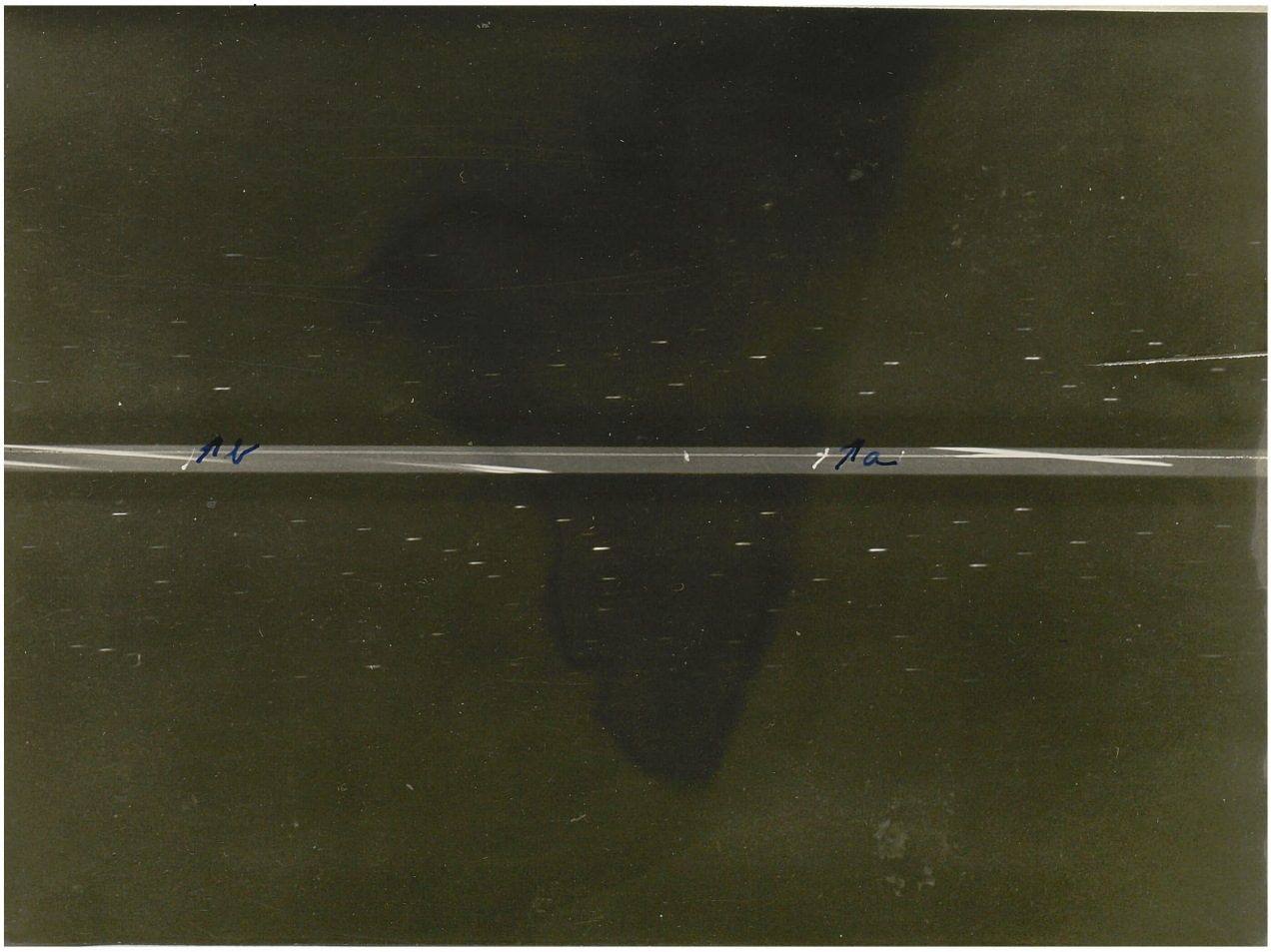


Fig. 50. Weissenberg Zero Layer Line Photograph- Orange Needles.

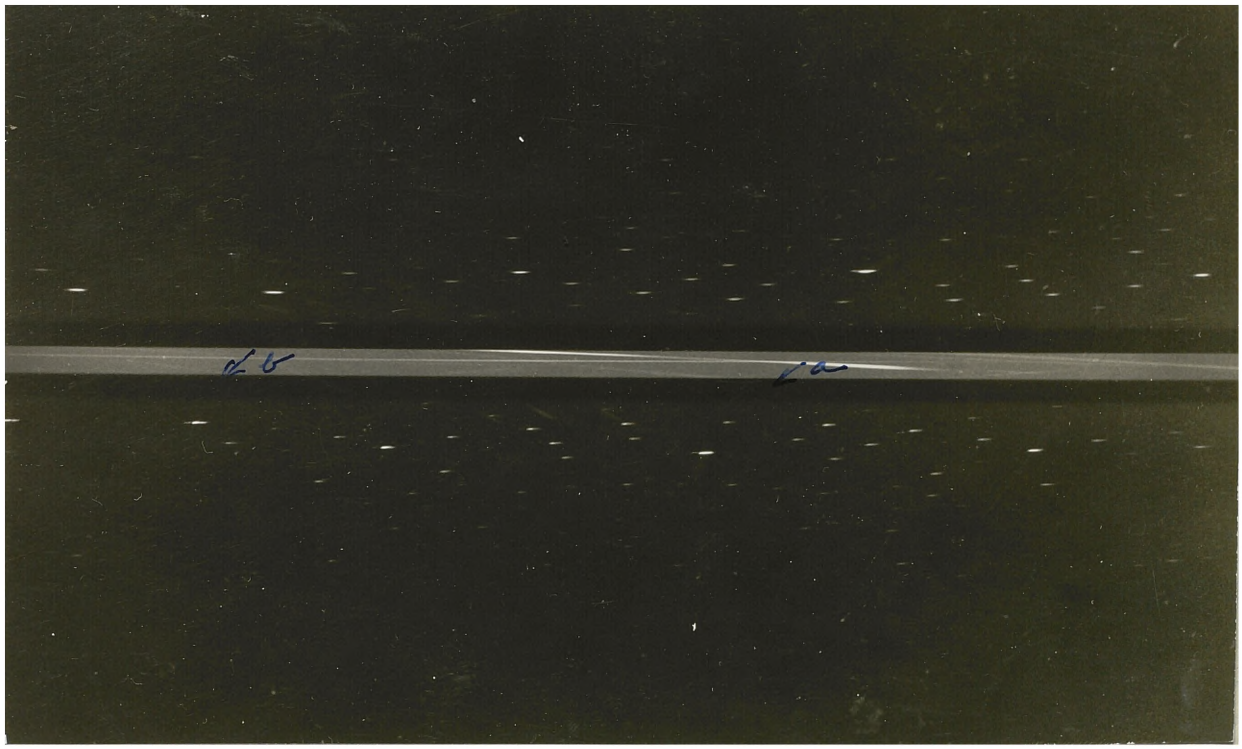


Fig. 51. Weissenberg First Layer Line Equi-Inclination Photograph. Orange Needles.

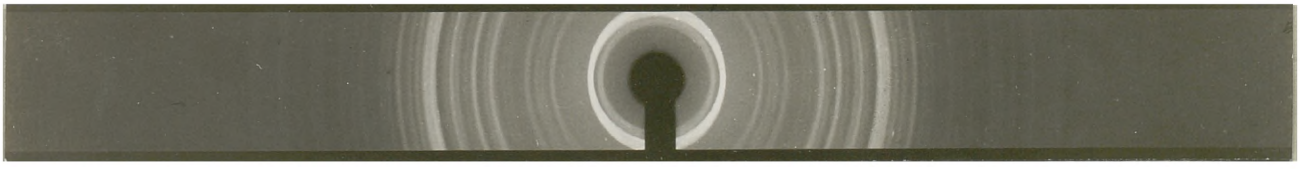


Fig. 52. Powder Pattern of Orange Needles. 7.00 cm. radius.

hk0 Present only where k= 2n

h0l " " " h = 2n

0kl " " " k = 2n + 1

From these Weissenberg patterns and the rotation pattern, the unit cell is orthorhombic.

a_o = 25.8 ± 1.0 A.

b_o = 25.0 ± 1.0

c_o = 7.0 ± 0.2

Fig. 52 is the powder pattern of the orange form. The sample used here, though appearing under the microscope to be of the pure orange crystals, may have contained some of the yellow crystals since a number of the lines in fig. 52 are common with those in fig. 48. Table IX lists the "d" values and relative intensities as measured with the microphotometer.

Table IX. Data From Powder Pattern of Orange Needles

#	D	I	"d"
1.	1.58	0.16	13.7
2.	1.85	1.00	11.7
3.	2.91	0.12	7.42
4.	3.17	0.08	6.80
5.	3.32	0.08	6.50
6.	3.59	0.10	6.00
7.	4.11	0.05	5.26
8.	4.29	0.05	5.05
9.	4.60	0.22	4.64
10.	4.79	0.09	4.41
11.	5.09	0.26	4.20
12.	5.29	0.09	4.08
13.	5.57	0.13	3.90
14.	5.72	0.23	3.80
15.	6.20	0.38	3.50
16.	6.24	0.29	3.48
17.	6.44	0.29	3.37
18.	6.69	0.13	3.24
19.	6.89	0.10	3.15
20.	7.20	0.12	3.03
21.	7.43	0.05	2.94

Amber Platelets: The third modification in which n-butyraldehyde 2, 4 dinitrophenylhydrazone crystallizes is in the form of amber platelets as seen from the photomicrograph fig. 53. These crystals were observed forming during the initial crystallization of



Fig. 53. Photomicrograph of Amber Platelets 20X

were observed forming during the initial crystallization of the derivative from the HCl-methyl alcohol solution. Successive recrystallization of these amber platelets resulted in the formation of the yellow and orange needles and was confirmed by the powder patterns of the recrystallized samples. The melting point of the amber platelets occurred at 122° C. (uncorrected). Fig. 54 is the powder pattern of these crystals. The absence of the inner intense lines of the yellow and orange needles indicates that this sample must have been essentially pure. Table X lists the data from this powder pattern.

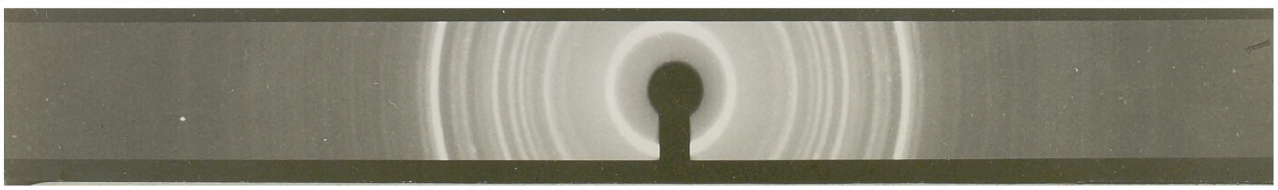


Fig. 54. Powder Pattern of Amber Platelets. 7.00 cm. Radius.

Table X. Data from Powder Pattern of Amber Platelets.

#	D	I	"d"
1.	1.71	1.00	12.6
2.	2.98	0.03	7.2
3.	3.12	0.04	6.9
4.	3.32	0.03	6.5
5.	3.47	0.20	6.25
6.	3.96	0.08	5.45
7.	4.18	0.14	5.18
8.	4.47	0.15	4.86
9.	4.91	0.26	4.33
10.	5.17	0.08	4.17
11.	5.42	0.05	4.00
12.	5.79	0.13	3.76
13.	6.12	0.09	3.55
14.	6.60	0.83	3.28
15.	6.79	0.08	3.20
16.	7.01	0.03	3.11

Furfuraldehyde 2, 4 Dinitrophenylhydrazone

Preparation: The two generally reported forms of furfuraldehyde 2, 4 dinitrophenylhydrazone have been investigated crystallographically. The samples were prepared in a manner similar to the other 2, 4 dinitrophenylhydrazones using freshly distilled furfuraldehyde b. p. 157.5-158.5° C. Bredereck (9) has observed two forms of 2, 4 dinitrophenylhydrazones of a number of furans, in particular furfuraldehyde. The red form was reported to have been prepared by recrystallization from pyridine while the yellow modification was prepared by recrystallization from acetone and ethyl alcohol. It has been found possible in this laboratory to prepare both of these forms in a fairly purestate by recrystallization from the same solvent, ethylene chloride. Apparently the key to the formation of these two modifications is the temperature at which crystallization occurs. The red form was prepared by keeping the temperature above 85° C. during crystallization. These crystals formed in ruby red pyramides, usually twinned, as observed in fig. 54. The yellow modification was prepared by evaporation of the ethylene chloride solution at room temperature

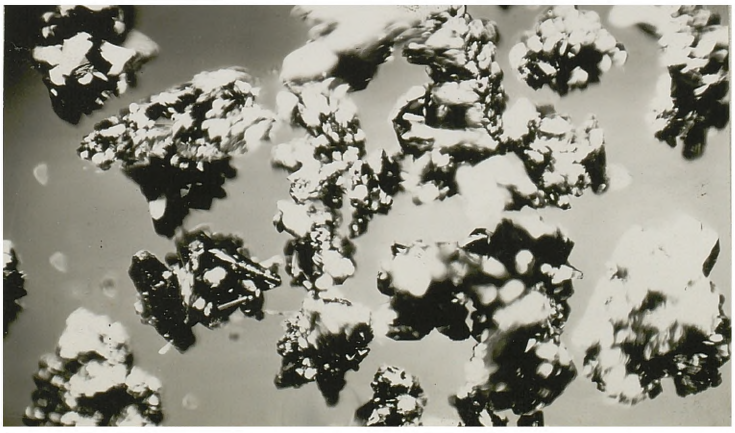


Fig. 54. Photomicrograph of Red Crystals, 50X.



Fig. 55. Photomicrograph of Yellow Needles 50X

producing the yellow needles shown in fig. 55. The melting point of thered form was observed to be 217° C. The yellow needles melted at 199° C. while 212-214° is the previously reported melting point (9). These two forms of the furfuraldehyde derivative have been observed and identified crystallizing from ethyl alcohol, ethyl acetate, and ethylene chloride solutions; hence the two forms can hardly be classed as alcoholates.

Experimental X-Ray Data: Fig. 56 is arotation pattern, 3.5 cm. radius, of one of the yellow needles rotated about the "c" axis. The unit cell value, c_o, calculated from this pattern is 3.62 A.

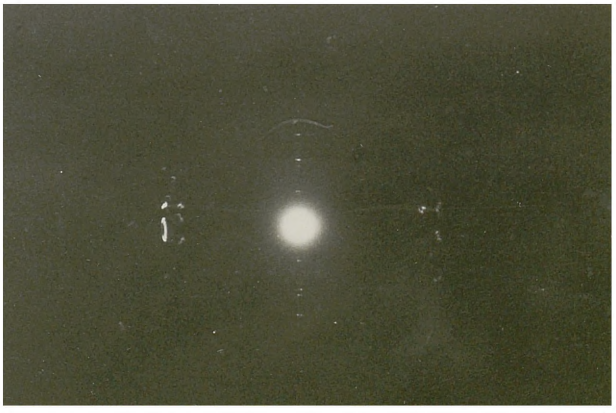


Fig. 56. Rotation Pattern 3.5 cm. radius, Yellow Needles.

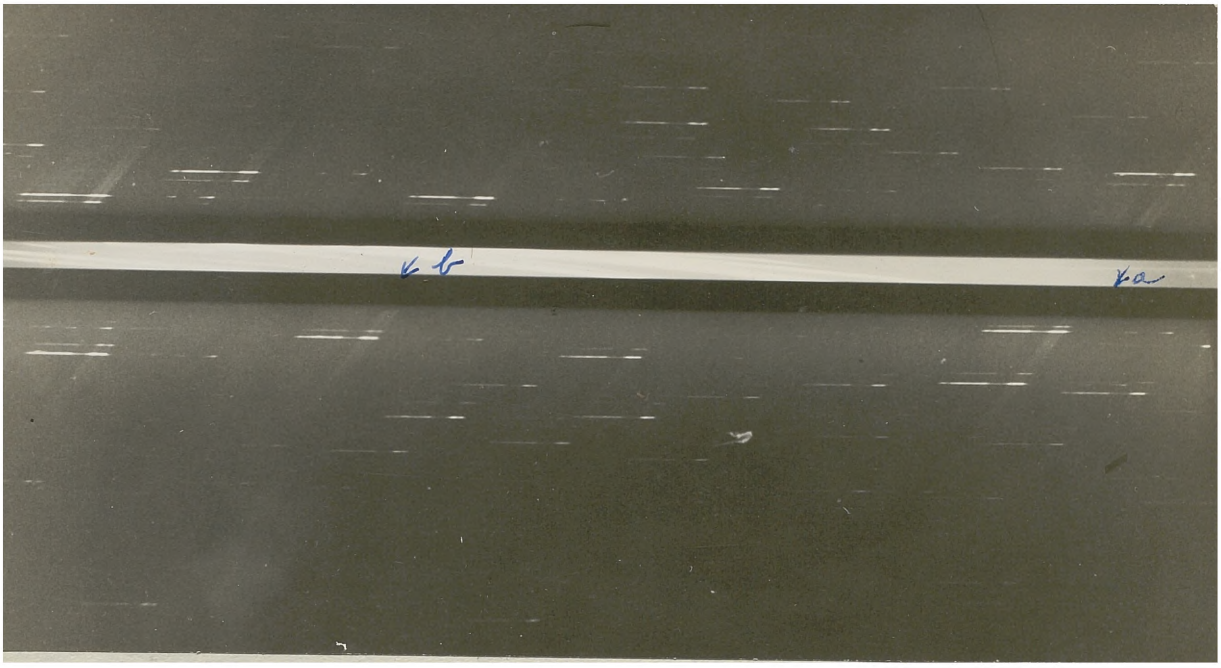


Fig. 57. Weissenberg Zero Layer Line Photograph. Yellow Needles.

Fig. 57 is a Weissenberg zero layer line photograph of one of the yellow needles. This needle was obviously poorly formed; however, a rough estimation of the unit cell may be made from this pattern. Fig. 58 is a powder pattern of the yellow needles. The data from this pattern is listed in table XI. Then intensity data were obtained from the microphotometer tracing. The hkl values were determined by visual comparison with the Weissenberg pattern.

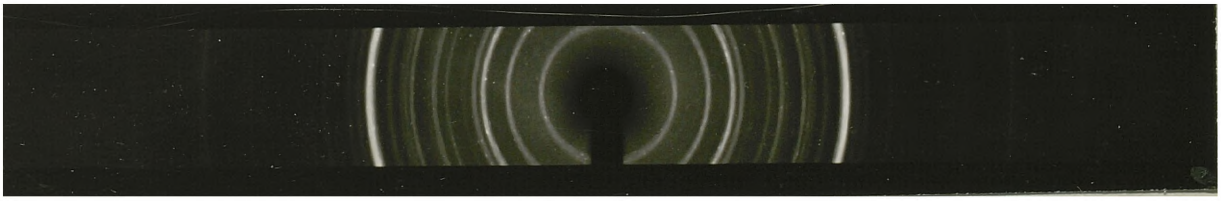


Fig. 58. Powder Pattern of Yellow Needles. 7.00 cm. Radius.

Table XI. Data for Powder Pattern of Yellow Needles.

#	D	I	"d"	hkl
1.	1.84	0.29	11.7	100
2.	2.80	0.34	7.7	010
3.	3.47	0.50	6.17	110
4.	3.74	0.23	5.77	200
5.	4.00	0.04	5.42	
6.	4.51	0.12	4.81	
7.	4.57	0.10	4.57	
8.	4.86	0.20	4.36	
9.	5.01	0.05	4.25	
10.	5.48	0.13	3.96	
11.	5.74	0.11	3.85	020
12.	5.77	0.05	3.78	
13.	6.10	0.04	3.56	
14.	6.65	1.00	3.26	
15.	6.96	0.10	3.12	
16.	7.22	0.09	3.01	
17.	7.91	0.08	2.76	
18.	10.26	0.06	2.154	

From these data the unit cell for the yellow form of furfuraldehyde 2, 4 dinitrophenylhydrazone is monoclinic.

$a_o = 11.7 \pm 0.5$ A. $\quad \gamma = 95^o$

$b_o = 7.7 \pm 0.5$

$c_o = 3.62 \pm 0.5$

No systematic extinctions are observed on fig. 57. Although layer line Weissenberg patterns might show that one ormoreof the above unit cell dimensions are half of the actual value because of systematic extinctions, it appears as though this were a primitive unit cell with the probable space group $P_m - C_s^1$ (21). The number of molecules per unit cell as calculated from the above unit cell values, a molecular weight of 276, and a reasonable density is one; hence the unit cell determines the actual size of the molecule.

The red form of furfuraldehyde 2, 4 dinitrophenylhydarzone crystallizes in even smaller crystals than the yellow variety; hence no Weissenberg patterns were obtained. Fig. 59 is an oscillation pattern giving one unit cell dimension of 7.85 0.05 A.

Fig. 60 is the powder pattern. The large amount of background is

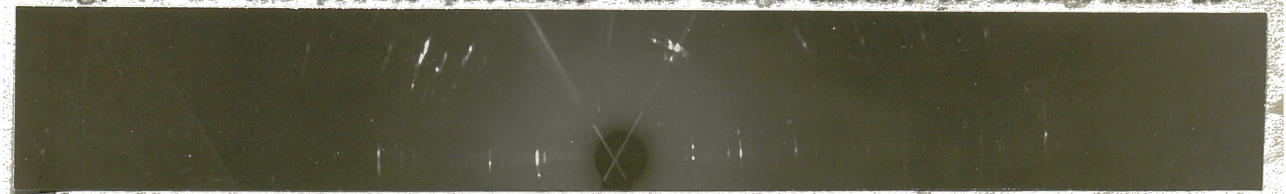


Fig. 59. Oscillation Pattern 7.00 cm. Radius. Red Crystal.

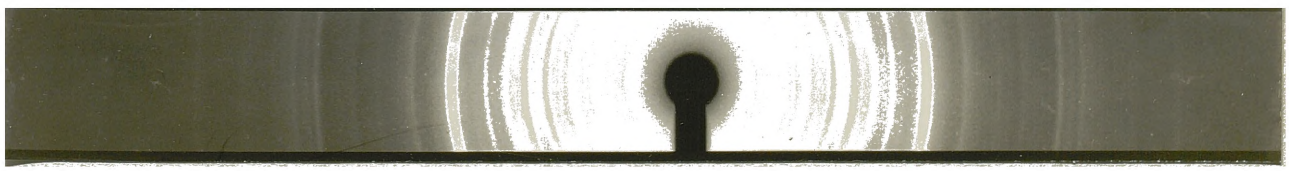


Fig. 60. Powder Pattern. 7.00 cm. Radius. Red Crystals.

difficult to account for unless the sample is impure. Though a microscopic examination did not indicate any crystals of the yellow variety in this ample, the lines common to figures 58 and 60 would seem to indicate that there was. Table XII lists the data obtained from fig. 60. The high intesity of the line with a "d" value of 3.25 seems to be common in both of these samples. This "d" value is probably indicative of the distance between the layers of molecules in the crystals.

Table XII. Data from Powder Pattern of Red Crystals.

#	D	I	"d"
1.	1.87	0.03	11.7
2.	2.82	0.03	7.85
3.	3.03	0.03	7.14
4.	3.49	0.04	6.17
5.	3.77	0.03	5.75
6.	4.05	0.17	5.35
7.	4.62	0.29	4.62
8.	5.00	0.05	4.25
9.	5.55	0.03	3.92
10.	5.71	0.06	3.80
11.	5.99	0.03	3.63
12.	6.65	1.00	3.26
13.	7.75	0.03	2.82
14.	10.41	0.05	2.12

Qualitiative X-Ray Analysis of Aldehydes in Micro Quantities

Introduction: The preceeding tables of "d" values from the powder patterns of the aldehyde 2, 4 dinitrophenylhydrazones offers a system of qualitative analysis. The amount of the 2, 4 dinitrophenylhydrazine derivative necessary for an x-ray powder pattern is about 0.1 - 0.5 mg.; however satisfactory single crystal patterns have been taken of crystals smaller than 10^{-6}cc. (1 (1 microgram). The amount of aldehyde necessary to prepare a sufficient quantity of the 2, 4 dinitrophenylhydrazine derivative for x-ray powder patterns depends upon the technique of crystallization. Fortunately, the required degree of purity is not nearly as great as that required for melting point determinations and the impurities themselves may be determined if present in quantities greater than 5%.

Apparatus: The apparatus necessary for preparing the derivative in micro quantities may be easily assembled from glass tubing and commercial semi-micro equipment. The essential equipment consists of:

1. Eye droppers with the ends drawn into short capillary tubes.
2. Small centrifuge tubes.
3. Centrifuge
4. Cellulose Acetate tubes
5. X-Ray Powder Camera
6. X-Ray and Photographic equipment.

The small centrifuge tubes should have the bottom constricted to collect the precipitate into a compact small space.

The cellulose acetate tubes are prepared in a manner similar to that described by Fricke and Lhorman (28). These tubes have been found to be quite uniform in size, produce very little scattering of the x-ray beam, are remarkably strong, serve as a permenent mounting for the sample and may be prepared easily. These tubes are prepared by dipping a copper or chromel wire, size 19-26 into a solution of cellulose acetate, prepared by dissolving 12 grams of dry powdered cellulose acetate in a mixture of 90 grams of chloroform and 10 grams of ethyl alcohol (95%), allowing the solution to drain uniformly from the wire, drying for aperiod of several hours, then stretching the wire to loosen the coat of cellulose acetate. For qualitative analysis of small amounts of aldehyes, the cellulose acetate tubes should be prepared on no. 24 chromel wire since in small sizes chromel wires are more easily handled than copper wires. After stretching the wire coated with the cellulose acetate, the tubes have an internal diameter of a proximately 0.35 mm.

The x-ray powder camera was specially designed for this type of work and was made by J. B. Hayes Scientific Appliances Co. Figures 61, 62, and 63 show the general design of the camera. The radius from sample to film is 7.00 ± 0.01 cm. The film is held in place by machined rings 1/8 in. in thickness and fitted to hold the film plus two thicknesses of black paper tightly to the circumference of the camera. The camera rests on the Machlett x-ray tube by means of thecollimating tube which is machined with a conical collimating tube. The use of this conical connection to the x-ray tube permits positive allignment in the x-ray beam. The

X-Ray Powder Diffraction Camera



Fig. 61. Side View.



Fig. 62. Bottom View.

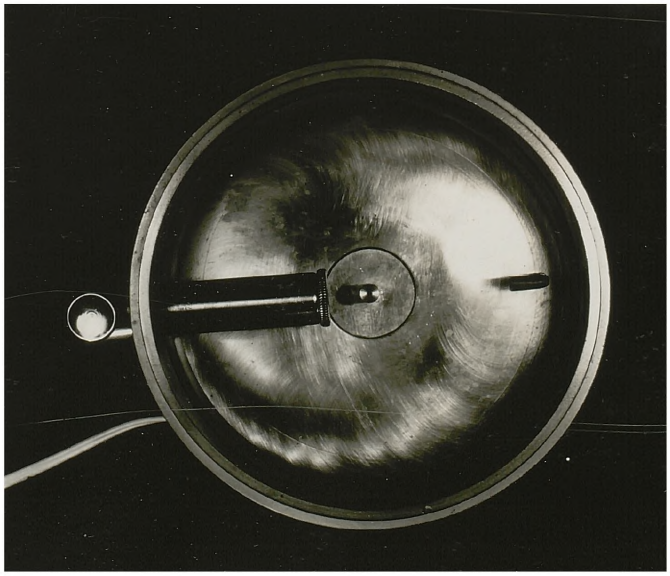


Fig. 63. Inside View.

The back pinhole is so designed to lay on the circumference of the camera thus making use of the maximum geometric focusing of the x-ray beam by the sample placed at the center of the camera. The beam trap is held in position by a spring but may be momentarily pulled from the beam to permit recording of the central x-ray beam on the film. The beam trap is elongated for use both with pinhole and slit collimating systems. The diffraction lines may be recorded on both sides of the central beam for greater accuracy of "d" value and intensity measurements. The cellulose acetate tube supported by its wire base is held in position on the central shaft by a small amount of Picene wax pilled into a hole in the shaft 0.040 in. in diameter. The shaft upon which the sample in the cellulose acetate tube rests is mounted in a ball bearing socket and connected to a Haydon 5 watt, 110 V. reversing motor rotating the sample at 1 RPM. The reversing switch is operated by means of pins placed in a circulat disk mounted on the shaft of the sample holder. The pins may be set to oscillate the sample through 10, 15, 20, 25, 30, 45, 60, 70, and 90° as well as rotate through 360° by removing the pins entirely. The use of such a mechanism for oscillating or rotating the sample permits the smoothing out of spots on the film arising from crystallites in the sample greater than 0.001 mm. in diameter, as well as versatility in using the camera for taking precision oscillation and rotation patterns of single crystals. The three legs of the camera protect the motor when placing the camera down and permit more convenient loading. A close fitting lid fits over the top of the camera as a further precaution against fogging the film.

The camera is equipped with a set of back pinholes 0.010, 0.025, 0.040 in. in diameter while the standard front pinholes may be obtained in sizes 0.010, 01025, 0.030, 0.04 and 0.060 in. in diameter as well as lits 1/8 in. long and 0.010 in. and 0.020 in. in width. Fig. 64 shows the effect of front and back pinhole sizes on the breadth of the the lines. It is observed that onlv

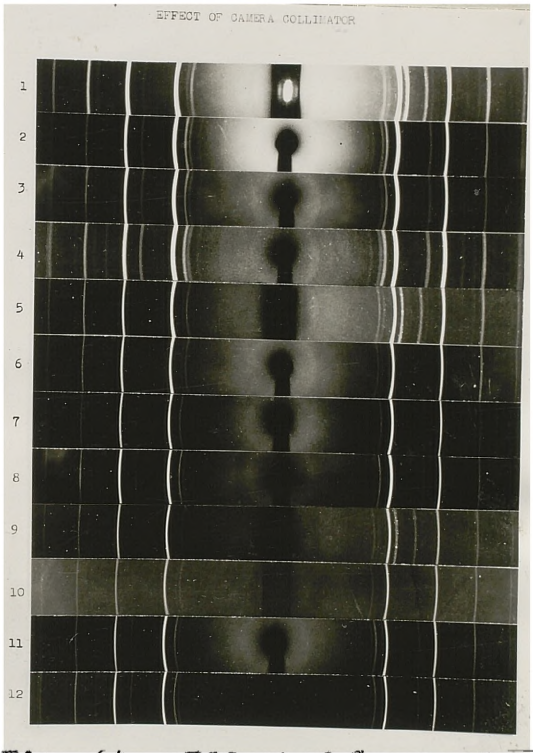


Fig. 64. Effect of Camera Collimation

back pinhole determines the line breadth for the lines lying relatively far out from the central beam. In the case where the diffraction lines occur close to the central beam ("d" greater than 4.0 A.(the size of the front pinhole begins to play a greater part in causing line broadening. The data for the set of powder patterns in fig. 64, are listed in table XIII. From this table and the measured intensities of the lines, the exposure data on the collimating systems may be determined. To a first

Table XIII. Data on Collimation Patterns

1. Sample: Sodium chloride C. P. sublimed in vacuum mounted in cellulose acetate tube 0.35 mm. in diameter.

2. Radiation: Copper, 40 KV., 15 MA.

3. Camera: 7.00 cm. radius, 30° oscillation.

4. Collimation: As described, back pinhole on circumference of film, front pinhole 1.0 cm. from sample.

#	back pinhole	front pin.	Filter	Hrs. Exp.
1.	0.040 in.	0.020s* in.	Ni	1/2
2.	0.040	0.040	-	1/2
3.	0.040	0.025	-	3/4
4.	0.040	0.010	-	1½
5.	0.025	0.020s	Ni	3/4
6.	0.025	0.040	Ni	1
7.	0.025	0.040	-	3/4
8.	0.025	0.025	-	1½
9.	0.010	0.020s	Ni	2
10.	0.010	0.010s	Ni	2
11.	0.010	0.040	-	2½
12.	0.010	0.010	-	7½

*Slit 1/8 in. long.

approximation the exposure time, for a given diffraction line instensity, is proportional to the first power of the radius of the front pinhole and is proportional to the second power of the radius of the back pinhole. The relationship of the exposure time with the radius of the back pinhole is determined by the cross sectional area of the x-ray beam passing into the collimating system while the effect of the front pinhole may be explained when it is understood that the samples were mounted in cellulose acetate tubes of only 0.014 in. in diameter and approximately 1/4 in. in length. This sample diameter is appreciably narrower than all but the smallest pinhole hence the length of the sample exposed to the x-ray beam is the determining factor.

Fig. 65 is a photograph of the calibration curve for this camera. The use of this graph of "d" values versus the diameter of the diffraction rings greatly facilitates the calculation of the powder and oscillation patterns.

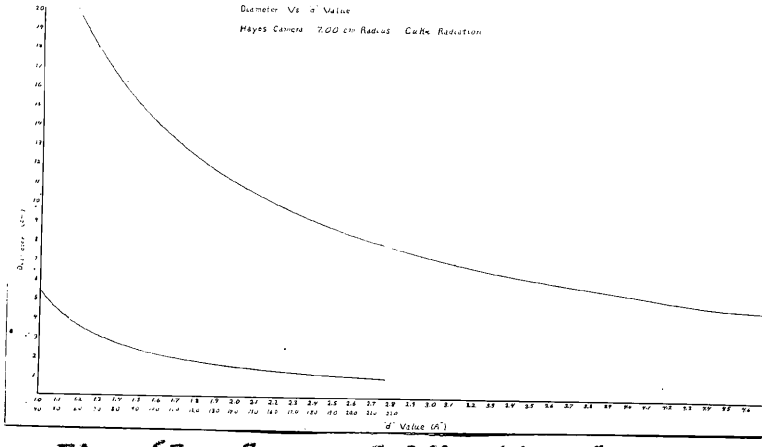


Fig. 65. Camera Calibration Curve

Technique of Qualitative Analysis: The sample for such an exposure as that of formaldehyde 2, 4 dinitrophenylhydrazone,

fig. 17, was prepared by adding approximately 1 drop of a 40% formaldehyde solution with an eye dropper, to a 0.3 ml. of a methyl alcohol-HCl solution of 2, 4 dinitrophenylhydrazine in one of the small centrifuge tubes. This solution of 2, 4 dinitrophenylhydrazine was prepared by dissolving 1 g. of 2, 4 dinitrophenylhydrazine in 25 ml. of methyl alcohol containing approximately two equivalents of HCl gas per liter of alcohol. Such a solution has been found to berelatively more stable for high concentrations of 2, 4 dinitrophenylhydrazine than ethyl alcohol-H_2SO_4 solutions. After allowing the solution of the formaldehyde derivative to stand ½ hour the tube was centrifuge, the liquid decanted, and the precipitate washed twice with 95% ethyl alcohol, then centrifuged and decanted again. A bit of filter paper was used to remove most of the wash liquid, then the remainder was removed by attaching the centrifuge tube to a vacuum pump for 15 minutes.

A portion of the dry dample in the constricted end of the centrifuge tube was then transfered to a cellulose acetate tube by forcing some of the sample into the open end of the cellulose acetate tube then tamping the sample solidly in to tube with another chromel wire. When the tube was filled with the sample to a length of about 1/4 in. the tube was cut approximately 1/4 in. below the end of the wire leaving 1/4 in. of wire in the tube for support. The tube was then transfered to the x-ray camera for an exposure of 1½-3 hours using 0.025 in. front and back pinholes and Eastman No-Screen film.

Evaluation of Powder Patterns: Since there is a possibility of contaminating the sample with unchanged 2, 4 dintrophenylhydrazine

and its hydrochloride, these powder patterns were taken. Fig. 66 is a powder pattern of the pure 2, 4 dinitrophenylhydrazine. The observed "d" values and intensities (by visual comparison) are listed in table XIV. Fig. 67 is a powder pattern of the hydrochloride. Table XV lists the data from this pattern. Fig. 68 is a powder pattern of the hydrochloride after "decomposition" in a vacuum for 2 hours. This decomposition is accompanied by a change in color from yellow to orange-red. Table XVI lists the calculated "d" values and relative intensities.

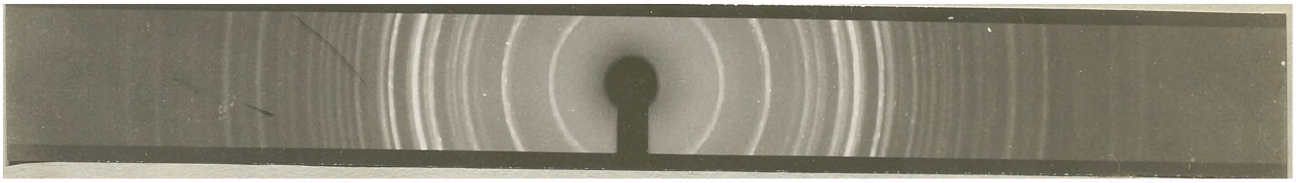


Fig. 66. Powder Pattern, 2, 4 Dinitrophenylhydrazine 7.00 cm. rad.

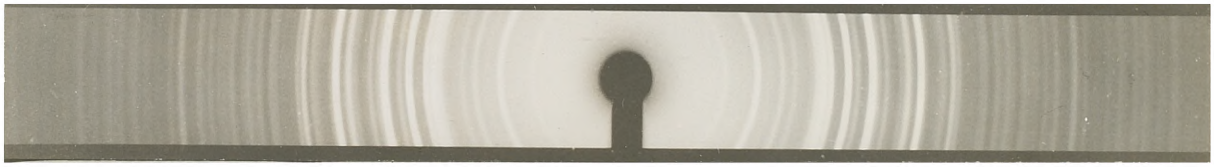


Fig. 67. Powder Pattern 2, 4 Dinitrophenylhydrazine Hydrochloride

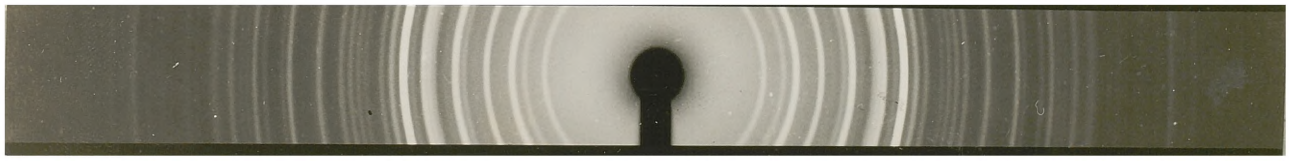


Fig. 68. Powder Pattern, 2, 4 Dinitrophenylhydrazine Hydrochloride "Decomposed" in a Vacuum.

Table XVII lists the three most intense lines in order of their relative intensities in a manner similar to that proposed by Hanawalt, Rinn, and Frevel (29). Since the innermost line in all cases is usually the most characteristic, it is also tabulated.

Table XIV. Data from Powder Pattern of 2,4 Dinitrophenylhydrazine

#	D	I	"d"
1.	2.40	0.5	8.9
2.	3.55	0.1	6.07
3.	3.71	0.6	5.81
4.	4.49	0.2	4.84
5.	4.80	0.4	4.42
6.	4.97	0.1	4.29
7.	5.13	0.2	4.18
8.	5.30	0.1	4.08
9.	4.76	0.5	3.78
10.	5.93	0.2	3.88
11.	6.21	1.0	3.50
12.	6.38	0.2	3.39
13.	6.89	0.6	3.15
14.	7.16	0.3	3.04
15.	7.47	0.1	2.92
16.	7.89	0.2	2.768
17.	8.09	0.1	2.689
18.	8.36	0.1	2.613
19.	8.63	0.1	2.534
20.	8.83	0.1	3.480
21.	9.16	0.1	2.398
22.	9.65	0.1	2.280
23.	10.00	0.1	2.203
24.	10.59	0.2	2.986
25.	11.49	0.2	1.927

Table XV. Data From Powder Pattern of 2, 4 Dinitrophenylhydrazine Hydrochloride.

#	D	I	"d"
1.	2.65	0.2	8.0
2.	3.59	0.4	6.0
3.	3.93	0.1	5.50
4.	4.29	0.2	5.05
5.	4.67	0.2	4.55
6.	5.11	0.1	4.18
7.	5.30	0.2	4.07
8.	5.47	0.4	3.98
9.	5.68	0.3	3.83
10.	5.90	0.1	3.69
11.	6.15	0.8	3.54
12.	6.40	0.2	3.38
13.	6.82	1.0	3.18
14.	7.03	0.1	3.09
15.	7.82	0.2	2.79
16.	7.62	0.1	2.86
17.	7.82	0.2	2.79
18.	8.17	0.5	2.6
19.	8.80	0.1	2.490
20.	9.06	0.2	2.422
21.	9.22	0.1	2.380
22.	12.46	0.2	1.786

Table XVI. Data from Powder Pattern of 2, 4 dinitrophenylhydrazine Hydrochloride - "Decomposed" in Vacuum.

#	D	I	"d"
1.	3.08	0.3	7.00
2.	3.61	0.2	5.95
3.	3.99	0.4	5.43
4.	4.69	0.3	4.51
5.	5.30	0.1	4.08
6.	5.55	0.4	3.91
7.	5.83	0.1	3.73
8.	6.19	0.2	3.51
9.	6.30	0.2	3.44
10.	6.44	0.3	3.36
11.	6.75	0.1	3.22
12.	7.00	1.0	3.11
13.	7.33	0.3	2.97
14.	7.62	0.2	2.86
15.	8.05	0.1	2.71
16.	8.25	0.1	2.645
17.	8.47	0.1	2.580
18.	8.42	0.1	2.508
19.	9.33	0.2	2.350
20.	10.17	0.2	2.170
21.	10.39	0.1	2.126
22.	10.86	0.1	2.035
23.	11.13	0.2	1.985

The use of this table facilitates the identification of the unknown aldehyde derivative. Further confirmation of the other weaker lines in the powder pattern of the unknown may be made by reference to the tables of "d" values listed under each compound.

Table XVII. "d" Values of Most Intense Lines of 2, 4 Dinitrophenylhydrazine and Its Aldehyde Derivatives in Order of Intensity.

#	Compound	I	II	III	IV*
1.	2,4 D.P.H.	3.50	3.15	5.81	8.9
2.	2,4 D.P.H-HCl	3.18	3.54	2.68	8.0
3.	2,4 D.P.H-HCl decomposed in vac.	3.11	3.91	4.51	7.0
4.	Formaldehyde 2,4.	3.08	3.62	3.47	10.3
5.	Acetaldehyde 2,4. yellow.	3.21	9.35	4.65	9.35
6.	Acetaldehyde w,4. orange	9.2	3.20	6.8	912
7.	Crotonaldehyde 2,4	3.22	3.26	10.9	10.9
8.	n-Butyraldehyde yellow	14.0	3.77	3.21	14.0
9.	n-Butryaldehyde orange	11.7	3.50	3.48	13.7
10.	n-Butyraldehyde	12.6	3.28	4.33	12.6
11.	Furfuraldehyde 2,4 yellow	3.26	6.17	7.7	11.7
12.	Furfuraldehyde 2,4 red.	3.26	4.62	5.35	11.7

*Innermost Line

Quantitative X-Ray Analysis

Introduction: The quantitative analysis of pure aldehydes by precipitation with 2, 4 dinitrophenylhydrazine has been studied carefully by Iddles and Jackson (12). They reported yields greater than 95% for simple aliphatic aldehydes. Their method, using standard quantitative procedures, is quite accurate when the aldehyde may be obtained relatively free of other carbonyl compounds. By the use of accurate density measurements of x-ray powder patterns of samples containing some internal standard it is possible to analyse quantitatively samples of mixed aldehydes and ketones.

Quantitative analysis by the x-ray powder diffraction method has been reported for the analysis of mineral and metallurgical samples (30, 31, 32) using sodium chloride as an internal standard. These articles have dealt rather carefully with the theory of line intensities but lack in the presentation of satisfactory laboratory procedures. These articles report an accuracy of 5% in the determination. This is probably a good estimate for most crystalline compounds, but under favorable circumstances the accuracy may be limited to 1%.

The following sections illustrate the quantitative x-ray powder method of analysis for the favorable case of a misture of sodium chloride and potassium chloride and the case for the aldehyde 2, 4 dinitrophenylhydrazones with the data necessary for their quantitative estimation.

Quantitative X-Ray Analysis of Mixtures of NaCl and KCl:

In order to develope the techniques necessary for the quantiative estimation of mixtures of organic compounds, a series of mixtures of NaCl and KCl was first analysed by the x-ray powder method.

The x-ray powder patterns of the NaCl-KCl mixtures were taken with new Afga-Ansco Non-Screen x-ray film. The film responce to x-rays of various wave lengths is shown by fig. 69 and table XVIII to be linear with respect to the milliampere seconds of exposure. i. e. density is directly proportional to the exposure (Busens Law). Since the response of the film was expected to vary with the wave length of the x-rays used, two curves for two different tube targets and voltages were graphed and tabulated with a third target giving almost the same values. All the exposures for a particular radiation were made on the same film and developed for 5 minutes in Eastman X-ray developer at 18°C. The density of the spots on the processed film was them measured with a Leeds and Northrup Recording Microphotometer. The slope of the lines in fig. 69 is not a measure of the relative

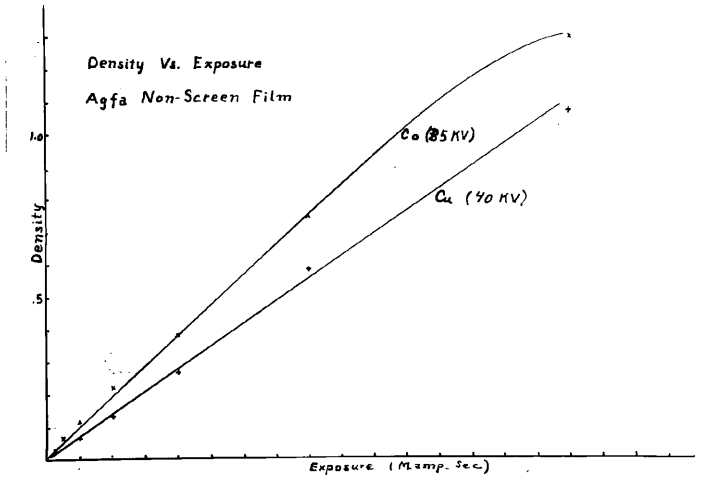


Fig.69. Density Vs. Exposure, Agfa Non-Screen Film.

speed of the film to derferent wave lengths since filters and tube to film distances was different for the different sets of exposures.

Table XVIII. Plate Calibration for Agfa Non-Screen film.

MAS	Co-35 KV	Cu-40KV	W-50KV
4	Fe filter	Ni filter	Fe filter
4	0.030		0.020
8	0.057		0.050
16	0.117	0.065	0.100
32	0.225	0.130	0.187
64	0.385	0.265	0.400
128	0.75	0.585	0.800
256	1.30	1.07	1.45
512	3.0	1.70	

From table XVIII it is apparent that the data in column four for tungsten radiation are more consistent than with the other radiations. This is due to the fact that the Picker radiographic unit was used for the tungsten radiation and this unit was regulated with an automatic timer whereas the timing on the other units had to be controlled by hand.

Since there are many variables which can cause erroneous measurements of line intensities, experiments were undertaken to try to find the best set of conditions. The errors produced by "spotty" diffraction lines on the powder patterns are large. To obviate this difficulty the samples must be in a finely divided state and preferably rotated during exposure. Since it is a time consuming operation to grind NaCl and KCl to a

sufficiently small size, some methods were tried of obtaining a small particle size. Fusion was tried as well as precipitation from concentrated aqueous solutions by the use of organic missible liquids of which acetone was found most satisfactory for this operation. Another method, suggested by L. G. Schulz, required the sublimation of the sample in a vacuum. Grinding the sample together in amortar using CCl_4 as a dispersing medium was fairly successful; however, the best method from the standpoint of time and convenience was one in which the aqueous solution of the mixture was evaporated rapidly. Since the anions were the same in this case there was no possibility of obtaining a new compound; however, even with mixtures of NaCl and KBr the powder patterns of the evaporated mixtures indicated the presence of NaCl and KBr only and no appreciable amounts (5%) of NaBr and KCl. This effect has been noticed previously for alkali halide salts by Link and Wood (33 when they summarized the effect in the following way, "In almost every case the heavy cation united with the heavy anion and the light cation with the light anion".

In fig. 70 is shown a series of powder photographs of mixtures of NaCl and KCl varying in the proportion of NaCl to KCl. The samples were prepared by the evaporation technique and were mounted in cellulose acetate tubes of 9.35 mm. internal diameter and photographed using a Hayes Universal camera of 5.00 cm. radius. 0.025 in. back and front pinholes were used and the sample was rotated through 360° during the exposures. The intensities of the lines were measured with the microphotometer. The results of this series is tabulated in table XIX. The rows of ratios of

Table XIX. Intensity Measurements of KCl - NaCl Mixtures

KCl Line	3.91	6.84	14.2	22.8	30.5	48.5	68.2	80.0	82.9	93.0
NaCl 111	.110 .134	.152 .159	.127 .098	.104 .082-	.067 .076	.047 .057		.040 .050		
KCl 200	.075 .082	.142 .145	.186 .152	.315 .242	.381 .410	.470 .362	.418 .468	.960 .770	.470 .508	.780 1.13
NaCl 200	1.16 1.35	1.58 1.53	1.20 .97	1.38 .990	.718 .740	.473 .367	.165 .189	.209 .168	.095 .097	.068 .066
KCl 220	.085 .101	.114 .120	.127 .110	.231 .178	.271 .300	.390 .290	.308 .345	.727 .640	.386 .442	.646 .928
NaCl 220	.903 1.01	1.124 1.17	.892 .782	.846 .697	.487 .545	.376 .282	.133 .153	.136 .114	.078 .107	.039 .056
KCl 200 NaCl 111	.681 .612	.935 .910	1.47 1.51	3.03 2.95	5.52 5.85	8.15 6.35		24.0 15.4		
KCl 200 NaCl 200	.065 .061	.090 .095	.155 .157	.228 .244	.531 .555	.993 .986	2.53 2.48	4.60 4.59	4.95 5.28	11.5 17.1
KCl 220 NaCl 220	.094 .100	.101 .102	.142 .140	.273 .256	.446 .550	1.04 1.03	2.32 2.26	5.35 5.60	4.95 4.13	16.6 16.6
NaCl 200 NaCl 220	1.29 1.34	1.40 1.27	1.35 1.24	1.63 1.42	1.47 1.36	1.26 1.26	1.24 1.24	1.54 1.47	1.22 .91	1.74 1.18
KCl 200 KCl 220	.88 .81	1.25 1.21	1.46 1.38	1.36 1.36	1.41 1.37	1.20 1.25	1.36 1.36	1.32 1.20	1.22 1.15	1.21 1.22

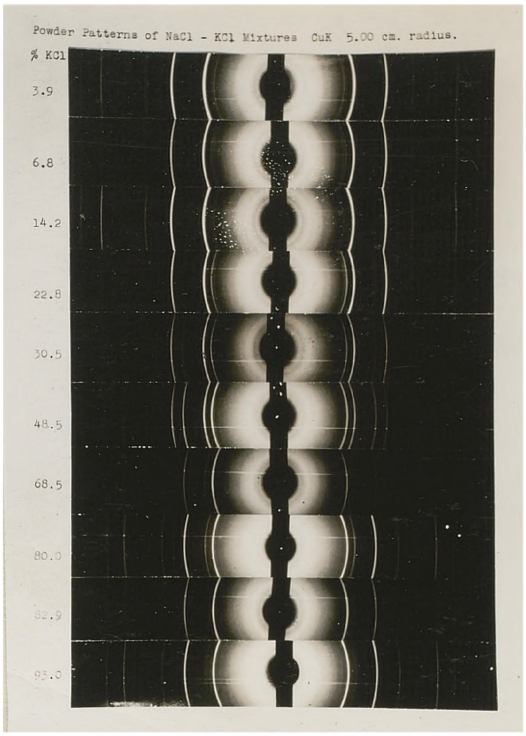


Fig. 70. Powder Photographs of NaCl-KCl

the intensities of lines NaCl 200/NaCl 220 and KCl 200/KCl 220 give some indication of the reliability of the density measurements. Measurements of the lines on a powder pattern of a pure sample of NaCl indicated that the K radiation penetrating the filter was about 2.5% as strong as the K radiation. Since the K interference of the NaCl 200 plane lies at almost the same position as the KCl 200 K interferenc, correction was necessary in order to obtain a reliable measurement of the density of the KCl line. The correction for this "double" line was made by subtracting 2.5% of the intensity of the NaCl 200 line from the measured intensity of the KCl 200 line. The final ratio of line intensities was then made using this corrected KCl 200 line intensity. These corrected intensities and final ratios are tabulated in table XX.

Table XX. Correction for Cu K_β radiation (2.5%)

% KCl	ratio KCl/NaCl	NaCl 200 K_α	NaCl 200 K_β	KCl 200 K_α	KCl 200 corr.	KCl 200 / NaCl 200
3.9	0.040	1.16	0.027	0.075	0.048	0.041
		1335	0.033	0.082	0.049	0.042
6.8	0.073	1.48	0.039	0.142	0.103	0.065
		1.53	0.038	0.145	0.105	0.070
14.2	0.165	1.20	0.030	0.186	0.156	0.130
		0.97	0.024	0.152	0.138	0.142
22.8	0.294	1.38	0.034	0.315	0.281	0.204
		0.99	0.025	0.242	0.217	0.219
30.5	0.432	0.718	0.017	0.381	0.364	0.506
		0.740	0.018	0.410	0.392	0.530
48. 5	0.947	0.473	0.012	0.470	0.458	0.958
		0.367	0.009	0.362	0.353	0.962
68.2	2.15	0.165	0.004	0.418	0.414	2.50
		0.189	0.004	0.468	0.464	2.45
80.0	4.00	0.209	0.005	0.960	0.955	4.56
		0.168	0.004	0.770	0.766	4.56
82.9	4.75	0.096		0.470	0.470	4.95
		0.097		0.508	0.508	5.24
93.0	13.3	0.068		0.780	0.780	11.5
		0.066		1.13	1.13	17.1

Table XX also lists the ratios of grams of NaCl to KCl. Comparing this ratio of grams of constituents with the ratio of densities of the diffraction lines shows a rather close correlation. No correction for density vs. intensity need be made since the response for this film was linear. The resulting pattern from a mixture of compounds, apparently, is the same as would be obtained if the two compounds were photographed separately on the same film. From the above table XX it appears that with the proper conditions standardized a quantitative estimate of one constituent in a mixture could be made with an error of less than 3% provided the samples gave rise to clear diffraction lines.

It would seem, at first, asthough there might be a better measurement of the total radiation from a particular plane in a crystal than is obtained by measuring only the peak density on the photographic film. The most likely measurement of such a total radiation would be the area under the curve in a graph plotting density vs. distance. Such a graph is shown in figs. 71 and 72. The area under these curves was measured with a Keuffel

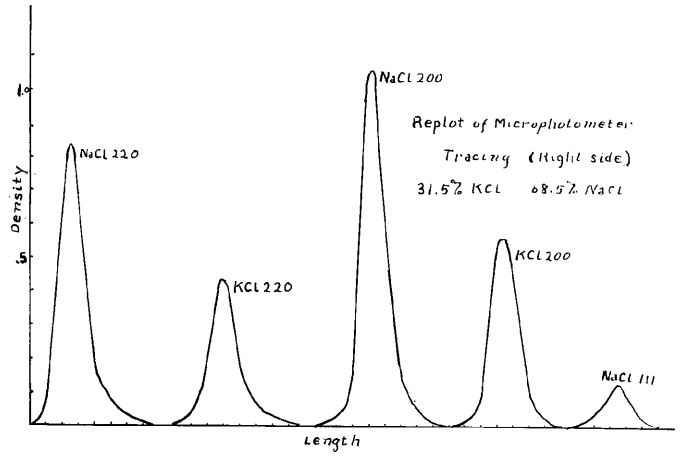


Fig. 71. Replot of Microphotometer Tracing.

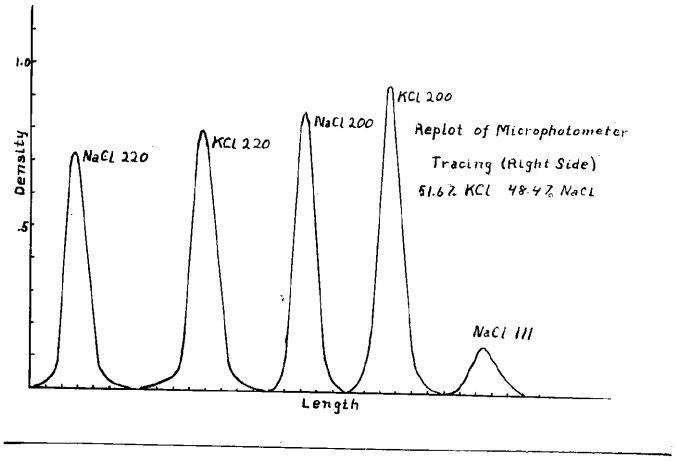


Fig. 72. Replot of Microphotometer Tracing (New Tube)

and Esser Polar Planimeter and the results are tabluated in tables XXI and XXII. By comparison of the ratio of the intensities of the lines as measured by the area and the height of the curve it is evident that the area is not as reliable a measure of relative total radiation as is the measurement of the maximum density. Observation of the shape of the curves in fig. 71 shows that one side of the curve exhibits a steeper slope than the other. Since the steeper side of the curve is on the long wave length side of the peak it seems that the most logical explanation of this broadening of the line lies in the presence of some tungsten radiation. Were the line broadening due to the CuK_{α} doublet alone the curve would exhibit a steeper slope on the short wave length side of the peak. This is further evidenced by the fact that the curves in fig. 72 exhibit a more symmetrical shape than those in fig. 71. The only difference between these figures, besides the sample, is the length of time the x-ray tube had been in operation. The tube used in photographing the pattern form which

Table XXI. Replot of Microphotometer Curves for Sample Containing 31.5% KCl (old tube)

Line	Max. Height	Area (planimeter)
NaCl 111	0.130	0.033
	0.122	0.037
KCl 200	0.566	0.154
	0.584	0.147
NaCl 200	1.07	0.268
	1.06	0.275
KCl 220	0.438	0.126
	0.390	0.115
NaCl 220	0.837	0.221
	0.768	0.198
$\frac{\text{KCl 200}}{\text{NaCl 111}}$	4.35	4.67
	4.78	3.97
$\frac{\text{KCl 200}}{\text{NaCl 200}}$	0.530	0.575
	0.550	0.535
$\frac{\text{KCl 220}}{\text{NaCl 220}}$	0.523	0.571
	0.509	0.581
$\frac{\text{NaCl 200}}{\text{NaCl 220}}$	1.28	1.21
	1.38	1.39
$\frac{\text{KCl 200}}{\text{KCl 220}}$	1.29	1.22
	1.50	1.28

Table XXII. Replot of Microphotometer Curve for Sample Containing 51.6% KCl (new tube)

Line	Height	Area (planimeter)
NaCl 111	0.145	0.037
	0.185	0.047
KCl 200	0.940	0.204
	0.900	0.184
NaCl 200	0.861	0.170
	0.816	0.193
KCl 220	0.804	0.198
	0.672	0.180
NaCl 220	0.727	0.154
	0.626	0.164
KCl 200 / NaCl 111	6.50	5.51
	4.86	3.92
KCl 200 / NaCl 200	1.09	1.20
	1.11	1.08
KCl 220 / NaCl 220	1.10	1.28
	1.07	1.10
NaCl 200 / NaCl 220	1.18	1.10
	1.29	1.18
KCl 200 / KCl 220	1.29	1.03
	1.34	1.02

fig. 71 was taken had been in operation more than 500 hours whereas the tube for fig. 72 had been in operation less than 100 hours.

The necessary steps for obtaining a good quantitative estimation of a mixture of two known compounds is then:

1. Calibration of the film used.
2. Preparation of a known mixture of the compounds in question with some definite amount of an internal standard such as NaCl. Care must be given to prepare the sample in a finely divided state and thoroughly mixed, either by rapid evaporation or fine grinding using some inert liquid as a dispersing agent.
3. Measurement of the relative line densities of the internal standard linesandthe lines of the sample under consideration.
4. Correction of the relative line densities to give line intensities by using the film calibration curve.
5. Calculation of the ratio of line intensitiesof internal standard and sample in question for a 1 to 1 mixture.
6. Preparation of the sample containing an unknown amount of the constituent in question with a known percentagepf the internal standard.
7. Determination of the relative line densities from the powder pattern.
8. Correction of density to give intensity of the lines.
9. Calculation of the ratio of line intensities of unknown to internal standard. Multiplication of this factor by the ratio determined in step 5 will givethe ratio of grams of

unknown to internal standard. Knowing the amount of internal standard in the sample subjected to the x-ray examination it is possible to calculate t e amount of constituent in question present in the original sample.

When a film is used with a linear response to the x-rays steps 4 and 7 may be omitted.

Quantitative X-Ray Analysis of Aldehydes: The quantitative analysis of Aldehydes was accomplished in a manner similar to that of the mixtures of NaCl-KCl. Sodium fluoride was chosen as the internal standard since it could be obtained in large quantities having a particle size small enough to give smooth sharp diffraction lines as well as produce a relatively simple powder pattern with a minimum of absorption of the x-ray beam.

For reasons of war shortages the Ansco-Non-Screen film could no longer be obtained and other types of x-ray film were investigated. Each of the films was place in the camera to record the pattern from sodium chloride in a manner similar to that used for the collimation data in table XIII. The negatives were microphotometered for the intensity data. In this manner the relative speed of each type of film to the CuK wave length as well as the relative grain size could be determined. The results of this investigation are summarized in table XXIII. Apparently the Eastmen No-Screen film is the best available incorporating speed with fine grain size.

Table XXIII. Relative Qualities of Commercial X-Ray Films to Copper K X-Ray Radiation.

Type Film	Speed	Grain size	background
Ansco Non-Screen	1.00	D	C
Eastman No-Screen	.85	B	A
Eastman Type A	.25	A	A
Eastman Type K	.60	C	A
Dupont Photo Roentgen	.54	C	A
Dupont Photo Roentgen with "detail" intensifier	.70	C	A

The graph of density vs. exposure for this Eastman No-Screen film is shown in fig. 73. All the exposures were made on the same film by exposing small sections of the film to the x-ray beam (Cu target, 15 KV, filtered through Ni foil). The exposure time was regulated by hand hence the accuracy was not great. The exposure scale is an arbitrary one, each unit corresponding to 1½ seconds exposure at ½ milliampere tube current. Table XXIV lists the data from which this graph was drawn. While the accuracy is not great due to timing control, the graph shows that the response of the film is a linear function of the exposure time as was observed for the Agfa-Ansco Non Screen film.(p. 133)

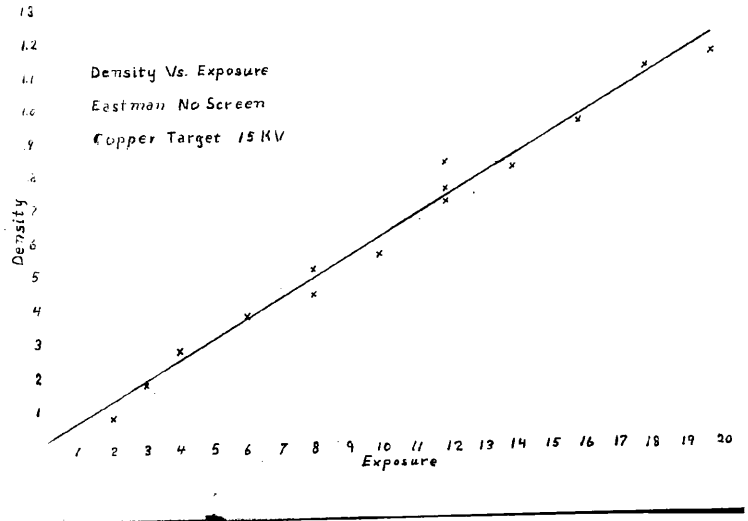


Fig. 73. Density vs. Exposure, Eastman No-Screen Film.

The samples were prepared by mixing weighed quantities of the aldehyde 2, 4 dinitrophenylhydrazone with sodium fluoride. These were ground together carefully in an agate mortar, filled in a 0.35 mm. diameter cellulose acetate tubes and exposed to the x-ray beam in the 7.00 cm. powder camera for 2½ - 3 hours using

Table XXIV. Density vs. Exposure, Eastman No-Screen Film
Copper Target 15KV. ½ MA. Direct Radiation.

Sec.	Exp.	Density
2½	2	0.07
33/4	3	0.17
5	4	0.27
5	4	0.27
7½	6	0.37
10	8	0.43
10	8	0.51
12½	10	0.55
15	12	0.71
15	12	0.71
15	12	0.75
17½	14	0.81
20	16	0.95
22½	18	1.11
24	20	1.15
26½	22	1.23

Eastman No-Screen film. The motor on the camera was set to rotate through 360° to smooth out any spots on the diffraction lines. The patterns were microphotometered with the Leeds and Northrup recording Microphotometer.

Table XXV lists the intensity data from the series of aldehyde 2, 4 dinitrophenylhydrazone - NaF patterns. The two sets of readings for each pattern were obtained from the two sidesof the film upon which the powder pattern was registered.

The 1:1 ratios of line intensities in table XXVI were calculated by dividing the ratio of intensities of the aldehyde 2, 4 dinitropheylhydrazone to NaF lines by the ratio of grams of the constituents the sample. These 1:1 ratios may now be used to calculate the ratio of grams of unknown to NaF in any given sample, after qualitative identification of the aldehyde, in a manner outlined for the NaCl-KCl mixtures p.143.

Table XXV. Quantitive Data On Aldehyde 2, 4 Dintirophenylhydrazone

Compd.	G. 2,4 g. NaF	NaF Pattern NaF 220	Naf 200	2,4 DPH	2,4 / 200	2,4 / 220
Form. .	2.54	.273	.566	.239	.42	.87
		.295	.607	.254	.43	.86
"	1.23	.490	.950	.185	.195	.378
		.472	.968	.207	.214	.440
"	1915	.303	.640	.090	.140	.296
		.328	.680.	.100	.147	.305
Acet. (Yellow p.)	1.70	.440	.876	.549	.63	1.25
		.428	.855	.506	.59	1.18
"	3.19	.281	.590	.685	1.16	2.44
		.274	.551	.579	1.05	2.11
"	2.66	.500	.992	.807	.81	1.61
		.521	1.11	.910	1.82	1.74
Crot.	1.90	.505	1.05	.458	.436	.907
		.534	1.06	.447	.420	.84
"	1.15	.715	1.32	.370	.280	.519
		.630	1.25	.367	.293	.58
Butry. 2,4 DPH (yellow)	1.95	.239	.400	.51	.127	2.13
		.203	.370	.45	1.22	2.21
"	1.63	.417	.845	.790	.935	1.89
		.398	.727	.770	1.06	1.93
Furfur. (red)	2.08	.610	1.20	.540	.45	.89
		.622	1.19	.470	.393	.755
" (yellow)	.870	.961	1.80	.450	.250	.524
		.800	1.63	.472	.290	.590
2,4 DPH	1.57	1.75	.885	.570	.325	.645
		1.87	.970	.738	.340	.657
2,4 DPH	1.60	2.07	.955	.635	.317	.665
		1.60	.910	.560	.350	.615

Table XXVI. Ratios of Intensities of 1:1 Aldehyde 2, 4 Dinitrophenylhydrazone - Sodium Fluoride Mixtures.

Compd.	$\frac{2,4}{220}$	Ave.	$\frac{2,4}{200}$	Ave.
Form. 2,4 DPH	.342		.165	
	.339		.165	
	.307		.158	
	.357		.174	
	.324		.153	
	.334	.338	.161	.165
Acet. 2,4 DPH	.735		.370	
	.695		.347	
	.765		.364	
	.662		.330	
	.695		.305	
	.655	.695	.308	.345
Crot. 2,4 DPH	.477		.230	
	.441		.221	
	.450		.244	
	.505	.465	.255	.235
Butyr. 2,4 DPH yellow	1.09		.652	
	1.13		.575	
	1.16		.510	
	1118	1.14	.650	
Furf. 2,4 DPH yellow	.601		.288	
	.678	.640	.333	.305
Furf. 2,4 DPH red	.428		.216	
	.362	.395	.189	.202
2,4 DPH	.410		.207	
	.410		.216	
	.415		.198	
	.384	.408	.218	.209

Discussion of the Strong Outer Spacing

The powder patterns for 2, 4 Dinitrophenylhydrazine and its aldehyde derivatives have been collected in fig. 74. A marked feature of all of these powder patterns is the high intensity of the lines in the neighborhood of 3.20 A. The data present in the preceeding tables permit a quantitative approach to a study of the reasons for this high line intensity. In the case of formaldehyde 2, 4 Dinitrophenylhydrazone it was proposed (p. 74) that this line ("d" = 3.08) arose from the $0\bar{2}1$ plane which was believed to be parallel to the plane of the benzene ring in the unit cell. The thickness of the aromatic molecule including the Van der Waals radii is reported as 3.7 A. (24). If the above planes are actually plane parallel to the plane of the aromatic nucleus with the distance between the planes equal to the distance between the aromatic nuclei, then the molecules

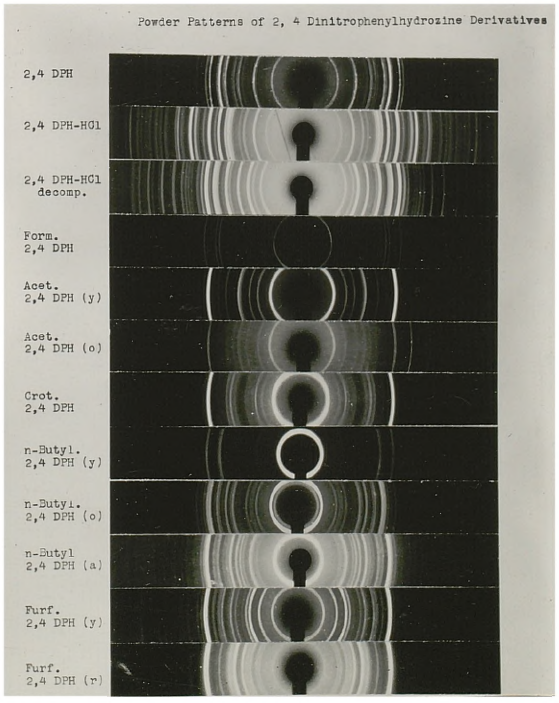


Fig. 74. Powder Patterns of 2, 4 Dinitrophenylhydrazones.

must lay unusually close to one another, perhaps by hydrogen bonding and interleaving of the straight chain portion of the molecule with the aromatic portion of the next molecule.

Table XXVII. Relative Intensities of Outer Strong Spacing of 2, 4 Dinitrophenylhydrazine and its Aldehyde Derivatives

Compound	"d"	$\frac{2,4*}{220}$	Int. outer line	Rel. Int. Outer line.
2, 4 DPH	3.15	.408	.60	.245
Form. 2, 4 DPH	3.08	.338	1.0	.338
Acet. 2, 4 DPH (y)	3.21	.695	1.0	.695
Crot. 2, 4 DPH	3.22	.465	1.0	.465
n-Butry. 2, 4 DPH (y)	2.31	1.14	.31	.355
Furf. 2, 4 DPH (y)	3.26	.640	1.0	.640
Furf. 2, 4 DPH (r)	3.26	.395	1.0	.395
	3.26	.39		

* From table XXVI

\# From tables of "d" values from Powder Patterns.

Column 3 of table XXVII lists the ratios of equal amounts of the strongest aldehyde 2, 4 dinitrophenylhydrazone line to the NaF 220 line taken from table XXVI. Column 4 lists the relative intensities of the strongest diffraction line of the powder pattern with the strong line of a "d" value close to 3.20 A. Column 5 tabulates the product of the values in column one and two. The values in this column now represent the intensities of the outer intense lines relative to one another, i.e. proportional to the absolute value of the scattering power of these planes through the crystal and therefore is probably a function of the

degree of planarity of the molecule. It will be observed that it is only by chance that a crystallographic plane through the unit cell would be parallel to the plane of the benzene ring of the molecule and have a "d" value equal to the thickness of the molecule; however, due to the large size of the unit cells of these derivatives the chance that some crystallographic plane should satisfy these requirements is good.

It is interesting that the outer intense lines of the two forms of furfuraldehyde 2, 4 dinitrophenylhydrazone have almost identical "d" values but widely varying intensities. One possible explanation may lie in the orientation of the furfural and benzene rings with respect to one another.

Another observation from this series is that there is no marked connection between the intensity of the lines and the presence of cleavage planes. One might expect a plane parallel to a cleavage plane to give unusually intense lines since the molecule would be expected to build up in the crystal in a lamellar manner. However, the line of acetaldehyde 2, 4 dinitrophenylhydrazine (y) exhibits no cleavage plane yet is almost twice as intense as the outer line of formaldehyde 2, 4 dinitrophenylhydrazine which possesses a definite cleavage plane.

Summary

1. The crystallographic parameters uniquely characterizing eight different crystalline aldehyde 2,4 dinitrophenylhydrazones from five different aldehydes have been determined using Weissenberg, rotation, oscillation, and powder patterns. The detailed data are summarized in table XXVIII. This series was selected because of its importance in organic analysis of aldehydes; because there is no previous record of investigation outside of fragmentary optical data; and because it afforded excellent experience in extending the most modern techniques to the problem of penicillin structure, particularly in distinction between polymorphic forms and in use of micro quantities of specimens.

2. The orientation of the molecule in the unit cell of formaldehyde 2, 4 hydrazine, which crystallizes in the triclinic system, has been proposed from the intensity measurements, cleavage planes and theoretical size of the molecule. This study has involved the first recorded practical reciprocal lattice interpretation of the powder pattern of a triclinic crystal.

3. Two forms of the acetaldehyde 2, 4 dinitrophenylhydrazone with melting points of 166° and 165° C. were investigated and structurally distinguished, One of these has not been previously reported in the literature which records two forms with melting points of 168° and 147° C. The melting point of the mixture of the two forms investigated in this thesis is not more than 4° lower than that of either of the pure forms. The form of acetaldehyde 2, 4 dinitrophenylhydrazone having a melting point of 147° and reported to have been prepared by sublimation and fusion

Table XXVIII. Crystallographic Data of Aldehyde 2, 4 Dinitrophenylhydrazones

Compd.	System	a_o	b_o	c_o	γ	p.	n	S.G.
Form.	Triclinic	10.40	10.00	4.23	87° $\alpha = 85^\circ$ $\beta = 86^\circ$	1.592	2	$P\bar{1}$
Acet. (y.)	Tetragonal	18.69	7.14	7.14		1.541	4	$P4_2/n$
Acet. (o.)	Orthorhombic	17,3	10.6	5.06		1.51	4	$P2_12_1-$
Croton.	"	18.90	13.08	4.63		1.43	4	$P2_12_1-$
Butyr. (y.)	"	54.	17.9	4.90		1.3		
Buty. (o)	"	25.8	25.0	7.0		1.3		
Furfur. (y.)	Monoclinic	11.7	7.7	3.62	95°		1	Pm
Furfur. (r.)				7.85				

of the stable form has not been found and powder patterns of samples prepared by fusing the acetaldehyde 2, 4 dinitrophenylhydrazone are similar to the patterns of the unfused samples. The close agreement between the theoretical and observed number of molecules per unit cell indicates that the molecular weight of both compounds is the same as the molecular weight calculated assuming no association or solvation.

4. Three crystallographically different forms of n-butyraldehyde 2, 4 dinitrophenylhydrazone were identified from their powder patterns. Hitherto the literature has not distinguished between these forms since their melting points all are within one degree of 123° C. and the depression in the melting point from mixtures of the forms is not morethan a few degrees.

5. The two previously reported forms of furfuraldehyde 2, 4 dinitrophenylhydrazone were investigated. It was found possible to prepare essentially pure samples of either forms by controlling the temperature at which crystallization occurred from ethylene chloride. Previously these two forms had been obtained from different solvents but essentially in the same manner since crystallization from the solvents must have occurred at different temperatures. Temperature is not considered to be the only variable controlling the formation of a particular type of crystal. Rate of crystallization seems to be the most important factor in determing the modification of n-butyraldehyde 2, 4 dinitrophenylhydrazone from methyl alcohol solutions considered in the previous paragraph.

Bibliography

(1) Purgotti, Gazz. chim. ital. 24, I, 55 (1894)

(2) Curtius and Dedichen, J. Prakt. Chem. (2) 50, 206, (1894)

(3) Allen, C. F. H., J. Amer. Chem. Soc. 52, 2955 (1930)

(4) Bryant, W. M. D., J. Amer. Chem. Soc. 54, 3758 (1932)

(5) Bryant, ibid. 55, 3201 (1933)

(6) Bryant, ibid. 58, 2335 (1936)

(7) Bryant, ibid. 60, 2815 (1938)

(8) Bell, F. O., Biochem. J. 35, 294 (1941)

(9) Dredereck, H., Ber. 65, 1833 (1932)

(10) Campbell, Analyst 61, 391 (1936)

(11) Allen, C. F. H. and Richmond, J. H. J. Org. Chem. 2, 222 (1937)

(12) Iddles, H. A. and Jackson, C. E., Ind. Eng. Chem. Anal. Ed. 6, 454 (1934)

(13) Weissenberg, K., Z. Physik 23, 229 (1924)

(14) Clark, G. L., "Applied X-Rays", McGraw Hill, New York third edition, 1941 p. 263.

(15) Barrett, C. S., "Structure of Metals", McGraw- Hill New York 1943 p. 111.

(16) Davey, W. P., "A Study of Crystal Structure and Its Applications", McGraw-Hill, New York 1934 p.204

(17) Buerger, M. J. "X-Ray Crystallography", John Wiley and Sons, New York 1942 p. 221.

(18) Clark, G. L., ibid. p.293

(19) Buerger, ibid. p. 252

(20) Clark, G. L., ibid. p.293

Bibliography (II)

(21) "Internationale Tabellen der Bestimmung von Kristalsturen" Gebruder Borntrager, Berlin 1935 vol I. p. 381.

(22) "International Tabellen", ibid. p. 95

(23) Davey, ibid. p. 182.

(24) Pauling, L., "Nature of the Chemical Bond", Cornell University Press, Ithaca, New York, 1940 p. 189.

(25) Allen, C. F. and Richmond, J. H., J. Org. Chem. 2, 2335 (1936)

(26) Brady, J. Chem. Soc. 1931, 756.

(27) Brady, E. Analyst 51, 77 (1926).

(28) Frick, R., Lohrmann, O., and Schroder, W., Z. Elektrochem. 47, 374 (1949). Chem. Ab. 35, 7826 (1941)

(29) Hanawalt, J. D., Rinn, H. W., and Frevel, L. K., Ind. Eng. Chem. Anal. Ed. 10,457 (1938)

(30) Ballard, J. W., Oshry, H. I. and Schrenk, Bureau of Mines Rept. of Invest. 3520 (1940); J. Opt. Soc. Amer. 33, 667 (1943)

(31) Schafer, K., A. Krist. 99, 142 (1938)

(32) Cross, S. T., and Martin, D., Ind. Eng. Chem. Anal. Ed. 16, 95 (1944)

(33) Link, H. L., and Wood, J. Am. Chem. Soc. 62, 766 (1940)

VITA

The author was born in Pelham Manor, New York, January 28, 1922. His primary education was received in the public schools of Pelham Manor and Lake Helen, Florida. His secondary education was completed in the high school of De Land, Florida in 1939. He entered Stetson University in the summer of 1939, and received the Bachelor of Science degree in June 1942. He attended the graduate school of the University of Illinois from July 1942 to January 1945. He held a teaching fellowship during the winter semester 1942-43 and 1944-45. During the summer semester of 1943 he held an industrial fellowship with the National Lead Company. Beginning June 1944, he was special reaserach assistant working on Penicillin under contract OEM cmr 439. He married Virginia Agett on February 7, 1944. The author is a member of the following: American Chemical Society, Sigma Xi, Gamma Sigma Epsilon, and Sigma Pi Sigma.

ProQuest Number: 29404084

INFORMATION TO ALL USERS
The quality and completeness of this reproduction is dependent on the quality
and completeness of the copy made available to ProQuest.



Distributed by ProQuest LLC (2022).
Copyright of the Dissertation is held by the Author unless otherwise noted.

This work may be used in accordance with the terms of the Creative Commons license
or other rights statement, as indicated in the copyright statement or in the metadata
associated with this work. Unless otherwise specified in the copyright statement
or the metadata, all rights are reserved by the copyright holder.

This work is protected against unauthorized copying under Title 17,
United States Code and other applicable copyright laws.

Microform Edition where available © ProQuest LLC. No reproduction or digitization
of the Microform Edition is authorized without permission of ProQuest LLC.

ProQuest LLC
789 East Eisenhower Parkway
P.O. Box 1346
Ann Arbor, MI 48106 - 1346 USA